Controlled Release of the Histone Deacetylase Inhibitor Sodium Butyrate for Increasing Recombinant Protein Production.

By

Ciara McCabe B.Sc.

Supervised by:

Dr. Tony McCabe

Dr. Ailish Breen

Dept. Life Science, IT Sligo

A thesis submitted to the Institute of Technology, Sligo, for the degree of Master of Science

June, 2019

Title: Controlled release of the histone deacetylase inhibitor sodium butyrate for increasing recombinant protein production.

Name: Ciara McCabe
Student Number: s00117254
Supervisors: Dr. Ailish Breen
Dr. Tony McCabe

Declaration: "I hereby declare that this project is entirely my own work and that it has not been submitted for any other academic award, or part thereof, at this or any other education establishment".

X_____

Ciara McCabe

Contents

Table of Figures

Table Of Tables

Abbreviations

BHK – Baby hamster kidney

Bp – Base pairs

CHO – Chinese hamster ovary

CHO K1-INS/GFP- Chinese hamster ovary cells insulin, green fluorescent protein fusion expressing cell clone

DNA - Deoxyribonucleic acid

E. coli - *Escherichia coli*

ELISA - Enzyme-linked immunosorbent assay

FDA - Food and Drug Administration

HAT – Histone acetyltransferase

HDAC – Histone deacetylase

HDACI – Histone deacetylase inhibitor

HEK 293 – Human embryonic kidney

HNSCC – Head and neck squamous cell carcinoma

IgG - Immunoglobulin G

PCR - Polymerase chain reaction

PI – Propidium iodide

PLGA - Poly(lactic-co-glycolic acid)

PTM – Post translational modification

SAHA – Suberanilohydroxamic acid

SEM – Scanning Electron Microscopy

tPA - Tissue plasminogen activator

VPA - Valproic acid

Acknowledgements

I wish to express my gratitude to my two supervisors, Dr. Ailish Breen and Dr. Tony McCabe, for their support and guidance throughout my research masters. I would also like to thank Dr. Thomas Smyth, for his time input and advice throughout the GC-MS process.

I would also like to thank all of the staff in the research office, the technicians and all the heads of science department for their help and support.

Finally, I want to thank my family, friends and colleagues who have supported and helped me throughout this project.

Abstract

Improving the yields of biopharmaceutical products from mammalian cell culture is of paramount importance to manufacturing companies; increasing product yield includes enhancing recombinant gene expression in mammalian cells. One avenue for investigation is the use of histone deacetylase inhibitors, such as sodium butyrate, which function by opening up genomic DNA for transcription. However, a limitation to the use of sodium butyrate is its toxicity. This research aimed to examine the controlled release of sodium butyrate onto CHO-K1 cells, to increase recombinant protein production, while minimizing loss of viability.

Reused lobster exoskeleton was demineralised and deproteinated and was used as a release vehicle due to its nanoporous biocompatible structure. Biocompatibility of the shell was confirmed by *in vitro* toxicity assays. Adsorption and release of butyrate was measured by GC-MS and the effect of sodium butyrate on recombinant protein (human insulin-GFP) production in CHO K1-INS/GFP clonal cells was quantified using fluorescent microscopy. Cell viability was quantified using the dyes neutral red, propidium iodide and Hoechst staining.

When compared on a per mM basis, controlled release of 100mM sodium butyrate via the lobster shell (7.69 mM actual release) at 24 hours ($p=0.0218$) and 48 hours (7.47 mM actual release) ($p=.0454$) resulted in statistically significant increases in protein production compared to 25mM bolus exposure. 250mM controlled release (21.86 actual release) was higher at 48 hours compared to 25mM bolus exposure ($p=0.0221$). Concurrently, cell viability for controlled release at 48hrs was 99.75% for 100mM and 99.46% for 250mM. For the bolus dose data, the viability at 48hrs was 99.70% for 5mM, 98.36% for 10mM and 93.20% for 25mM, indicating a moderating effect of controlled release on butyrate associated toxicity.

A *burst release mechanism* for the release of sodium butyrate from the shell is suggested based on release data. Meanwhile, the activation of autophagic prosurvival and anti-apoptotic pathways; which are likely to be active under the conditions of increased protein production by controlled butyrate exposure in comparison to bolus dosing, are proposed as mechanisms for improved cell survival. The study concludes that controlled release of sodium butyrate could be used to significantly improve protein yields in biologics manufacturing, and the use of reused lobster exoskeleton presents a viable vehicle for release.

1. Literature review/ Introduction

1.1 Recombinant protein production

Biopharmaceutical products represent a wide range of products including proteins, monoclonal antibodies, vaccines and blood products; they are produced using biotechnology for therapeutic and diagnostic uses (Moorkens *et al.*, 2017). Insulin was one of the first approved recombinant proteins; it was produced in the 1980s using *Escherichia coli* (*E.coli)* (Zhu, 2012). The first therapeutic protein to be produced in mammalian cells which was approved for market was human tissue plasminogen activator (tPA); this was derived from Chinese Hamster Ovary (CHO) cells in the 1980s (Wurm, 2004). Recombinant proteins are made in host cells of a different species; as the DNA encoding them has been engineered or recombined with plasmid and/or recipient host DNA they are called recombinant proteins (Overton, 2014). There are a number of possible hosts for recombinant protein production, including microbial, plant, insect and mammalian cells (Sharifi-Sirchi and Jalali-Javaran, 2016).

The process for the production of a recombinant protein involves many steps which generally follow a well-established scheme. Once the gene of interest is selected, for example GFP, codon optimisation may be carried out, as different species can have preferences for certain codons which encode the same protein. Following codon optimisation, the recombinant gene of interest is cloned into the plasmid along with a selectable marker; for example a gene for antibiotic resistance. After transfection of the gene into the cell line, the non-transfected cells are eliminated through selective culture. Only the cells which have the selection gene will survive. Eventually the clones expressing the highest amounts of protein are selected for further cultivation. From these candidates, one cell line with the appropriate growth and productivity characteristics is chosen for production of the recombinant protein (Figure 1;Wurm, 2004).

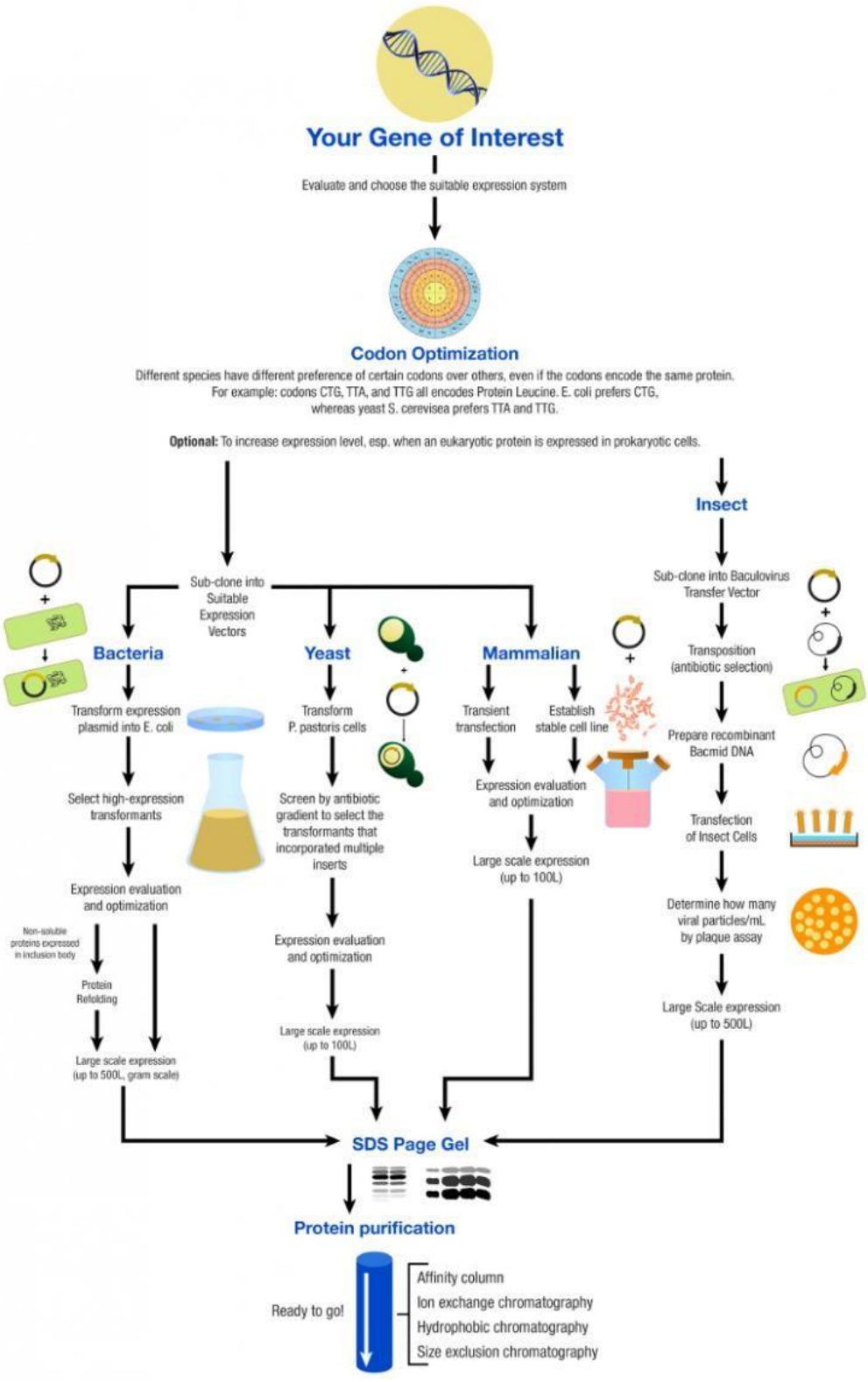

Figure 1: Overview of recombinant protein production (Rbpaonline, 2018).

1.1.2 Post-Translational Modifications

Most of the approved recombinant proteins require some form of post translational modification (PTM), (Walsh and Jefferis, 2006). Post translational modification refers to modifications of the protein after translation from mRNA to peptide by the ribosomes, and are catalysed by enzymes. There are a number of possible PTMs that occur including glycosylation, phosphorylation, sulphation, glycation, deamidation, and deamination (Figure 2) (Jefferis, 2016). Monoclonal antibodies and recombinant proteins need correct PTMs in order to have the correct structure and to be functional. Monoclonal antibodies represent today the vast majority of new therapeutic proteins, and require extensive PTMs. Mammalian cells also have the ability to correctly fold and assemble mammalian proteins along with preforming necessary post-translational modifications, and possess efficient glycosylation abilities relevant to mammalian proteins; because of this they have become the dominant system used for the production of recombinant proteins for clinical applications (Wurm, 2004; Lalonde and Durocher, 2017).

Post-translational modifications are often required for efficient secretion, drug efficacy, and stability of the recombinant protein (Jenkins, Murphy and Tyther, 2008). Production of recombinant proteins has shifted over the last number of years to production in mammalian cell expression systems.

Although the amino acid sequence of a protein is determined by the gene sequence, the structure and function are determined by the amino acid sequence and posttranslational modifications (PTMs). These PTMs are species and cell specific and are a challenge for the production of recombinant proteins (Jefferis, 2016). A substantial amount of currently approved recombinant protein pharmaceuticals need glycosylation in order to exhibit maximum therapeutic efficacy, as glycosylation can affect a number of processes at both cellular and protein levels (Solá and Griebenow, 2010). Only some PTMs are associated with recombinant proteins currently on the market (Walsh and Jefferis, 2006).

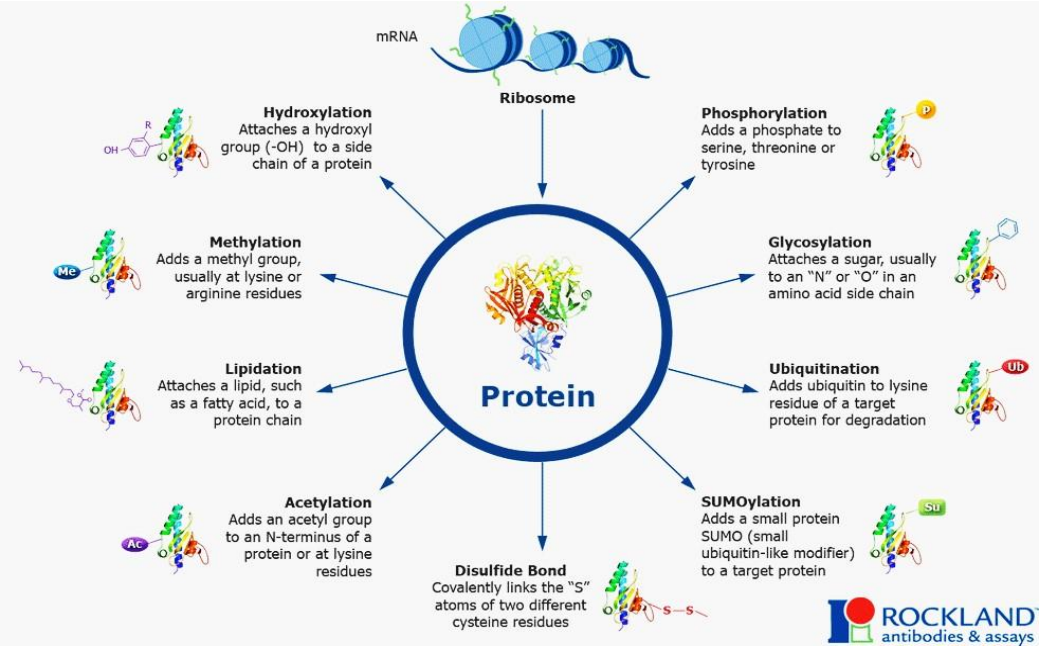

Figure 2: An overview of post-translational modifications of proteins. (Moncada, 2018).

1.1.3 Host cells

The choice of host cell for recombinant protein expression is dependent on the final protein product. Protein production in prokaryotic systems is cheaper and faster, however these systems are limited as they lack the ability to form correct post translational modifications which produce functionally active proteins (Almo and Love, 2014). *E. coli* is fast, easy and cheap to culture, however its ability to process PTMs is limited resulting in proteins that are incorrectly folded or insoluble and sometimes may result in very low or no protein expression (Ahmad *et al.*, 2018; McKenzie and Abbott, 2018). The main disadvantage of using bacteria as a host for recombinant protein production is their failure to preform PTMs in ways that eukaryotic cells can, another issue with bacterial hosts is that the protein produced will accumulate in the cytoplasm which can result in protein degradation due to the presence of proteases in the cytoplasm (Overton, 2014). Yeast can also be used for recombinant protein production, as it can produce high product titre, however the protein produced by yeast is less potent in humans and can be immunogenic (Lalonde and Durocher, 2017). Due to this, mammalian cells are a favourable host as the final product requires complex post-translational modifications (Almo and Love, 2014; Sharifi-Sirchi and Jalali-Javaran, 2016).

1.1.4 Mammalian cells

Mammalian cells have the ability to produce proteins which are biochemically similar to proteins naturally occurring in humans (Zhu, 2012). Only one third of revenue from the top selling biopharmaceutical products has come from microorganisms including yeast and *E. coli* (Zhu, 2012). Over 50% of recombinant proteins are produced in mammalian cells (Bandaranayake and Almo, 2014). Therapeutic protein drugs are now a critical component of the overall health-care industry and have revolutionized therapy options in many disease areas, due to their efficacy and targeted therapeutic design. These medications, however, are also some of the most expensive in the marketplace (Table 1; Lagassé *et al.*, 2017). For example, the recombinant drug Humira® is used to treat Rheumatoid arthritis, the cost per unit of Humira is $2,705.13 while Vimovo® which is not a recombinant drug costs per unit is $43.33. Similarly Herceptin which is a recombinant drug used for the treatment of breast cancer has a cost per unit of $1,635.49, compared to Methotrexate which has a cost per unit of $2.64 (*drugs.com*, 2019). Over the past ten years, over one hundred new biopharmaceutical products have been approved by the Food and Drug Administration (FDA) for market in both the United States and the European Union (Lalonde and Durocher, 2017). This has resulted in an increase in the demand for recombinant therapeutics which are produced in mammalian cell lines (Noh, Sathyamurthy and Lee, 2013). There are over 200 approved recombinant proteins which are FDA approved, of that about 50% are produced in mammalian cells, indicating these cells as the dominant choice in manufacturing (Zhu, 2012). In order to make protein therapeutics more affordable, it is important that the host has a high productivity and high product titre (Richelle and Lewis, 2017). Mammalian cell lines most often used to produce proteins include, CHO cells, Baby hamster kidney (BHK) and Human embryonic kidney (HEK 293) (Noh, Sathyamurthy and Lee, 2013).

Table 1: The 20 top-selling biopharmaceutical products in 2017. Financial data from La Merie Business intelligence(Walsh, 2018). Highlighted in yellow are recombinant proteins, blue are mono clonal antibodies.

Rank	Product	Sales, 2017 ($ billions)	Cumulative sales, 2014–2017 ($ billions)	Year first approved
1	Humira (adalimumab; anti-TNF)	18.94	62.6	2002
2	Enbrel (etanercept; antiTNF)	8.34	35.4	1998
3	Rituxan/MabThera (rituximab; anti-CD20)	7.78	29.1	1997
4	Remicade (infliximab; anti-TNF)	7.77	35.6	1998
5	Herceptin (trastuzumab; anti-HER2)	7.39	27.1	1998
6	Avastin (bevacizumab; anti-VEGF)	7.04	27.0	2004
7	Lantus (insulin glargine)	6.72	27.4	2000
8	Eylea (aflibercept; antiVEGF)	5.93	18.0	2011
9	Opdivo(nivolumab; antiPD-1 receptor)	5.79	11.4	2014
10	Neulasta (pegfilgrastim)	4.53	20.1	2002
11	Stelara (ustekinumab; anti-IL-12 & IL-23)	4.01	12.2	2009
12	Keytruda (pembroli-zumab, anti-PD-1)	3.81	5.7	2014
13	Prolia/Xgeva (deno-sumab, anti-RANKL)	3.54	11.6	2010
14	Lucentis (ranibizumab; anti-VEGF)	3.38	14.3	2006
15	Novolog/Novorapid (insulin aspart)	3.31	11.7	1999
16	Soliris (eculizumab; anti– C5 complement protein)	3.14	10.7	2007
17	Simponi (golimumab; anti-TNF)	2.94	9.7	2009
18	Humalog mix 50:50 (insulin lispro)	2.86	11.3	1996
19	Xolair (omalizumab) anti-IgE	2.75	8.7	2003
20	Aranesp/Nesp (darbe-poetin alfa)	2.62	10	2001

1.1.5 Chinese Hamster Ovary (CHO) cells

CHO cells are perhaps the most important host for large scale production of recombinant proteins as they are the most commonly used to date, with 7 of the 10 top selling biologics produced in CHO cells (Noh, Sathyamurthy and Lee, 2013; Harcum and Lee, 2016). As mammalian cells, CHO cells can perform complex post-translational modifications, can be readily transfected and their safety has been proven for recombinant therapeutic production (Kumar, Gammell and Clynes, 2007). In 2012, the top selling biologic was Humira, a monoclonal antibody used to treat rheumatoid arthritis, that is made in CHO cells (Almo and Love, 2014). CHO cells have also proven to adapt to grow in serum free conditions which reduces the risk of contamination from bovine serum, which results in simplified downstream processing (Bandaranayake and Almo, 2014). They also have the ability to resist human viral infections, and the quality of glycoproteins produced has correct PTMs and is compatible and bioactive with humans (Noh, Sathyamurthy and Lee, 2013; Lalonde and Durocher, 2017). As the protein production rate of CHO cells is relatively low, this contributes to the high cost of CHO cells which is of concern for the biotechnology industry as the cost of biopharmaceuticals is driven up due to this (Noh, Sathyamurthy and Lee, 2013; Harcum and Lee, 2016).

One major issue with using CHO cells and other mammalian cells as hosts for recombinant protein production is that the yield of protein from these cells is relatively low with final titres of around 100 mg/L. Over the past 20 years, there have been developments such as cell line development and media optimisation which have increased the yield of proteins from these cells. The final titre of protein has been improved and can be 1-5 g/L (Wlaschin *et al.*, 2007). In contrast the bacteria *R. eutropha* produce up to 10 g/L*, and S. cerevisiae, a species of yeast* can produce 9 g/L and another yeast species, *P. pastoris* can make 20–30 g/l of recombinant proteins (Demain and Vaishnav, 2009). While yeast and bacteria can produce higher amounts of proteins, they often lack the ability to correctly fold and modify mammalian proteins, which is why CHO cells are preferred.

1.1.6 Increasing recombinant protein production

There are currently a number of different methods which aim to improve protein yield; these include development of growth media (Huang *et al.*, 2010; Fan *et al.*, 2015), improved transfection methods, optimisation of culture conditions (Krause *et al.*, 2010) and supplementation with short-chain fatty acids (Coronel *et al.*, 2016). For example, an accumulation of lactate in mammalian cell culture can negatively impact the culture performance and restrict the production of recombinant proteins. Matthews *et al.*, (2016) found that controlling the lactate concentration in mammalian cell culture leads to improved cell viability, density and protein production. Glucose and lactate levels were monitored using a Raman spectroscopy probe, when the lactate levels dropped below the set point of 4.0 or 2.5 g/L glucose was automatically added. The automated control of lactate by restricted glucose feeding lead to an increase in protein production with the protein titre on day 13 of cultures with 85% higher protein production than the normal process.

Another approach to optimizing the media to improve expression is to supplement the cell culture media with additives which act as histone deacetylase inhibitors. Histone deacetylase inhibitors affect gene transcription, they do so by reducing the interaction between the histones and the DNA, leaving the chromatin open and leading to increased transcriptional activity of genes which can result in an increase in protein production (Almo and Love, 2014; Lalonde and Durocher, 2017).

1.2 Histones

Epigenetics refers to changes in gene expression which do not alter the Deoxyribonucleic acid (DNA) sequence. These changes are caused by epigenetic processes such as histone modification, acetylation, phosphorylation or DNA methylation (Handy, Castro and Loscalzo, 2011). One of the more significant epigenetic processes is chromatin modification (Weinhold, 2006). DNA in cells is stored in chromatin. Chromatin were first discovered by Walter Flemming in 1879, when he observed the banded chromatin in the nuclei of eukaryotic cells (Fazary, Ju and Abd-Rabboh, 2017). DNA within eukaryotic cells is packaged together with proteins; this protein/DNA complex is referred to as chromatin. Within this complex, the DNA is wrapped tightly around histone proteins to fit into the nucleus (Weinhold, 2006). As the DNA is wrapped around the nucleosome, it becomes compacted and therefore the binding sites for transcription factors on the DNA are blocked, leaving them unavailable for transcription (Berg, Tymoczko and Stryer, 2001; Weinhold, 2006). The basic unit of the chromatin is the nucleosome, this is composed of 147bp of DNA wrapped around a core histone octamer (Figure 3) (Agarwal and Weinstein, 2017).

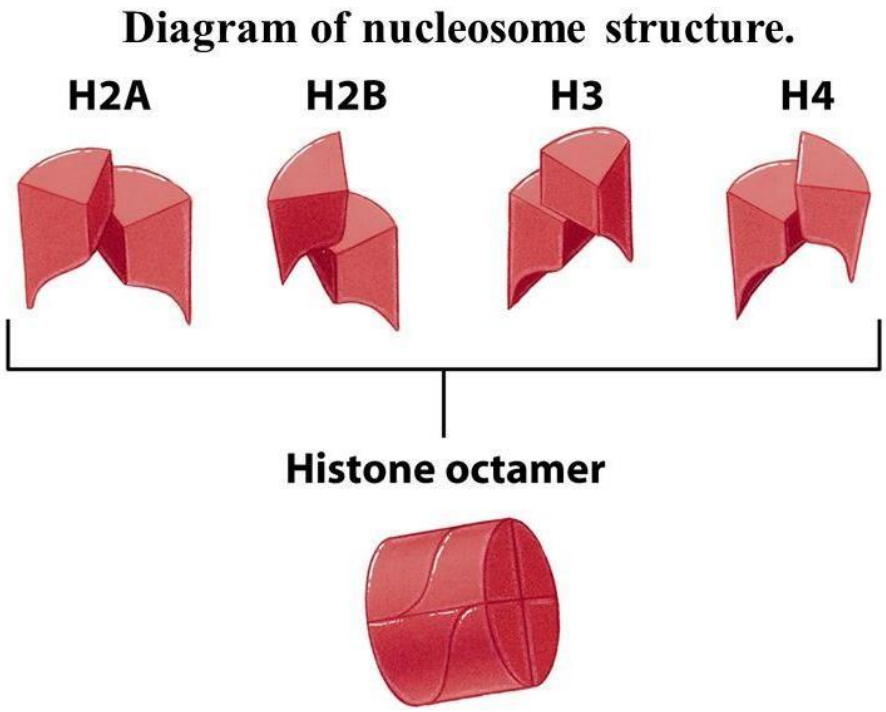

Figure 3: Histone octamer as comprised of H2A, H2B, H3, H4 (Horton *et al.*, 2006).

Eukaryotic cells have five histones, H1, H2A, H2b, H3 and H4; four of these histones, (H2A, H2B, H3, H4) form the histone octamer. In addition to these main four histones, the H1 histone is bound to the outside of the core nucleosome particle and stabilizes the chromatin structures (Figure 4) (Chrun, Modolo and Daniel, 2017). The DNA is condensed and wrapped around the octamer (Horton *et al.*, 2006). The histone octamer contains two copies of each of the four histone proteins (H2A, H2B, H3 and H4), part of these proteins remain unwrapped and form the histone tail. The histone tail makes up 20–25% of the mass of each core histone and is unstructured and flexible and protrudes from the nucleosome (Azad *et al.*, 2018). The regulation of transcription is influenced by post translational modifications of histones. (de Ruijter *et al.*, 2003). These histone tails are rich in lysine and since they protrude out of the nucleosome they are targets for post translational modifications such as acetylation, methylation, phosphorylation, ubiquitinylation, sumoylation, ADP ribosylation, and deamination, which can lead to changes in the chromatin structure (Lawrence, Daujat and Schneider, 2016).

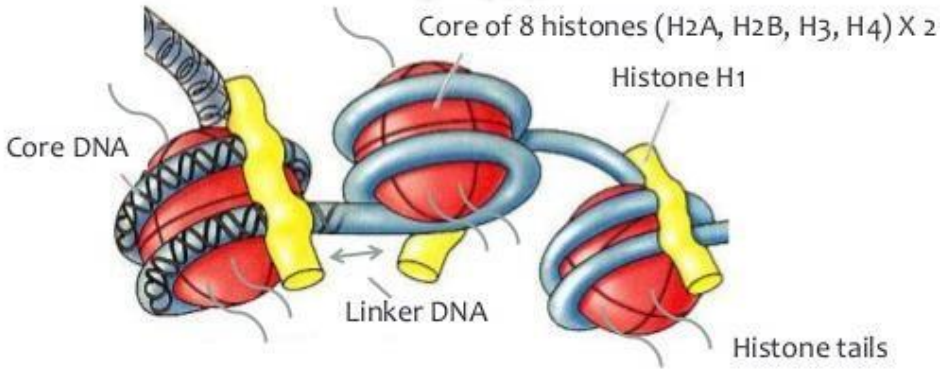

Figure 4: Nucleosome structure showing the 147bp of DNA wrapped around a complex of histones. Represented in red in the image is the histone core particle, which is made up of two copies of each of the core histones (H2A, H2B, H3, H4). Represented in yellow is the histone H1 protein binds to the linker DNA and helps to stabilize the chromatin. The histone tails can be seen in grey in the image and are the portion of the protein which remains unwrapped from the histone core (Horton *et al.*, 2006).

1.2.1 Histone acetylation

Histone acetylation is considered a very common post translational modification (PTM) and is associated with active transcription (Kouzarides, 2007). DNA interacts with the histone proteins resulting in the histones being tightly bound to the DNA preventing the DNA from being exposed; however during transcription the DNA is required to make proteins (Goodsell, 2003).

Histone acetyltransferases (HAT) is the enzyme which controls acetylation in cells (Figure 5). When chromatin are acetylated the DNA is less condensed and more relaxed, which allows DNA transcription (Chrun, Modolo and Daniel, 2017). HAT causes the DNA to relax and unwind from the histones; this is done by the addition of acetyl groups to lysine residues in the histone tail (Berg, Tymoczko and Stryer, 2001). This addition neutralises the DNA causing it to unwind leaving it more accessible for binding of transcription factors and RNA polymerase to access the DNA and transcription (Elvir *et al.*, 2017). Changes in the chromatin structure leads to the exposure of binding sites for transcription factors, this suggests that acetylation can activate transcription. As stated by Berg *et al*., 2001; this occurs due to reducing the affinity of histones for DNA, by recruiting other components of the transcriptional machinery, and by initiating the active re-modelling of the chromatin structure.

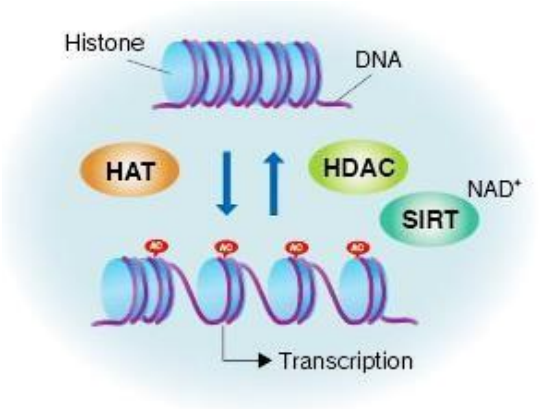

Figure 5: The top of the image is showing deacetylated DNA which is tightly wrapped around the histones supressing transcription, this deacetylation is catalysed by histone deacetylase (HDAC). Some classes of HDAC are SIRT or NAD dependant. The bottom half of the image shows acetylated DNA, here the DNA histone complex is loosened and the DNA becomes unwound allowing transcription. (MBL International, 2016).

1.2.2 Histone Deacetylation

Deacetylation is the opposite of acetylation, reversing its effects, and is catalysed by the enzyme histone deacetylase (HDAC) (Goodsell, 2003). During deacetylation HDACs, remove the acetyl groups from amino acids on the histone tail which restores the positive charge, causing the DNA to compact and become unavailable for transcription (Misztak, Pańczyszyn-Trzewik and Sowa-Kućma, 2018). Currently there are 18 different human HDACs which are divided into four classes based on their activity and homology with yeast proteins (Wang *et al.*, 2012). These include; Class I, Class II, Class III and Class IV. Classes I,II and IV are grouped together as they share a similar Zn^{2+} - dependant mechanism of action and are found mainly in the nucleus (Witt *et al.*, 2009). Class III the sirtuins are NAD+ dependant (Agarwal and Weinstein, 2017). Even though both class I and class II HDACs have a conserved HDAC domain, they have quite different characteristics; class I enzymes have similarity to yeast transcriptional regulator RDP3 and are located mainly in the nucleus (Ververis and Karagiannis, 2012). The class II HDACs share homology with yeast Hda1 and are located in the nucleus and cytoplasm. Class III histone deacetylases are nicotinamide adenine dinucleotide (NAD) - dependant and are referred to as sirtuins. The Class IV protein (HDAC11) shares sequence similarity to both Class I and II proteins (Yang and Gre, 2005).

Table 2: The different classes of histone deacetylases (Lakshmaiah *et al.*, 2014).

Group	Class	Name	Location in cell	Location in body
Classical (Zn dependent)	Class I (Rpd3)	HDAC1 HDAC2 HDAC3 HDAC8	Nucleus	Ubiquitous
	Class IIa (Hda1)	HDAC4 HDAC5 HDAC7 HDAC9	Nucleus/ cytoplasm	Tissue specific
	Class IIb (Hda1)	HDAC6 HDAC10	Cytoplasm	Tissue specific
	Class IV (Rpd3/Hda1)	HDAC11	Nucleus/ cytoplasm	Tissue specific
NAD dependent	Class III	SIRT (1-7)	Nucleus/ cytoplasm	

HDAC=Histone deacetylase, NAD=Nicotinamide adenine dinucleotide, SIRT=Sirtuin

1.2.3 Histone deacetylase inhibitors

Histone deacetylase inhibitors (HDACI) are a class of natural or synthetic chemicals that alter the function of histone deacetylases by inhibiting their function and restoring the level of histone acetylation (Mottamal *et al.*, 2015). HDAC inhibitors can be classed into groups according to their chemical structures (Table 2) (Grant and Dai, 2012). There are 4 classes of HDACI; hydroxamic acids, cyclic peptides, benzamides and short chain fatty acids (Micelli and Rastelli, 2015). The different classes vary in potency and specificity, meaning that each HDAC inhibitor will target different HDACs (Table 3) (Mottamal *et al.*, 2015). Histone deacetylase inhibitors have been identified as epigenetic modifiers due to their abilities for modulation of gene expression. Many HDAC have been shown to be involved in cancer pathways and for this reason, HDAC inhibitors have proven to be a promising family for anticancer therapies (Bertrand, 2010). As a result of this, HDAC inhibitor based therapies have gained interest for their potential use in treatment of cancers and other diseases including diabetes and heart disease (Mottamal *et al.*, 2015).The regulation of the chromatin structure and gene expression is controlled by the acetylation or deacetylation of histones; for this reason histone deacetylase is a target for epigenetic therapies (Grant and Dai, 2012).

1.2.4 HDACI Mechanism of Action

Histone deacetylase inhibitors act as epigenetic agents and although the mechanism by which they work is not fully understood, it is believed that they function by inducing acetylation and exposing sites on the DNA (Mottamal *et al.*, 2015). One mechanism by which HDACIs can affect cells is by the down regulation of antiapoptotic proteins. Apoptosis is induced in some cases by the activation of caspase proteins. HDACI's inhibit the activation of caspases by the down regulation of these anti-apoptotic proteins (Bose, Dai and Grant, 2014). Conversely HDACI's can also up regulate pro-apoptotic proteins such as Bim and Bmf; this is done through acetylation of p53 gene. Other mechanisms of HDACI include induction of cell cycle arrest, relaxation of DNA, interference with chaperone proteins and de-repression of gene transcription (Park *et al.*, 2017).

Although histone deacetylase inhibitors are believed to inhibit ZN^{2+}- dependant histone deacetylases, the inhibitors have little selectivity and can affect all members of the histone deacetylase families (Witt *et al.*, 2009). Their inhibitory effects are transient and only result in partial inhibition of activity (Haberland, Montgomery and Olson, 2009; Wang *et al.*, 2012). By disrupting the activity of histone deacetylases chromatin structure and function are altered which can subsequently affect cellular events including the cell cycle, apoptosis and differentiation (Griffith *et al.*, 2011; Mottamal *et al.*, 2015).

The largest class of HDACIs is the hydroxamic acids, this class contains suberoylanilide hydroxamic acid (SAHA) which is currently an FDA approved HDACI for the treatment of cancer (Advanced Primary Cutaneous T-Cell Lymphoma). Datta *et al.*, (2016) found that through SAHA treatment it may be partly possible to enhance the efficacy of standard chemo-/radiation therapy in head and neck squamous cell carcinoma (HNSCC). In this study, miR expression profile was used to identify the tumour suppressor miRs that are re-expressed following SAHA treatment in HNSCC. Through real-time PCR analysis it was shown that two tumour suppressors, miR-107 and miR138, were significantly up-regulated in CAL27 and SCC25 cell lines, following SAHA treatment. In the CAL27 cell line, miR-107 expression increased 3 fold with treatment of 5µM SAHA compared to the untreated control. It was also found that SAHA treatment in a dose dependent manner inhibited the cell proliferation, cell migration, and anchorage dependent clonogenic survival in CAL27 and SCC25 cell lines. Following SAHA treatment cell proliferation was decreased by 80% in CAL27 and 90% in SCC25 cells. It was found that miR suppression plays a role in progression of HNSCC, and that treatment with SAHA can increase the expression of tumour suppressor miRs, miR-107 and miR-138.

Table 3: Table of different classes of histone deacetylase inhibitors with examples, applications, potency ranges and HDAC specificity.

Class of HDACI	Example	Applications	Potency	HDAC specificity	Reference
Hydroxamic Acids	Suberoylanilide Hydroxamic Acid (SAHA)	Treat Cutaneous T Cell Lymphoma	Micro/nano molar range	Classes I and IIa	(Edelstein *et al.*, 2009)
Cyclic Peptides	Romidepsin	Treatment of peripheral T-cell lymphoma	Nano molar range	Class I	(Petrich and Nabhan, 2016)
Benzamides	Entinostat (MS-275)	Treatment of various cancers	Milimolar range	Class I	(Connolly, Rudek and Piekarz, 2017)
Short Chain Fatty Acids	Sodium Butyrate, VPA, and Phenyl Butyrate	VPA approved for epilepsy, bipolar disorders and migraine	Milimolar range	Classes I and IIa	(Eckschlage r *et al.*, 2017)

1.2.5 Short chain fatty acids as histone deacetylase inhibitors

Short chain fatty acid class members include sodium butyrate, VPA, and phenyl butyrate; these HDACI's selectively inhibit class I and IIa HDAC's (Lakshmaiah *et al.*, 2014; Qiu *et al.*, 2017). Sodium butyrate is a short-chain fatty acid that is produced by anaerobic bacterial fermentation of dietary fibers (Deacetylase and Davie, 2003). It is known that short chain fatty acids can induce a variety of changes within the nucleus, including histone hyperacetylation, and DNA methylation. Sodium butyrate treatment results in histone hyperacetylation through a non-competitive and reversible inhibition of HDAC1, a major HDAC subtype (Chen, Faller and Spanjaard, 2003). As early as 1971 sodium butyrate was considered to be a biological response modifier, meaning it had reversible effects on a number of cell processes including halting DNA synthesis, arresting cell proliferation and altering cell morphology. Uretsky *et al.*, found that in neuroblastoma cells, 0.5mM sodium butyrate inhibited the multiplication of cells after only 24 hours.

Similarly Ginsburg *et al.* (1973) have shown that XC sarcoma line cells did not change their morphological appearance in the presence of 2.5 mM of sodium butyrate, but that cell division was inhibited. Wright (1973) demonstrated that Chinese hamster ovary cells cultured in the presence of sodium butyrate (0.5 mM) show a decrease in the growth rate. Xiong, Mou and Xiang, (2015) found that sodium butyrate, could inhibit the growth of B16 melanoma by supressing tumour associated macrophage proliferation and reduce relevant pro-tumour macrophage factors expression. For the *in vitro* study, mouse melanoma cell lines-B16 were used. It was found that after treatment with 5mM sodium butyrate for 48 hours, the cell viability decreased ~25%, compared to 100% cell viability of the control. For the *in vivo* study C/57 female mice of 5-7 weeks of age were used. Sodium butyrate was injected into the mouse every other day. Tumour size was tested every 3 days. With the addition of sodium butyrate the tumour volume decreased. The most notable growth suppression was obtained when sodium butyrate was administrated at 5.0 g/kg, where a statistical significant retardation of tumour growth was observed on days 13-19 as compared with control. Sodium butyrate treated tumour volume was 300mm^3 compared to the control which was 900mm^3.

Mu *et al.*, (2013) examined the effect of sodium butyrate on viability of two human prostate cancer cell lines (PC3 and DU145). Cells were seeded at $2x10^5$ cells per well in a 24 well plate, cells were cultured at 37°C, 5% CO_2. 24hrs after seeding, a bolus dose of sodium butyrate was added to the cells (0, 5, 10mM). The cells were exposed to the sodium butyrate for 12-120hrs. It was found that the viability of both cell lines reduced in a time and dose dependant manner. At 48 hrs both cell lines had 60% cell survival compared to the control which had 100% survival. This shows the potential of sodium butyrate as an anticancer treatment and also demonstrates that adding a bolus dose of sodium butyrate negatively affects cell viability.

1.2.6 Increasing recombinant protein production using sodium butyrate

Short chain fatty acids are a class of histone deacetylase inhibitors. The most prominent members of this class are sodium butyrate, valproic acid and phenyl butyrate (Qiu *et al.*, 2017). They can induce apoptosis, by up regulating pro-apoptotic genes or down regulating anti-apoptotic genes, they can inhibit cell growth, by induction of cell cycle arrest and increase recombinant protein production in mammalian cell culture (Chen *et al.*, 2011). The addition of sodium butyrate to cell culture has been shown to increase protein production in mammalian cells (by causing the DNA to unwind from the chromatin, resulting in increased availability of binding sites for transcription), it has also been approved by the FDA for therapeutic protein production (Joon *et al.*, 2008; Sunley and Butler, 2010). Carinhas *et al.*, (2013) treated CHO cells (cultured at 37°C) with 0.75 mM sodium butyrate, samples were collected at intervals of 8-14 hours. It was found that the IgG productivity increased on average 1.5-3 fold. They noted that sodium butyrate negatively impacts cell growth by capping peak cell densities and inducing early entry of the cells into the stationary phase.

Although sodium butyrate has been shown to increase protein production in mammalian cells, they also have unwanted side effects, including apoptosis, decreased cell growth and reduced viability. Joon *et al.*, (2008) examined the effect sodium butyrate has on the gene expression in CHO cells and a mouse hybridoma cell (MAK) cells. The cells were cultured at 37°C with 1 mM sodium butyrate added to the culture. After 27 hrs gene expression was examined, 27 hr time point was chosen as this was the time before viability of the cells decreased. In CHO cells three antiproliferation genes were up regulated, along with a decrease in four anti-apoptotic genes. This result is not surprising as sodium butyrate is known to cause apoptosis. Mimura *et al.*, 2001 showed sodium butyrate increases IgG production in CHO-K1 cells (cultured at 37°C). 24 hours after cells were seeded, butyrate was added to final concentrations of 0–5 mM. It was found that antibody production was increased 2-4 fold using 0-5 mM of sodium butyrate over 13 days. The optimal concentration was determined to be 2 mM sodium butyrate which, after 13 days resulted in 4 mg/ml of antibody production compared to 1 mg/ml antibody in the control. Antibody titres were measured using ELISA. They also noted that cell viability decreased gradually as the sodium butyrate concentration increased. At day 6, cells treated with 5 mM sodium butyrate had 82% viability compared to 100% viability of non-treated cells. There have been studies which combine the addition of these HDACIs with mild hypothermia in order to attempt to prolong cell survival (Lalonde and Durocher, 2017). Chen *et al.*, (2011) examined the effect of sodium butyrate and low temperature on antibody production in CHO cells. The cells were treated with 0-5 mM sodium butyrate and cultured at 30°C and 37°C. They found an increase in antibody production at 37 °C but this resulted in dramatic reduction in cell viability. At 37 °C, after 5 mM sodium butyrate addition the percentage cell viability dropped to 40% compared to the control which had a percentage viability of approximately 100% after 72 hrs. They found that decreases in cell viability could be delayed by lowering the culture temperature. While they reported the highest antibody production of 180 mg/L at 30°C with 1 mM butyrate, compared to 100 mg/L for the control it was noted that the effect of sodium butyrate on cell growth reduced its benefits on protein production.

Similarly Kantardjieff *et al.*, (2010) cultured CHO cells with anti-apoptotic genes at 33°C; after treatment with 2 mM sodium butyrate they found a 3-fold increase in specific IgG productivity. This cell line generally produces 40 pg/cell/day of IgG,; but with treatment of 2 mM sodium butyrate at 33 °C, the IgG secretion increased to over 100 pg/cell/day (2.5 fold increase). They found the sodium butyrate to have a negative effect on peak culture density as at 118 hrs, butyrate treated cells had a peak culture density of $1.4x10^6$ cells/ml whereas the control had $1.65x10^6$ cells/ml.

A number of studies have been conducted using the addition of different short-chain fatty acids to mammalian cells with the hopes of increasing protein production. A strategy to circumvent apoptosis is to control the release of sodium butyrate. It is hoped that in this study through controlled release of the sodium butyrate the effects on apoptosis or cell death can be reduced, whilst increasing protein expression.

1.3 Controlled Release

Controlled release drug delivery is a system that delivers the drug at a predetermined rate, locally or systemically, for a specified period of time. The aims of controlled release are, protecting the drug from degradation, prolong the drugs half-life and maximise therapeutic effects of the drug (Miao *et al.*, 2018). There are a number of benefits of controlled release drugs versus conventional drug delivery, these include more effective treatment of chronic illness, prolonged efficacy, improved biological responses, a reduction in required dose level and toxicity and a reduction in side effects (Uddin *et al.*, 2011; Nayak *et al.*, 2018). As the number of recombinant proteins being used for therapeutic applications increases, the area of protein drug delivery is becoming an important area of research (Kim *et al.*, 2001). Many biologic drugs are proteins, peptides or unstable compounds which need to be protected from degradation, therefore these drugs would benefit from controlled release through an appropriate carrier (Miao *et al.*, 2018). Bolus dose addition of drugs can lead to an inconsistency in drug concentration, with a peak in drug concentration at the time of administration, followed by a decrease in drug concentration.

Controlled release can prevent this issue of inconsistent drug concentration as an appropriate concentration of drug can be released for the desired time. As seen in Figure 6 with conventional release systems, the drug levels in the plasma peak above the maximum desired level after the patient takes a dose, it then drops below the minimum effective level before the next dose. However in the controlled release system the drug level in the plasma remains at a constant level (Sasiak and Sesardic, 1997; Kohrs *et al.*, 2019).

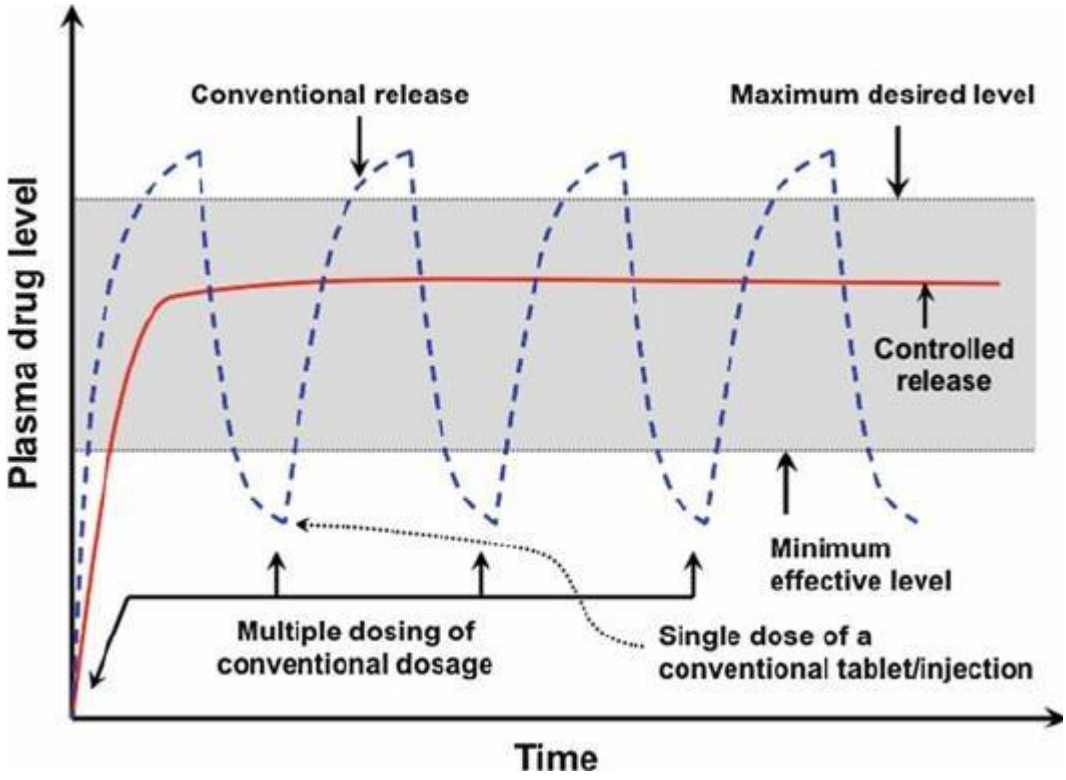

Figure 6: Drug levels in the plasma released from conventional release system, (blue dashed curve), and controlled release system (red continuous curve).

An ideal drug delivery system is one that would deliver the drug to the location needed and when required (Uddin *et al.*, 2011). Drug delivery systems allow for antibiotics, growth factors, hormones and other therapeutic agents to be delivered in a controlled manner to the required area (Kohrs *et al.*, 2019). It is important to choose the correct delivery mechanism in order to allow controlled release, the delivery system can affect the dosage and release rate (Lam *et al.*, 2015).

Some mechanisms of controlled release include, diffusion of the agent within the device, osmotic pumping, swelling, and hydrolysis (Weiser and Saltzman, 2014). Controlled release systems have been used often in bone regeneration; by controlled release of growth factors and cells, functional bone formation can be accelerated.

One of the earliest examples of controlled release was proposed in the 1960s by Judah Folkman; he determined that if he implanted silicone tubing into rabbits and ran anaesthetic gases through the tube that the rabbits would fall asleep. This was the first idea of a constant release rate drug delivery system *in vivo* (Hoffman, 2008).

In the last few decades there has been significant advances in drug delivery including the development of controlled release systems, this can be seen by the rise in the number of patents and commercial controlled release products delivering bioactive agents (Uddin *et al.*, 2011), expected to reach a 14% compound annual growth rate (CAGR) in the next 6 years (Market Watch, 2018).

Our interest in this research is to examine the use of a material to control release *in vitro*, so specifically some studies examining controlled release of molecules *in vitro* are outlined.

Nguyen *et al.*, (2015) carried out a study to examine the release of two growth factors (BMP-4 or FGF-2) from microspheres. In this study researchers incubated gelatin microspheres with varying concentrations of growth factors overnight. After incubation the tubes were centrifuged and the supernatant assayed for growth factors. This determined the loading efficiency (percentage of the drug which is adsorbed) which was found to be, on average between 69.2% and 43.9%. They measured release by ELISA, the adsorption of growth factors was determined by subtracting the amount of growth factor in the supernatant from the input amount. A plateau was observed at 50 hr with most being released at 12 hrs. They observed longer release of up to 170 hrs when they treated the microspheres with enzymes to break them down (Nguyen *et al.*, 2015).

Osswald and Kang-Mieler, (2016) demonstrated the controlled release of two bioactive anti-vascular endothelial growth factor agents (ranibizumab and aflibercept) from an injectable microsphere-hydrogel drug delivery system.

The growth factors were injected into the microspheres, which were then suspended in a hydrogel. Hydrogels, are polymer material that has the ability to swell and retain a large amount of water within its structure, but will not dissolve in water (Ahmed, 2015). Release was conducted at 37°C under mild agitation; cumulative release was measured as a percentage of the encapsulated drug. It was found that in the first 24 hours there is an initial burst release of 22.2 and 13.1 µg of ranibizumab and aflibercept respectively followed by controlled release of ranibizumab at 0.153 µg/day, and 0.065 µg/day aflibercept was released with approximately 25% of the encapsulated drug remaining trapped in the hydrogel. This shows that is it possible to have a controlled release of both growth factors for up to 196 days. Chitin and chitosan are widely studied polymers for drug release.

1.4 Chitin

Chitin is a natural polysaccharide which was first discovered in 1811 by Prof. Henri Braconnot (Hamed, Özogul and Regenstein, 2016). Chitin is a simple β-linked repeating sugar polymer which is the second most abundant natural polymer after cellulose (Chakravarty *et al.*, 2018). In its native form, chitin occurs as ordered crystalline microfibrils (Younes and Rinaudo, 2015). Chitin and cellulose have quite similar structures (Figure 7), cellulose has a hydroxyl group at C-2 while chitin has an acetamide group at C-2 (Hamed, Özogul and Regenstein, 2016). Chitin occurs naturally as three polymorphic forms: α chitin, β-chitin and γ-chitin (Duan *et al.*, 2018). The α-chitin is the most commonly found form in nature. Chitin can be found in a range of sources in nature including: insect cuticles, the cell wall of fungi, the wings of cockroaches and in the exoskeleton of crustaceans (Abdel-Rahman *et al.*, 2015).

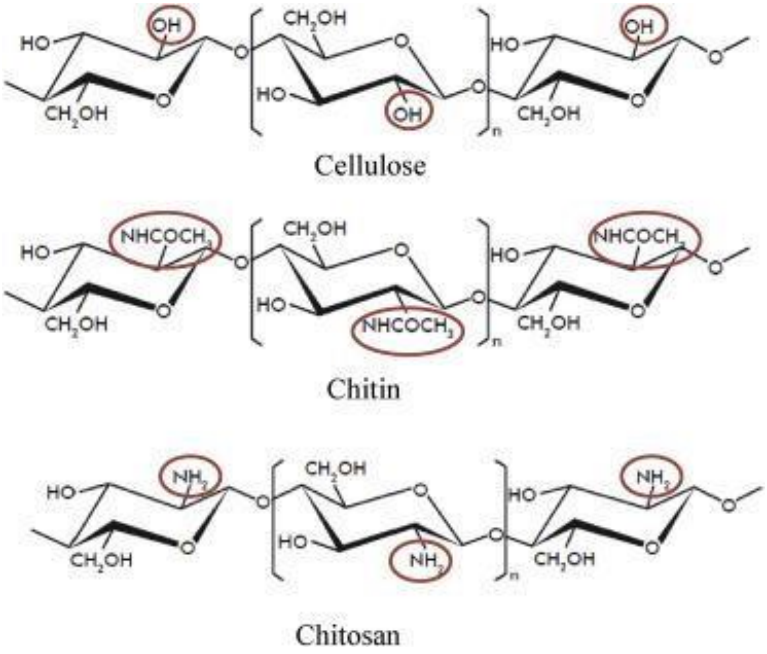

Figure 7: Comparison between the chemical structures of cellulose, fully acetylated chitin and fully deacetylated chitosan (Ramírez *et al*., 2010).

During industrial processing of crustacean shells, large amounts of waste are produced around 60% of that waste is exoskeleton of lobsters, crab and shrimp; this waste is usually dumped in a landfill which can be an environmental challenge (Asiedu *et al.*, 2017). The crustacean processing sector produces approximately 6,000 tonnes of crab waste a year (Archer, 2008). In general, it is very costly for producers of sea food to dispose of their waste, it can cost up to €60 per tonne for the waste to be sent to a landfill. If this waste was recycled by being donated or sold onto the life sciences industry, this waste exoskeleton can be used to further research and can have added value (Zhang *et al.*, 2017). In order to reuse or recycle waste from the seafood processing industry, chitin is extracted from the shells of crustaceans (Hamed, Özogul and Regenstein, 2016). In order to produce pure chitin an acid treatment is used to remove the calcium carbonate, followed by an alkaline treatment to remove proteins (Younes and Rinaudo, 2015). Samrot *et al*. (2018) collected crab shell from local fish markets and then demineralised and pulverised the shell, resulting in a chitin powder. This chitin powder was then deacetylated resulting in chitosan, which was used to make polymeric nanoparticles for drug delivery *in vitro*. Similarly (Peng *et al.*, 2019) used crab and shrimp shells and ground them to a fine powder to produce chitin nanowhiskers hydrogels for drug release.

As chitin originates from the exoskeleton of crustaceans, it is associated with many proteins, minerals and pigments, all of which must be removed by deproteinization in order to obtain a high purity chitin for biomedical applications (Abdel-Rahman *et al.*, 2015; Soon *et al.*, 2018). This extraction of chitin produces a compound with applications in a number of fields, including the food industry, pharmaceuticals and medicine, including tissue engineering (Hamed, Özogul and Regenstein, 2016).

1.4.1 Chitin properties

Chitin has many properties which make it appealing for biomedical applications. These include acceleration of wound healing and suppression of tumour cell growth, food, agriculture, medicine, pharmaceuticals and water purification (Hassainia, Satha and Boufi, 2018). It is also non-toxic, biocompatible and biodegradable, flexible, durable and bioresorable (Chakravarty *et al.*, 2018). Chitinases are enzymes which degrade chitin , as chitinases are widely found in nature (in bacteria and in digestive systems of numerous animals) (Rinaudo, 2006). Chitin and its derivatives, including chitosan are renewable, biocompatible, biodegradable and non-toxic. They have a wide range of biomedical applications including artificial skin, bones, cartilage regeneration and drug delivery (Hamed, Özogul and Regenstein, 2016). While chitin has a number of desirable properties it is not soluble in most solvents or water and this results in chitin being underutilised (Chakravarty *et al.*, 2018).

1.4.2 Chitin fibres

Chitin fibres are being developed for biomedical applications including controlled drug release and wound dressings, these fibres are favourable to use due to the fact that they are non-allergenic, deodorizing and antibacterial (Rinaudo, 2006). They also have remarkable mechanical properties combining toughness with strength (Ling *et al.*, 2018). Due to the low cost, availability and biocompatibility of biopolymer nanofibrils they have gained attention in research over recent years. Chitin nanofibrils can be moulded into different shapes; this is a valuable propriety with regards to bone tissue engineering as different shaped materials will help attachment and proliferation of osteoblast cells (Ling *et al.*, 2018).

For use in bone tissue engineering, generally chitin nanofibrils are blended with calcium minerals, resulting in improved biochemical and mechanical properties (Ling *et al.*, 2018). Kawata *et al.*, 2016 have used chitin nanofibrils as templates for mineralization of calcium phosphate crystals; this resulted in accelerated differentiation of osteoblasts in subcutaneous tissue of rats.

Chitosan is a partially or fully deacetylated form of chitin (Sayari *et al.*, 2016). Chitosan is rarely found in nature, however it can be found in the mycelia, stalks and spores of some yeast and filamentous fungi (Liaqat and Eltem, 2018). The annual production of chitosan is estimated to be several gigatons, most of this chitosan is obtained from the deacetylation chitin (Liaqat and Eltem, 2018). Chitosan has applications in a wide range of areas including pharmaceutical and medical applications, paper production, textiles, wastewater treatment, biotechnology, cosmetics, food processing, and agriculture(Lim and Hudson, 2003). Chemical deacetylation with an alkali solution is performed on chitin to produce chitosan, which is the most common chitin derivative (Sayari *et al.*, 2016; Liaqat and Eltem, 2018). The amount of acetylation of the D-glucosamine unite is used to identify chitin and chitosan. Chitin and chitosan are very similar in structure, they vary in the fraction of acetylated repeating units (Figure 8) (Wan and Tai, 2013). Unlike chitin, chitosan is soluble in organic acid solutions and in dilute acids with a pH below 6 (Abdel-Rahman *et al.*, 2015; Liaqat and Eltem, 2018).

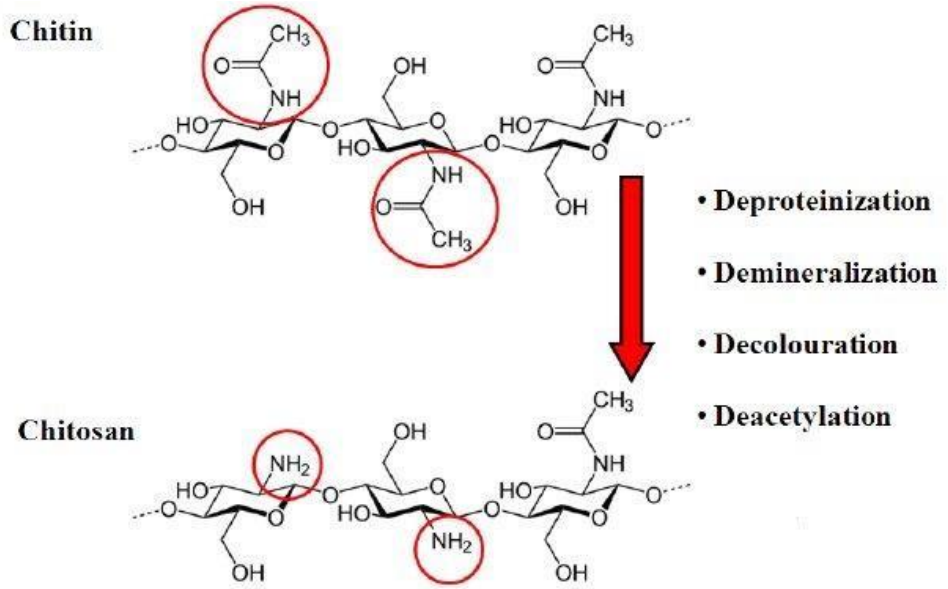

Figure 8: Molecular structures of chitin and chitosan. (Tran *et al*., 2011).

1.4.3 Chitosan properties

Chitosan has been a more widely studied material for controlled release and due to its similarity with chitin, a review of chitosan is presented here. Chitosan also has very good properties in terms of biomedical applications, including adsorption, filmforming and antimicrobial properties (Abdel-Rahman *et al.*, 2015). Chitosan is biocompatible, biodegradable and antimicrobial. Due to these properties chitosan is attracting attention as a component of wound dressing and is widely used as a biomaterial (Wan and Tai, 2013; Abdel-Mohsen *et al.*, 2016). Chitosan is popular as it can be processed into many different forms, from gels to fibres, however another reason for its popularity is that it can be mixed with both natural and synthetic polymers, which can lower the cost and improve its properties (Archana, Dutta Kumar and Dutta, 2015). In recent years chitin and chitosan have gained attention for use in biomedical applications, with studies being carried out on its potential use in drug delivery, treatment of optical and colon diseases (Elgadir *et al.*, 2015).

1.4.4 Chitin as controlled release matrices

Chitin and chitosan can be used for controlled drug delivery in the form of modified hydrogels. These hydrogels can be used for applications including drug delivery and tissue engineering systems while some polymers used for chitosan modification include gelatin, starch and polyethylene glycol (Giri *et al.*, 2012). The naturally porous structure makes chitin an attractive material for controlled release of drugs, as found by previous work in this laboratory the pore size to be 2-3µm in diameter and an approximate visual estimation shows porosity to be 50%.

The pore size of our lobster samples can be classed as mesoporous as the width of mesopores are classified as between 2 and 50 nm; it has been reported that mesoporous materials can increase the availability of poorly soluble drugs and also influence the amount of drug loading (Ahuja and Pathak, 2009). Recently there has been increasing interest in the use of porous materials as carriers for the controlled release of drugs, as the presence of pores provide sustained release systems (Ahuja and Pathak, 2009). Work by Pastor *et al.*, 2011 using mesoporous silicon microparticles, found that with an average pore size of 35 nm and porosity of approximately 50%, that the release of their proteins was quite fast with over 80% release in under two hours. In subsequent work Pastor *et al.*, 2015 examined the effects of tailoring pore size on controlled release, with all samples having much smaller pore sizes. Samples with a pore size of more than 10 nm reached 100% release after 24-48 hours, however samples with a smaller pore size of 6 nm sustained release for more than 96 hours. They found that burst release was reduced in samples with the smaller pore sizes (below 10 nm) compared to the previous study where the pore size was 35 nm. This shows the importance of pore size for materials to be used in controlled release mechanisms.

One example of a chitin controlled release system is porous chitin microspheres developed by Wang, Li and Li, (2017) for colon specific delivery of anthocyanins. Anthocyanins are compounds found in fruit and vegetables and have gained interest over recent years due to their beneficial properties including antioxidant activity, anti-inflammatory effects and anticancer effects, especially in the colon. Microspheres of chitin (80 µm diameter) were loaded with anthocyanins.

These spheres have a maximum loading capacity of 2718 mg/g. It was found that at a pH of 1.2, only 25% of the loaded anthocyanins were released, possibly due to a strong hydrophobic interaction between the chitin and the anthocyanins. When release was carried out *in vitro* under stimulated stomach conditions 37% of the loaded anthocyanins were released after 2hrs. In an attempt to slow the release of the anthocyanins the microspheres were coated with ethyl cellulose. The release for the coated microspheres was found to be 8% at 2hrs under stimulated stomach conditions. This coating must be digested when it arrives at the colon which results in a slower release compared to the non-coated spheres. Similarly, Shang *et al.*, (2014) formulated cross-linked chitin microspheres (300 µm diameter) for the pH controlled release of vancomycin. Scanning electron microscopy (SEM) of the microspheres showed a honeycomb-like structure with a pore size of 100 µm (Figure 9). It was found that at a pH of 7.4 it took only 10 minutes for 100% of the drug to be released compared to 30 hr release at lower pH of 4.0 and 1.2 for release of 90% of the drug. When the microspheres were cross-linked with chitosan the release at pH 7.4 was extended from 10 minutes to 10 hrs.

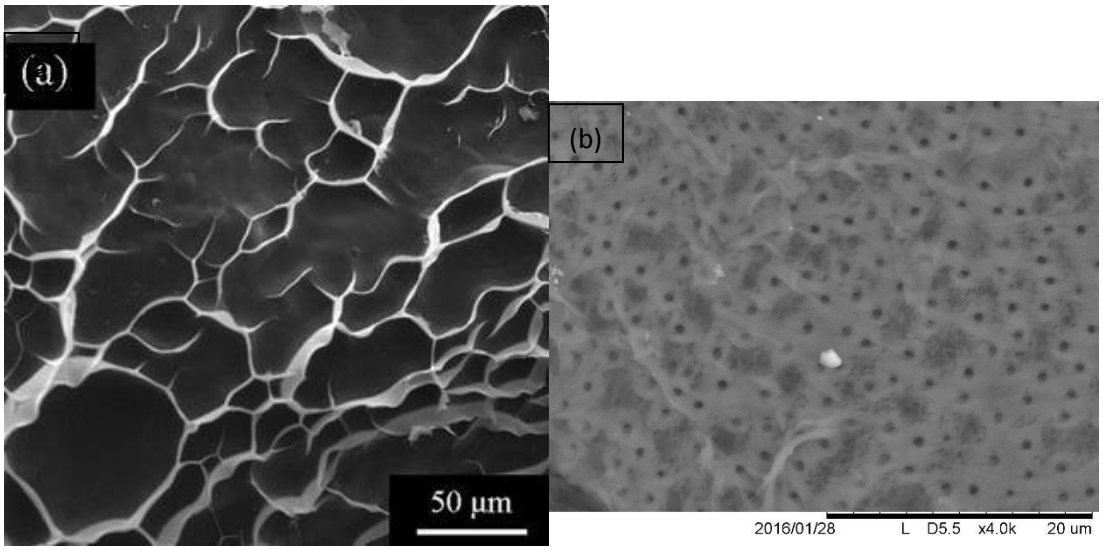

Figure 9: (a) scanning electron microscopy (SEM) images of the ferric crosslinked acrylamidemodified chitin microsphere with a pore size of 100µm from Shang *et al*., (2014). (b) scanning electron microscopy (SEM) images of the lobster claw sample used in this research with a pore size of 2-3µm in diameter.

1.4.5 Chitosan in drug delivery

Due to its unique structure chitosan is a promising candidate for specific drug targeting and delivery (Puvvada, Vankayalapati and Sukhavasi, 2012). Chitosan gels are frequently used for controlled release of proteins and drugs (Rinaudo, 2006). Chitosan is used for sustained release as a drug carrier matrix for the gastrointestinal targeted drug Naproxen (Bernkop-Schnürch and Dünnhaupt, 2012). Chitosan based systems also have potential to be used in nasal drug delivery and topical eye treatments (Bernkop-Schnürch and Dünnhaupt, 2012). Teijeiro-Osorio *et al*. (2009) studied the use of chitosan and cyclodextrin nanoparticles in nasal delivery of insulin in rabbits. Their results showed significantly decreased plasma glucose levels in rabbits, proving that these nanoparticles have potential for improving movement of complex molecules across the nasal barrier. Fisher *et al.* (2010) carried out a study in 18 human volunteers to evaluate fentanyl nasal spray formulations with chitosan and chitosan-poloxamer 188. It was found that the systemic exposure significantly improved and times to peak plasma values decreased. Na *et al.* (2010) conducted a study on co-administration of chitosan with isosorbide dinitrate (used to treat angina pectoris) this showed significant improvement in nasal uptake of the drug in rats. Chitosan is used in many types of drug delivery including oral, parenteral, nasal, transdermal and topical (Puvvada, Vankayalapati and Sukhavasi, 2012).

Chitosan, owing to its mucoadhesive nature, is gaining interest for use in the controlled release delivery of oral drugs (Kumar, Vimal and Kumar, 2016). As chitosan molecules are positively charged and mucosal surfaces are negatively charged this results in a strong electrostatic force between chitosan and the mucosal surfaces. The gastrointestinal tract (GIT) is a harsh environment for drugs, especially protein drugs, this is due to digestive enzymes and shifting pH (Kumar, Vimal and Kumar, 2016). Chitosan can protect the drug from this harsh environment due to its mucoadhesive nature and permeation enhancing effects (Kumar, Vimal and Kumar, 2016). By incorporating acyclovir (used to treat herpes simplex virus infections) with chitosan and thiolated chitosan Dhaliwal *et al.*(2008) improved the oral bioavailability of the drug by 3-fold and 4-fold respectively.

The research presented in this thesis aims to exploit the use of chitin as a delivery vehicle, which has already been described, but also to use a novel approach in harnessing the intricate architecture already supplied by the chitin lobster exoskeleton as a depot for controlled release.

1.5 Exoskeleton of anthropods/ crustaceans

1.5.1 Exoskeleton

Crustaceans are part of a group within the arthropod family. They can be marine or land dwelling species (Boßelmann *et al.*, 2007). All arthropods have an exoskeleton, which is their tough outer shell, it provides movement and mechanical support to the body but also to provides protection from predators (Raabe *et al.*, 2006). A lobster's first line of defence against parasites and pathogens is its chitin-containing exoskeleton. (Davies *et al.*, 2014). It is believed that the exoskeleton was essential to the arthropods' evolutionary success. The American lobster is a large crustacean, whose body can be divided into the head, thorax and the tail (Figure 10) (Raabe, Sachs and Romano, 2005).

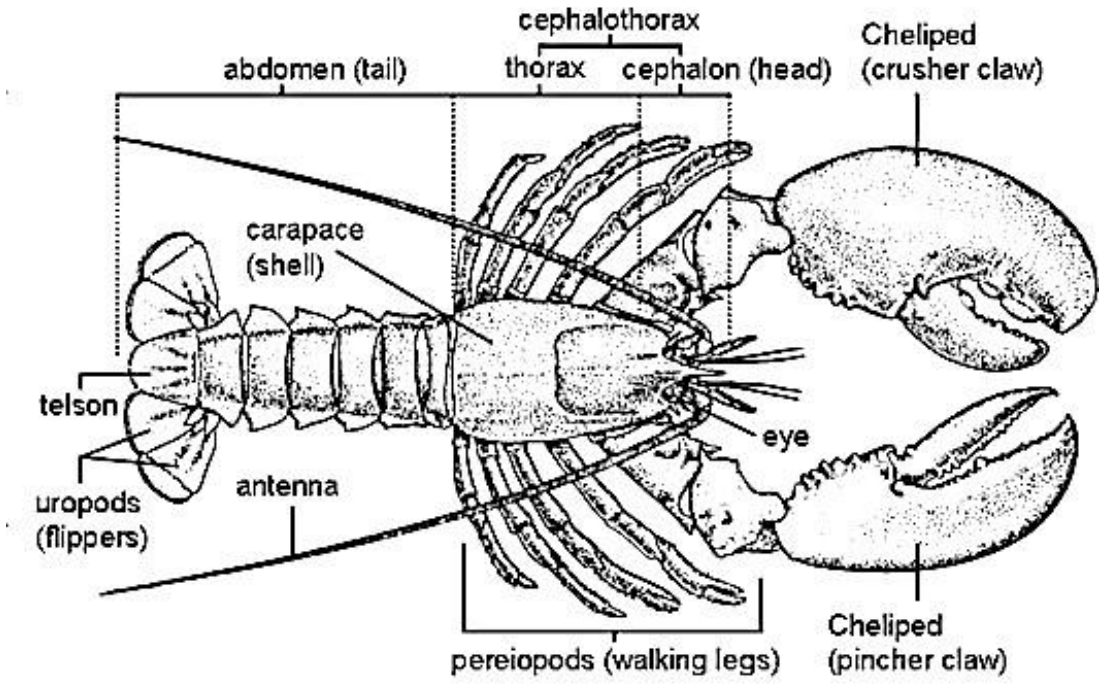

Figure 10 : Dorsal view of Homarus americanus. The schematic overview depicts the main body parts of the American lobster. (Raabe *et al*., 2006).

1.5.2 Exoskeleton composition

The exoskeleton is made up of multiple layers containing mineralized, fibrous, chitinbased tissue (Raabe, Sachs and Romano, 2005). Arthropod exoskeletons have a welldefined hierarchical organization, this shows off their different structural levels (Chen *et al.*, 2008). The cuticles of the lobster generally acts as an exoskeleton, which provides mechanical support to the body as well as allowing movement through the joints (Romano, Fabritius and Raabe, 2007). Most arthropods cuticles have two main layers that are secreted by a single layer of epidermis cells. This includes 1) an outer epicuticle, and 2) a pro cuticle which is comprised of the outer exocuticle and inner endocuticle and a thin membranous layer (Figure 11) (Coffey *et al.*, 2017).

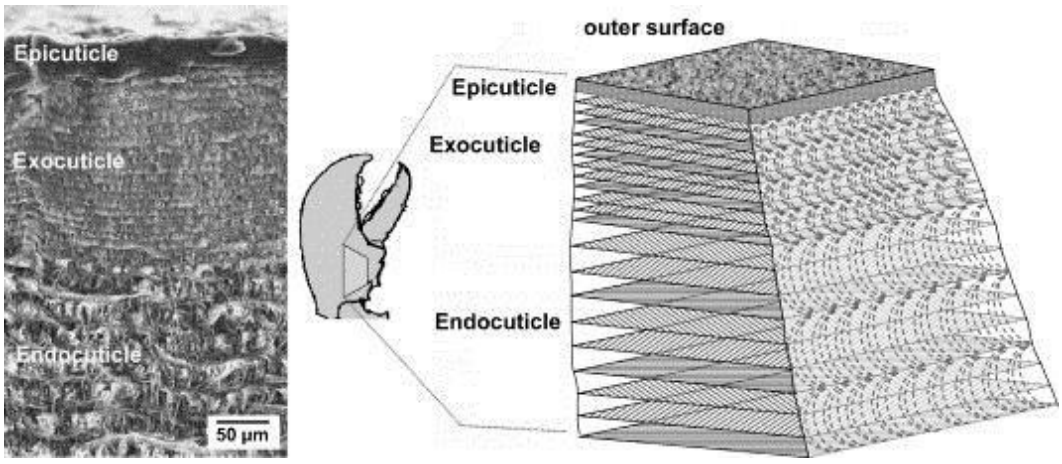

Figure 11: The organization of the cuticle of Homarus americanus, SEM (scanning electron microscope) micrograph of a cross section through the cuticle of a cheliped and schematic representation showing the layers of the cuticle. The outer epicuticle, and a pro cuticle which is comprised of the outer exocuticle and inner endocuticle (Sachs, Fabritius and Raabe, 2006).

1.5.3 Epicuticle

The epicuticle is the outer layer, which contains a lipoprotein layer for protection and a waterproof waxy layer and a protein layer referred to as a cuticulin (Davies *et al.*, 2014). The outermost layer is the epicuticle, this is a thin waxy layer which acts as a diffusion barrier to the surroundings (Raabe, Sachs and Romano, 2005). The epicuticle provides a permeability barrier to the environment.

1.5.4 Procuticle

The procuticle is the layer that provides mechanical support and can be sub-divided into the exocuticle and endocuticle. In the lobster exoskeleton, the highest level in the hierarchical organization is the epicuticle and the procuticle (Sachs, Fabritius and Raabe, 2008). The procuticle is under the epicuticle and is the main structural part of the exoskeleton and designed to resist mechanical loads (Chen *et al.*, 2008). The procuticle is thicker and is made up of a lattice of protein and chitin (Davies *et al.*, 2014). The layers within the procuticle carry the mechanical loads and are made up of hard mineralised fibrous chitin-protein tissue. The sub layers of the procuticle are both made up of mineralised chitin-protein fibres, which forms a twisted plywood structure, different rotation angels result in different thickness in the endocuticle and exocuticle (Sachs, Fabritius and Raabe, 2007).

1.5.6 Endocuticle and exocuticle

The mineralised exocuticle and endocuticle are composed of chitin-protein nanofibrils which are grouped into fibrous bundles (Coffey *et al.*, 2017). The outer exocuticle and the inner endocuticle have a similar structure and composition (Chen *et al.*, 2008). The outer part of the endocuticle is calcified and the inner layer is not, the inner layer is in close association with the underlying single layer epidermal cells that secrete the cuticle (Davies *et al.*, 2014). Approximately 90% of the volume of the exoskeleton is made up by the endocuticle (Chen *et al.*, 2008). The exocuticle has a very fine woven structure which is made up of a matrix of the fibrous chitin-protein; this gives a twisted plywood structure (Figure 12). The structure of the endocuticle is a much coarser twisted plywood structure (Raabe, Sachs and Romano, 2005). From micrographs taken by Romano, Fabritius and Raabe, (2007) it be seen that the twisted plywood structure of the exocuticle is more densely packed than the endocuticle (Figure 12).

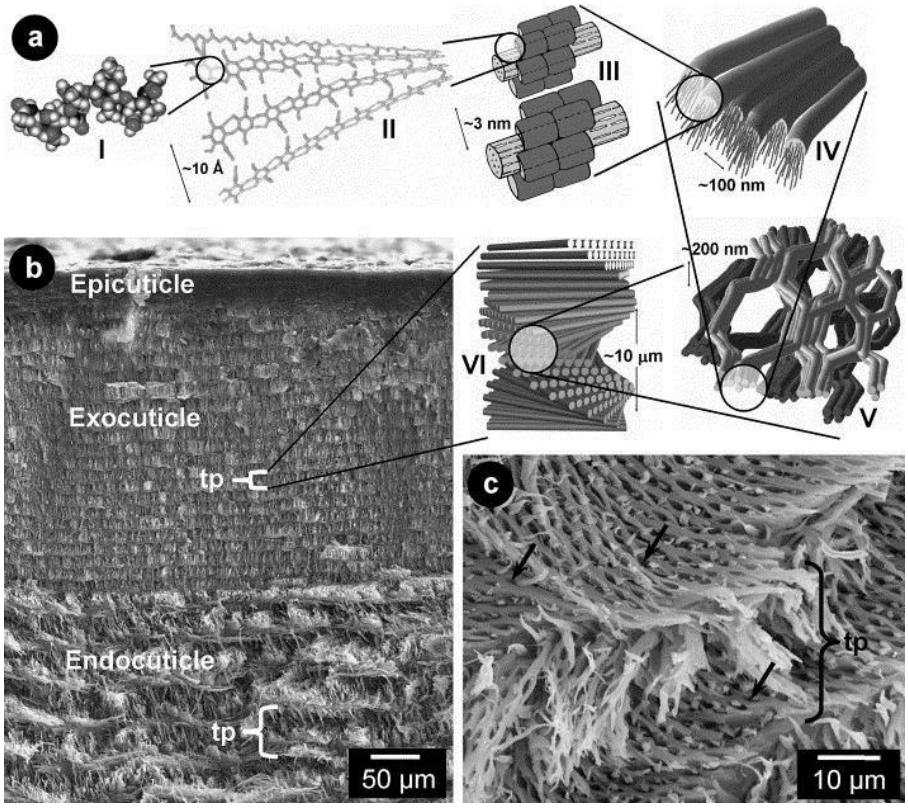

Figure 12: Microstructure of lobster cuticle. (a) Schematic representation of the different hierarchical levels in the microstructure of lobster cuticle. (b) SEM micrograph showing a cross-section through the three-layered cuticle.(c) SEM micrograph of obliquely fractured endocuticle displaying two superimposed twisted plywood layers (tp) and showing their typical honeycomb-like structure. The arrows indicate the pore canals (Romano, Fabritius and Raabe, 2007).

Each layer in the procuticle is made up of chitin planes. Once one of these planes completes a 180° rotation it is referred to as a Bouligand structure. These structures repeat to form the exocuticle and the endocuticle. The endocuticle is thicker than the exocuticle, due to the thickness of the Bouligand layers, this results in denser packing of Bouligand layers in the exocuticle (Coffey *et al.*, 2017). This same Bouligand structure can also be found in collagen networks in compact bone and in cellulose fibres in plant cell walls (Chen *et al.*, 2008). Bones and cellulose both have this structure naturally present to facilitate the movement of proteins, nutrients and ions, this same structure in lobster is also good for the movement of ions and proteins, it is hoped this will allow for the movement and release of sodium butyrate.

The brittle chitin-protein bundles are arranged in a Bouligand pattern with ductile pore canal creating a 3D composite (Chen *et al.*, 2008). Many skeletal tissues found in nature are composite materials with associated organic fibrils and mineral particles where the fibrous matrix is first deposited and then orientates the subsequent mineral nucleation and growth (Romano, Fabritius and Raabe, 2007).

After the lobster moults, ions and nutrients need to be transported for the formation of the new exoskeleton. This is done through the pore canals, these pore canals are well-developed, of high density and contain long flexible tubules which penetrate through the exoskeleton (Chen *et al.*, 2008). The presence of a well-developed pore canal system is characteristic of the lobster cuticle; many of these canals penetrate the twisted plywood structure perpendicular to the surface. A honeycomb like structure is developed by the presence of the periodically arranged pore canal system.

To look at the exoskeleton at a molecular level we first see a long chain of polysaccharide chitins that form fibrils (Figure 12). The fibrils (3nm diameter, 300nm long) then wrap with proteins to form fibres which are approximately 60nm in diameter. These fibres are than assembled into bundles, which arrange themselves parallel to each other forming planes. Alpha chitin is the most abundant of the three crystalline chitin polymorphic forms occurring in nature (Raabe, Sachs and Romano, 2005). Long chitin molecules are the smallest subunit in the lobster cuticle. Between 18-25 chitin molecules form nanofibrils which are approximately 300 nanometres long and have a diameter of about 2.5 nanometres which are wrapped by proteins. The protein wrapped chitin nanofibrils cluster forming long chitin protein fibres that are arranged parallel to each other forming horizontal planes (Romano, Fabritius and Raabe, 2007). It is envisioned that the pore canal system will act as a conduit for controlled release of sodium butyrate, the short chain fatty acid.

Scanning Electron Microscopy (SEM) analysis of lobster shell samples previously conducted in this laboratory by Patton, 2014 showed that the samples all maintained the structural characteristics of the raw samples after demineralisation.

It was noted that the structure of the lobster samples remains apparent after demineralisation, with the pore structure remaining clearly defined, therefore showing negligible effects of demineralisation on porosity and pore size, this is also supported by further SEM work in our laboratory by Thornton, 2016. Lobster shell is an industrial waste product. Owing to it's natural properties, we aimed to investigate a novel use for this waste product.

1.6 Short chain fatty acid controlled release

As previously mentioned, sodium butyrate can increase protein production, however it affects cell growth, viability and apoptosis. It is possible that through controlled release, this can be rebalanced in favour of recombinant protein production and greater cell viability. Roda *et al.*, (2007) evaluated the controlled release of sodium butyrate in the ileocecal region and the colon, for extended delivery of sodium butyrate. Sodium butyrate tablets containing 10% weight/weight of C-sodium butyrate and coated with shellac (shellac is a natural polymer resin obtained from the secretions of lac bugs (Baek *et al.*, 2018)) (80µm thick), were given to 24 subjects (12 healthy and 12 with Crohn's disease). The rate of C-sodium butyrate adsorption was measured by CO_2 breath test analysis. Breath samples were taken every half an hour for 8 hours. For the uncoated tablet breath tests, the maximum excretion was reached 45 minutes after administration of the tablet. For the coated tablets, the maximum excretion time was 180 minutes, showing the extended release of two to three hours, of sodium butyrate from the shellac coated tablets. Valproic acid, which is in the same family as sodium butyrate, also has applications in treating a number of diseases. However, its poor bioavailability and systemic side effects limit its use for long term treatment. Through controlled release of valproic acid using implants, these issues can be overcome (Uddin *et al.*, 2011). Uddin *et al.*, (2011) have carried out *in vitro* studies on the controlled release of valproic acid (VPA) using a titania ceramic matrix. The VPA was released into methanol for a period of 800 hrs. The initial release up to 100 hrs is a fast release with release slowing down and equilibrating after this. The pellet was loaded with 30.3 mg VPA; by 100 hrs approximately 0.20 mg/ml was released, after 100 hrs there was steady release of 0.25 mg/ml VPA.

The total amount of VPA released was 22% of the concentration loaded. This paper had no control, but one could assume that if this was compared to a bolus dose of VPA that the total 30.3 mg/ml of VPA would instantly be released compared to the controlled release which results in a steady release of 0.25 mg/ml VPA released over a period of 800 hrs.

The aim of this research is to investigate the controlled release of sodium butyrate onto a CHO-K1 cell clone which is expressing a recombinant form of insulin, fused to a GFP reporter molecule (CHO-k1 INS/GFP cells). The controlled release system is demineralised lobster shell claw (chitin).

The chitin shell has naturally occurring pores (~500 nm) and pore channels. It is hypothesised that once the shell is loaded with the sodium butyrate, that the shell will allow for controlled release through the pores harnessing the pore channel transport system existing in the exoskeleton. It is hypothesised that release of butyrate will be controlled over a longer period of time and enhance the recombinant protein production while minimizing cell toxicity. The choice to use sodium butyrate for increased protein production was supported by examples in the literature discussed previously showing sodium butyrate increases protein production (Sung *et al.*, 2004). Previous experience in this laboratory has shown sodium propionate to be inefficient at increasing protein production (McCabe, 2015). An alternative short chain fatty acid, valproic acid is sometimes used for increasing protein production however it has been shown to have negative effects on cell viability at concentrations as low as 1 mM (Catalano *et al.*, 2005).

2 Materials and methods

2.1 CHO-K1 cell culture

CHO-K1 cells were obtained from the American Type Culture Collection (LGC standards, UK). CHO-K1 cells were previously transfected with the plasmid pReceiverM03 containing the open reading frame for a human insulin-GFP fusion protein (Genecopiea, USA). CHO-K1 cells were transfected using lipofectamine 2000 (Life Technologies, UK) and selected using G418 sulphate (Sigma, UK) (unpublished data). This transfected cell line was designated CHO-K1 INS/GFP.

CHO-K1 INS/GFP were routinely cultured in MEM medium (VWR, cat. No L0415-500) supplemented with 10% foetal bovine serum (Fisher Scientific, cat. no 10270106) and 1% penicillin-streptomycin (Thermo Fisher, cat. No. 15140122). Cells were maintained at 37°C and 5% CO_2/95% air in a fully humidified atmosphere in a New Brunswick Galaxy CO_2 Incubator (Eppendorf).

2.2 Sodium Butyrate preparation and addition

Sodium butyrate (98%) (Sigma Aldrich, cat. No. 303410) was dissolved in 1X PBS (Fisher Scientific, cat. No. 1282-1680) to a concentration of 1000 mM. This was then diluted further to the working concentrations of 5, 10, 25, 50, 100 and 250 mM. Sodium butyrate was prepared fresh on the day of each experiment. Cells were exposed to a range of concentrations for a set time period dictated by the particular experiment.

2.2.1 Bolus dose Sodium butyrate

To check that sodium butyrate does increase protein production, cells were incubated with increasing concentrations of sodium butyrate (0-250mM). The effect of sodium butyrate on protein production was determined by measuring insulin/GFP protein production by quantifying GFP. Fluorescent (GFP) analysis was used to determine amount of protein produced. Three independent experiments were performed.

CHO-K1 INS/GFP cells were seeded in triplicate at a concentration of $2.5x10^3$ cells per mL in a 24 well plate (Iwaki, cat. no. 3820-024) in 1mL of MEM. Cells were cultured at 37°C in 5% CO_2 and allowed adhere for 48 hrs. Following cell adherence, medium was removed and 1mL fresh medium with or without sodium butyrate was added. The cells were exposed to the sodium butyrate for 4, 8, 24 and 48 hours. At each time point, the media was removed, and the cells were stained using fluorescent viability stains, using the staining procedure as outlined below.

2.3 Cell Viability

The viability for the cells was calculated through analysis of fluorescent images taken during the experiments (Figure 13).

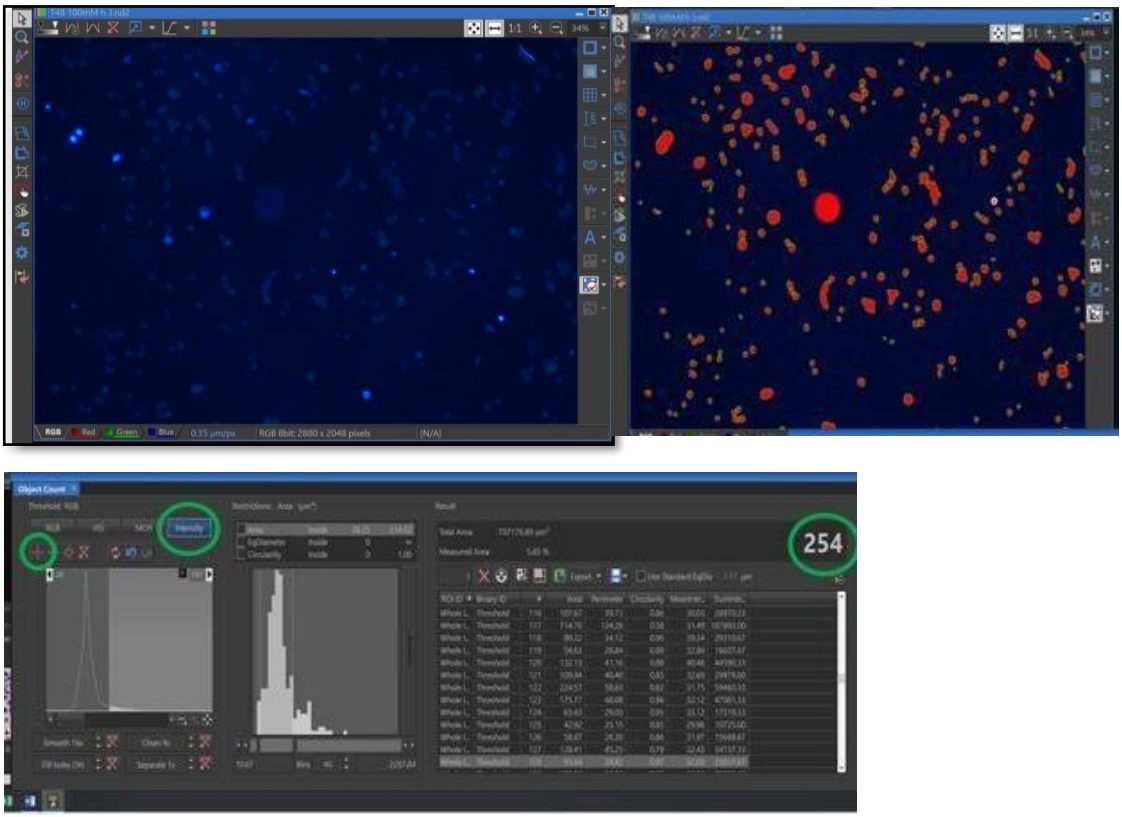

Figure 13: Screenshots from Nikon analysis. Starting with the original image, right click to bring up analysis controls and select object count as performed for GFP cells.

Once the cells are selected you can adjust which cells are selected. For example, in this image the large red circle is not a cell so that can be selected and removed from the count. You can see here there are 254 cells in this sample. The same process is done with the cells stained with propidium iodide (PI). Once image analysis has been completed, the results of both hoechst and PI stained cells are analysed to get percentage viability. The blue cells (hoechst) equal total cells and the red cells (PI) are dead. Taking the number of the dead cells away from the total cells gives number of live cells. Live cells divided by total cells multiplied by 100, gives percentage viability.

2.4 Fluorescent staining

Fluorescent stains were used in order to measure the number of dead cells and the total number of cells. Hoechst stain 33258 (Sigma Aldrich, cat. no. 94403) is a blue dye used for fixed- and live-cell fluorescent staining of DNA and nuclei in cellular imaging techniques. Propidium iodide (PI) (Sigma Aldrich, cat. no. P4864) is a popular red-fluorescent nuclear and chromosome counterstain; it is also commonly used to detect dead cells in a culture.

To stain the cells, the dyes were made up to a final volume of 2 mL in sterile 1X PBS (Fisher Scientific, cat. no. 1282-1680), with 10 µl hoechst and 2 µl PI giving a final concentration of 5 µg/ml hoechst and 1µg/ml PI. The dyes were made up immediately before use (the eppendorfs used to prepare the dyes were covered in tinfoil to protect the dyes from the light).

Before adding the dyes, media was removed from the cells, each well was then washed three times with 1x PBS (500 µl each). 300 µl of dye solution was added to each well and incubated at 37°C for 20 minutes. Following incubation, the stain solution was removed and the cells were washed twice with PBS (300 µl each wash). A small amount of PBS was left on the cells to prevent them drying out during fluorescent imaging. Images of each well were taken using a Nikon eclipse Ts2 fluorescent microscope. For each sample, an image was taken in phase contrast, green filter (GFP), blue filter (hoechst) and red filter (PI). Images were analysed using Nikon basic research package.

Following staining, the cells were viewed under a fluorescent microscope and the images were later analysed using ImageJ software (this method of analysis for protein production has been validated by comparing an ELISA with ImageJ analysis for the measurement of protein production – Figure 17).

2.5 ELISA preparation

Increasing numbers of cells were seeded in triplicate onto a 24 well plate, $1x10^3$, $2.5x10^3$, $5x10^3$, $1x10^4$, $2x10^4$, in 1 mL media. After 24 hrs, fluorescent GFP images of each well (1 image per well) were captured and analysed using ImageJ analysis. Image J measured the amount of fluorescence per cell. Following imaging, the cells were lysed according to the Abcam GFP ELISA Kit procedure for sample preparation of extracts from adherent cells.

2.5.1 Sample preparation by cell lysis

The growth medium was removed and the cells were washed twice with PBS (500 µl). The cells were kept on ice during the extraction procedure and were then centrifuged at 18,000 x g for 20 minutes. The supernatant was transferred into clean tubes and the pellet was discarded. Samples were then frozen at -80°C for further analysis.

Table 4: Plate layout for GFP ELISA: Highlighted in blue are the standards, highlighted in purple and orange are the samples extracted from the 24 well plates. The purple samples were diluted to 1/1000 and the orange samples were diluted to 1/5000.

0pg/ml	0pg/ml	$1x10^3$	$5x10^3$	$1x10^3$	$1x10^4$
2.7pg/ml	2.7pg/ml	$1x10^3$	$1x10^4$	$1x10^3$	$1x10^4$
8.2pg/ml	8.2pg/ml	$1x10^3$	$1x10^4$	$2.5x10^3$	$1x10^4$
24.7pg/ml	24.7pg/ml	$2.5x10^3$	$1x10^4$	$2.5x10^3$	$2x10^4$
74.1pg/ml	74.1pg/ml	$2.5x10^3$	$2x10^4$	$2.5x10^3$	$2x10^4$
222.2pg/ml	222.2pg/ml	$2.5x10^3$	$2x10^4$	$5x10^3$	$2x10^4$
666.7pg/ml	666.7pg/ml	$5x10^3$	$2x10^4$	$5x10^3$	
2000pg/ml	2000pg/ml	$5x10^3$	$1x10^3$	$5x10^3$	

2.5.2 Assay procedure

All materials and reagents were equilibrated to room temperature before use.

- 50 µL of all samples and standards were added to appropriate wells. (See plate layout Table 4).
- 50 µL of antibody cocktail was then added to each well.
- The plate was covered and incubated at room temperature for 1 hour on a plate shaker set to 400 rpm.
- Following incubation each well was washed 3 times with 350 µL of 1X wash buffer PT. After the last wash blot the plate against paper towel to remove any access liquid.
- 100 µL of TMB substrate was added to each well and incubated at room temperature in the dark on a plate shaker set to 400 rpm.
- 100 µL of stop solution was added to each well and shaken for 1 minute on a plate shaker set to 400 rpm.
- Absorbance was measured at 450 nm.

2.6 ELISA correlation to ImageJ

In order to validate ImageJ as a method for quantifying protein production, results from the ELISA were correlated with the amount of fluorescence produced as a result of insulin/GFP protein production from increasing numbers of cells. The ELISA used was GFP ELISA Kit (abcam, cat. No. ab171581). GFP fluorescence was also quantified using image analysis. The results of both tests were correlated to validate image analysis as a method of determining protein expression.

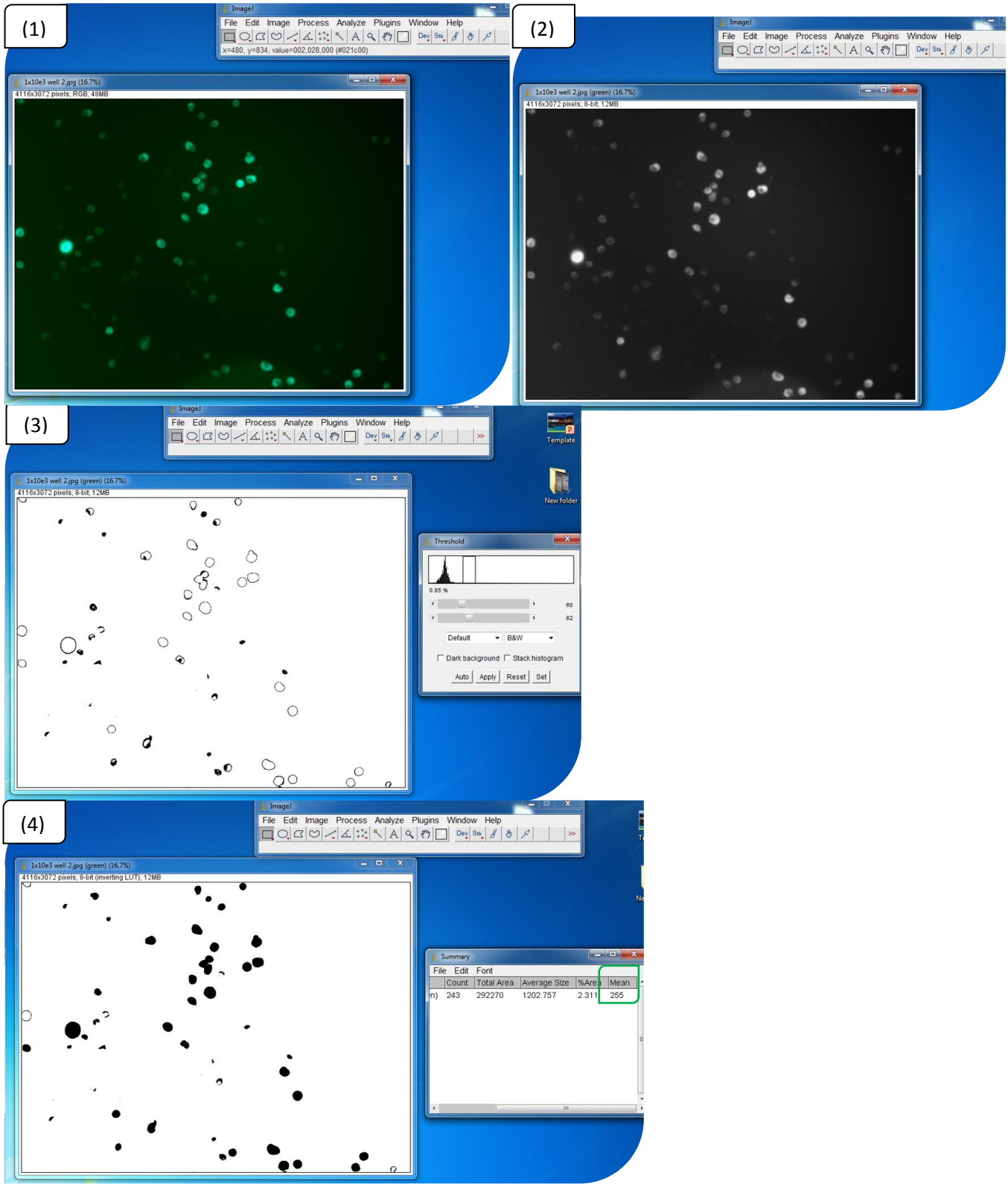

Figure 14: Screen shots from ImageJ analysis.

As shown in Figure 14, open image in ImageJ (1). Select image, colour, split channels, this separates the image into green, red and blue. Since this analysis is for GFP the green layer to the image is used which gives us the green image with no background

(2). You then select image, adjust, threshold, you can select the cells you want (3).Then you convert the image to binary and select fill holes, then you select analyse and analyse particles. And the % area result is the amount of the image that is green *i.e.* the amount of green fluorescence (4).

2.7 Lobster demineralization and Armins method

Frozen lobsters were obtained from Mullaghmore sea farm. The exoskeleton was removed and a Rotacraft Mini Rotary Tool was used to cut the crusher claw shell into 1 cm^2 pieces. To demineralize, claw shell samples were placed into 25 mL tubes with 10 mL of 1M Hydrochloric acid HCL (Fisher Scientific cat. No. H/1200/PB15) for two weeks. After one week, the samples were removed and placed into fresh HCL for the second week. Following HCL treatment, Armin's method was carried out to confirm demineralisation. Armin's method was used as it is a quick reliable method to test for demineralisation and is reported in the literature (Romano, Fabritius and Raabe, 2007). Armin's method solution was prepared immediately before use. 5% Ammonium Hydroxide and 5 % Ammonium oxalate solutions were combined in equal measure into a working solution. 10 mL of Armin's solution was added to 5 mL of the HCL from each sample. If any calcium remained in the HCL solution this resulted in a cloudy/milky solution, while a clear solution indicated that no calcium present and that demineralisation was complete. Following demineralisation, samples were placed into 1M Sodium Hydroxide (NaOH) (Lennox, cat. No. 1310-73-2) for one week to remove proteins. The demineralization process renders the shell pliable and it was then cut into 0.25 cm^2 pieces using a sterile scissors in order to fit into the 24 well plate inserts. Finally, the samples were rinsed with sterile PBS then sonicated for 1 hour, then placed into fresh sterile PBS and stored in the fridge.

2.8 Lobster shell viability test

In order to determine the effects of the lobster shell on cell viability, a number of tests were performed. The first method tested was a direct contact assay; though this method was not progressed with as in the initial test there was a loss of cells due to mechanical damage of the direct contact of the shell touching the cells (Figure 20).

To overcome the mechanical damage issue, it was decided that the shell would be suspended in a 24 well insert to determine the effects of the shell on the cells viability while also avoiding any mechanical damage due to direct contact. Cells were seeded in triplicate at a concentration of $2.5x10^3$ cells per well with 1 mL media.

Three independent experiments were performed giving a final sample size of n=9. Lobster samples were placed into 24 well inserts which were then added to the cells.

The samples were incubated at time points of 24, 48, 72 and 96 hrs. Following incubation, cell viability was determined using the neutral red assay. The medium was removed from the cells and the cells were washed twice with 1 mL PBS. In order to determine cell viability, the neutral red assay was performed.

The neutral red uptake assay offers a quantitative estimation of the number of viable cells in a culture. It is based on the ability of viable cells to incorporate and bind the neutral red in the lysosomes, meaning samples with more live cells will be able to take up more dye, resulting in a higher absorbance value (Repetto, del Peso and Zurita, 2008). 1 mL of neutral red containing MEM medium (50 µg/ml neutral red) was added to the cells. This was incubated for 2 hours at 37°C. Following incubation, neutral red was removed and cells were washed twice with 1 mL PBS. 1 mL of neutral red destain (50% ethanol, 49% water, 1% glacial acetic acid) was then added to the each well and the plate was shaken by hand for 5 minutes. The destain was then removed and placed into plastic cuvettes to measure the absorbance at 540 nm using a spectrophotometer.

2.9 Pilot adsorption and release study

As lobster has not previously been used for such adsorption and release, little is known regarding the shell's ability for adsorption or release of sodium butyrate. Accordingly, a pilot study was launched (n=3) to determine the dose and exposure time required for sodium butyrate adsorption and release.

Experimental conditions were:

- Concentrations of Sodium Butyrate tested: 0, 10, 25, 50, 100, 250, 500 and 1000 mM.
- Adsorption times: 24, 48, 72 hours.
- Release times: 4, 8, 24, 48, 72 hours.
- For this initial pilot study single samples of each concentration were run and then diluted to 1mM and 5mM. These dilutions were necessary in order to check which dilution of the samples fit best on the standard curve for the GCMS instrument.

The lobster shell was exposed to a range of sodium butyrate concentrations for 24, 48 and 72 hours. Following adsorption, the media was stored in the freezer for analysis on GC-MS at a later date. The release samples were treated the same, after each release time point the media was removed and stored to be extracted, diluted and analyzed on GC-MS. This was done to determine the optimum sodium butyrate concentration and exposure period. The hypothetical optimal concentrations are those which release a tolerable concentration of sodium butyrate to the cells, *i.e.* a concentration which will not significantly affect cell viability but still increase protein production. It was also important to determine the adsorption and release capability of the shell, as this is needed to determine what concentration of sodium butyrate will be released from the initial amount added to the shell. These samples were run in triplicate comprising 360 samples prior to diluting to 1 mM and 5 mM.

Due to the quantity of samples to be analysed, one sample from each experimental condition (time and concentration) was initially run on the GC-MS (120 samples X two dilutions) which allowed an initial analysis of results to narrow the range of conditions to be investigated further.

Following the initial examination described above, the experimental parameters were reduced to 0, 50, 100 and 250 mM sodium butyrate and a 48 hour adsorption and release time and these were investigated in more detail. *i.e.* the entire sample set was analysed (n=3) for these conditions.

2.10 Calculating sodium butyrate adsorption and release

In order to determine the amount of butyrate that the shell had adsorbed we worked backwards from the amount of butyrate which was left behind in the media. When the adsorption samples were run on the GC-MS this was measuring the media which was left behind by the shell*, i.e.* not adsorbed. From there, the amount adsorbed could be calculated. To calculate the amount released, the final concentration determined from GC-MS analysis was multiplied by the dilution factor.

2.11 Controlled release Sodium butyrate

From initial GC-MS adsorption and release, and bolus dose experiments it was found that 100 mM and 250 mM Sodium Butyrate were the optimal concentrations to move forward with. The concentrations 100 mM and 250 mM sodium butyrate were used for adsorption onto the shell as they released concentrations which were tolerable for the cells (seen in initial bolus dose experiments – Results 3.7; Figure 22). It was also found that a 48 hr period of adsorption and release was optimal. For controlled release, the cells (CHO-K1 INS/GFP) were seeded at $2.5x10^3$ cells per mL in a 24 well plate in 1 mL MEM. Cells were left to adhere for 48 hrs. During this 48 hrs the lobster shell samples (0.25 cm^2) were placed into 1 mL media containing either 100 mM or 250 mM sodium butyrate to adsorb.

Following this 48 hr period, 4 pieces of shell, each 0.25 cm^2 were placed into a 24 well cell culture insert Pore Size: 8.0µm (Cruinn, cat. No. 662638CI). The inserts were cut along the bottom to provide immediate exposure to sodium butyrate and as such, acted merely to suspend the shell in the cell culture. The inserts were then added into the well containing the cells. The media, which had contained the shell during the 48 hour adsorption period was stored and this was analysed by GC-MS, to determine the amount of sodium butyrate which had not been adsorbed by the shell. The controls in this experiment were samples of shell which had been placed in media alone and cells, and cells only. At each time point (4, 8, 24, 48 hrs) the media was removed from the cell culture experiments and stored for analysis on GC-MS. Following the removal of the media the cells were stained using hoechst dye and propidium iodide.

This was done to measure total cells and dead cells under fluorescent microscope imaging; during this imaging, insulin/GFP protein production was also measured by capturing the fluorescence of the GFP produced by the cells.

Table 5: Adsorption 24 well plate layout for controlled release of sodium butyrate. Each well above contained 4 pieces of lobster shell (0.25 cm^2).

Media	Media	Media	100mM	100mM	100mM
250mM	250mM	250mM			
Media	Media	Media	100mM	100mM	100mM
250mM	250mM	250mM			

Media	Media	Media	100mM	100mM	100mM
250mM	250mM	250mM			
Media	Media	Media	100mM	100mM	100mM
250mM	250mM	250mM			

Each well above (Table 5) contained 4 pieces of lobster shell (0.25 cm^2). The control used for this experiment was shell and media. Experimental groups were 100mM and 250mM sodium butyrate. Samples were prepared in triplicate as above.

All samples were left to adsorb for 48 hours. The samples highlighted in orange were used for the release plate that would test release after 4 hours. The samples highlighted in green were used for the 8 hour release plate. Purple were used for the 24 hour release and blue were used for 48 hour release.

2.12 Nikon image analysis to determine GFP expression

Figure 15 shows the measurement of GFP using the Nikon analysis. The original image was opened (1), analysis controls were used to select object count, intensity selected (2), threshold the image by selecting one of the cells, which then auto selected all the cells (3). This was then adjusted to add more or less cells, highlighting all the cells expressing GFP. The measured area was equal to the amount of GFP (3).

This is the same process as ImageJ analysis; however the software is newer and involves less steps and is a much faster method of analysis.

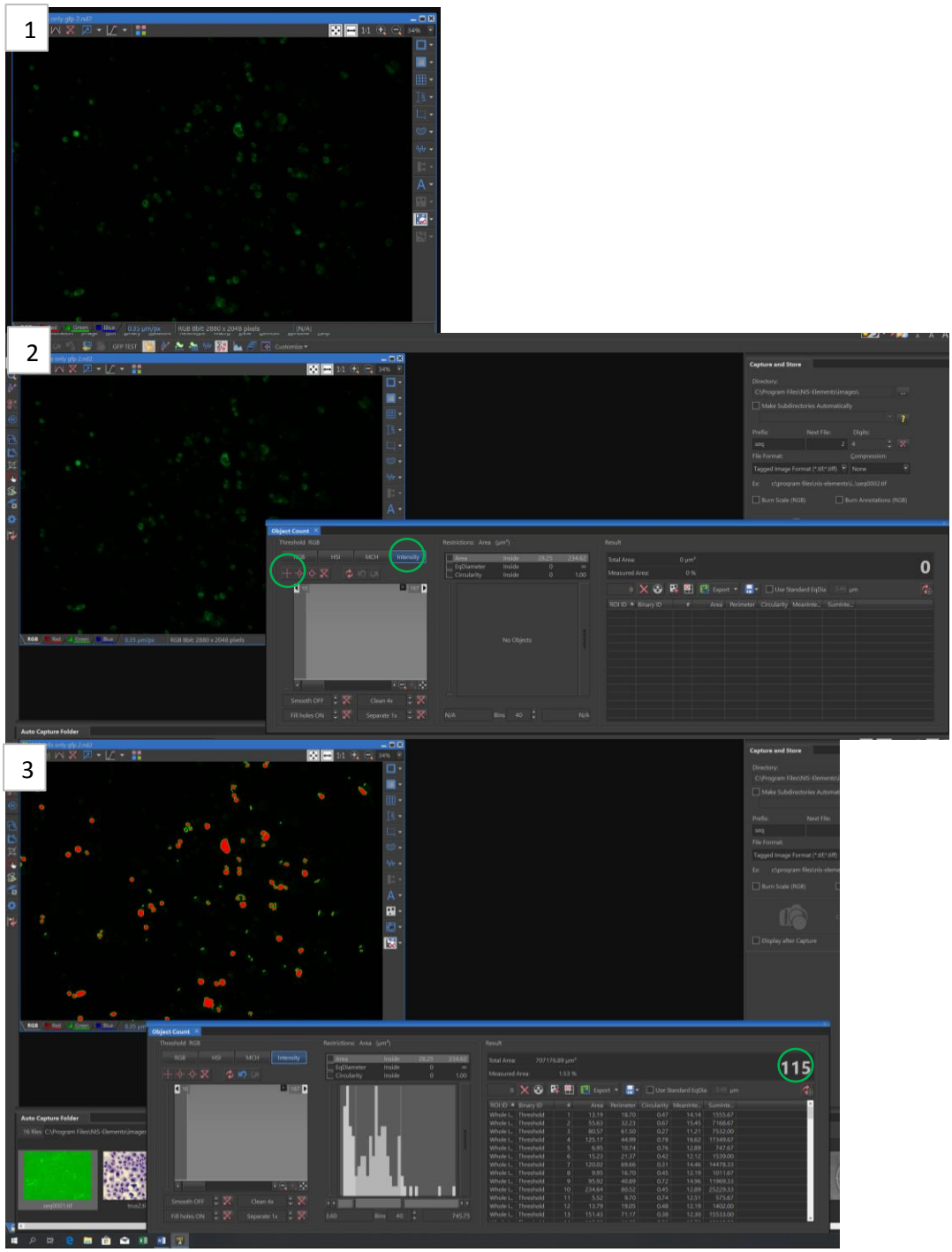

Figure 15: Measurement of GFP using Nikon basic research package.

2.13 GC-MS sample extraction

1 mL of samples from the controlled release experiment was added to separate 2mL micro centrifuge tube and phosphoric acid was added to a final concentration of 0.5% i.e. 5 µL in 1 mL. This was vortexed for 30 seconds to homogenise and then centrifuged at 15,000 RPM for 10 minutes.

The supernatant was filtered through 0.2 µm sterile filters. Following filtration, 500 µl of sample was removed and 500 µL of ethyl acetate was added to each sample. Samples were vortexed to extract the short chain fatty acids (SCFA), and left for 2 minutes for solvent phase separation and subsequently centrifuged at 15,000 RPM for 10 minutes. The organic phase was removed and transferred into fresh micro centrifuge tubes for analysis. Samples were diluted to 5 mM in ethyl acetate. Samples were diluted to ensure that the concentration of the target analyte was within the range of the standard curve and was based on the original concentration of added during the cell experiments.
120 µL of each sample was transferred to GC vials with a 250 µL glass insert.

2.14 GC-MS Analysis

The GC-MS system consisted of an Agilent Technologies 6890N GC connected to an Agilent Technologies 5973 inert mass selective detector and equipped with an automatic liquid sampler Agilent Technologies 7683B series injector. Data analysis was completed using mass hunter software. The GC was fitted with DB-WAXetr column, length 30m, internal diameter 0.250 mm, particle size 0.25 µm. Helium was the carrier gas at 1.2ml/min. Sample (1µl) were injected in split less mode with an inlet temperature of 250°C. The oven temperature was initially 90°C, then increased by 15°C/min until it reached 150°C, followed by an increase of 5°C/min to 170°C with a final ramp of 20°C/min to 230°C and held for 2 minutes with a total run time of 14 minutes. After every 8 samples a blank of ethyl acetate was inserted to check for memory effects. The detector conditions included the ion source at 230°C, quadrupole at 150°C and the interface at 280°C.

Data was collected in SIM mode with a scanning range of 30-120 m/z. Identification of the sodium butyrate was based on the retention time of standard compounds and NISD database analysis. Quantification was based on external sodium butyrate calibration curves using standards (10 µM-10000 µM).

2.15 Statistical Analysis

Paired one tailed t-test was performed using Microsoft Excel. One-tailed paired t-test was used to identify statistically significant differences between test samples and controls or between different time points and different sodium butyrate concentrations. Pearson's correlation analysis was performed using Minitab software.

3 Results

3.1 ELISA measurement of recombinant INS/GFP protein

In order to quantify the recombinant INS/GFP protein production, fluorescence was measured. To demonstrate that protein production can be measured by fluorescence, the relationship between fluorescence produced and protein expression was investigated. This investigation measured protein (measured by ELISA, standard curve Figure 16) and fluorescence (measured by Image J) in increasing numbers of CHO K1 INS/GFP cells grown in culture. It was found that as the number of cells increased so did the amount of fluorescence (Figure 18).

A correlation between fluorescence produced by the recombinant INS/GFP protein (measured by ImageJ) and the absolute INS/GFP protein produced (quantified by ELISA) was demonstrated. Correlation analysis (Pearson's test) and the relationship between protein produced and fluorescence was strongly correlated (Pearson's correlation coefficient 0.715) and showed a statistically significant correlation between protein production and fluorescence (Figure 17). This allowed us to move forward using fluorescence imaging and measurement as a method of quantifying protein production rather than an ELISA.

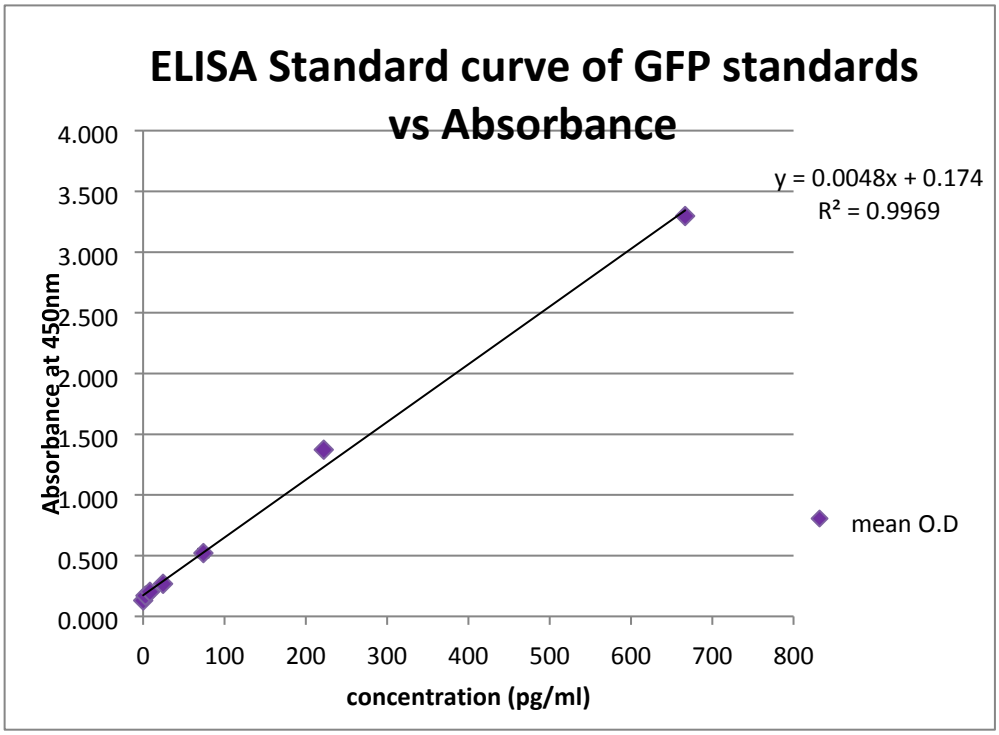

Figure 16: *Standard curve for GFP ELISA, standards were run in duplicate from 0-2000 pg/ml. (error bars are present here but are very small) (see appendix for raw data).*

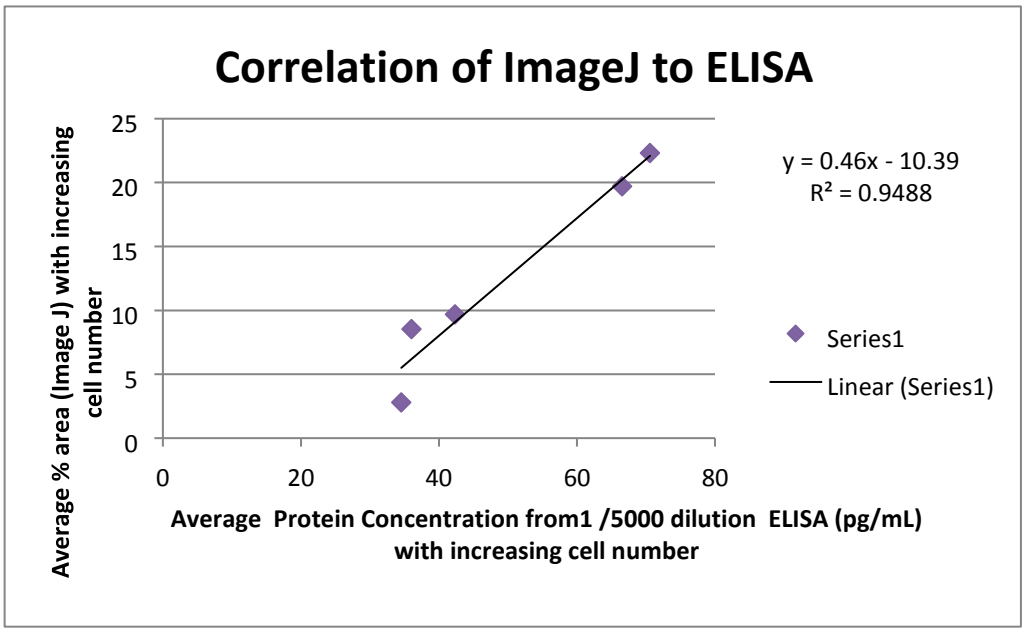

Figure 17: *Correlation ImageJ analysis to GFP ELISA A statistically significant correlation can be seen (Pearson's correlation coefficient 0.715, P = 0.003).This established a sound method of quantifying protein for the remainder of the study. (For raw data see appendix).*

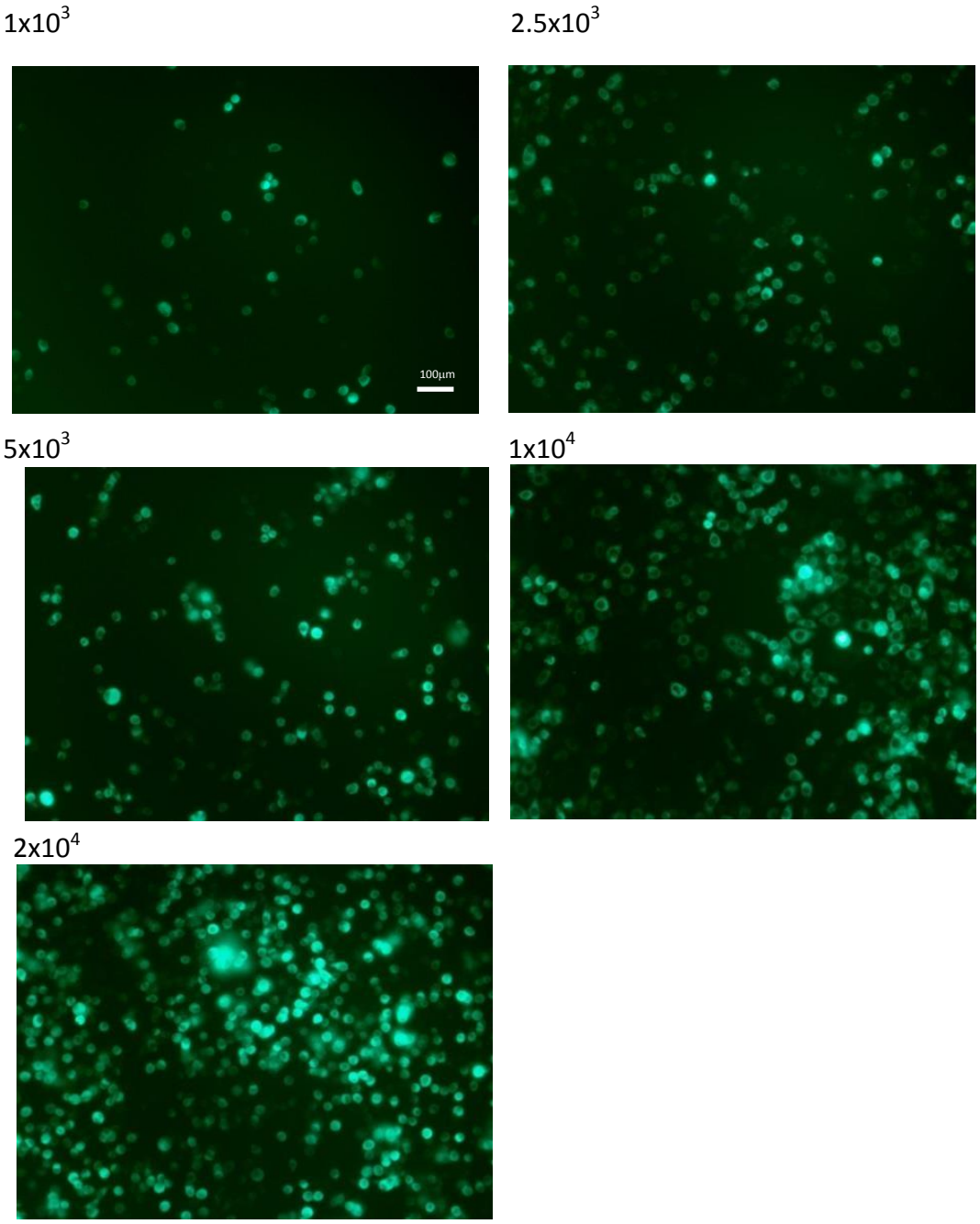

Figure 18: A sample of images taken (100x magnification) of CHO K1 INS/GFP cells which were used for the ELISA correlation to Image J. It can be seen in the images above that as the number of cells increased so does the fluorescence emitted. Image J analysis of these images were used to correlate fluorescence to protein production (Figure 16).

3.2 Lobster preparation

Lobster claws were demineralised and deproteinated. Determination of adequate demineralisation was performed using Armin's method; a clear solution indicates that demineralisation was complete (Figure 19a). Following treatment, it can be seen that the appearance of the claws changed indicating that pigments, proteins and minerals have been removed (Figure 19b). After treatment, the claw has no colour and is almost translucent. The claw is much softer and pliable and can easily be cut using a sterile scissors.

3.3 Lobster shell cytotoxicity analysis

3.3.1 Direct contact

To determine the effects of lobster shell on the cell viability, both direct contact and a modified MEM elution assay were explored. The first method used was a direct contact assay; the decision to start with this method is due to it being a standard test of biocompatibility for biomaterials (ANSI/AAMI/ISO 10993-5:2009). This method was not progressed as in the initial test there was a loss of cells due to mechanical damage of the direct contact of the shell touching and physically removing cells (Figure 20).

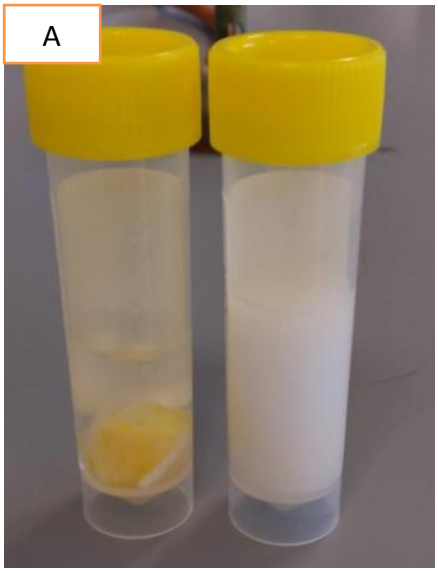

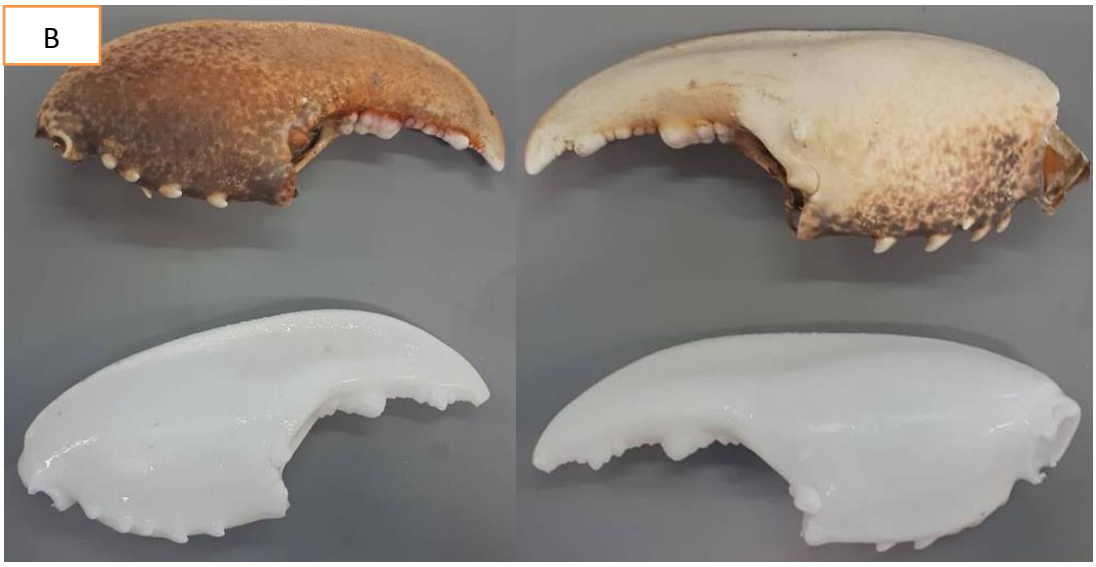

Figure 19: Figure 19: (a) An example of the Ammonium Hydroxide / Ammonium oxalate solution used to test for presence of calcium in the demineralising solution (HCL). If any calcium remained in the HCL solution this would result in a cloudy/milky solution, as seen from the tube on the right, while the clear solution shown indicates that no calcium is present and that demineralisation is complete, as seen in the tube on the left. (b) Images of the lobster shell before and treatment. Top left is the top side of the claw before treatment. Top right is the underside of the claw before treatment. Bottom left is the top side of the claw after treatment, bottom right is the underside of the claw after treatment.

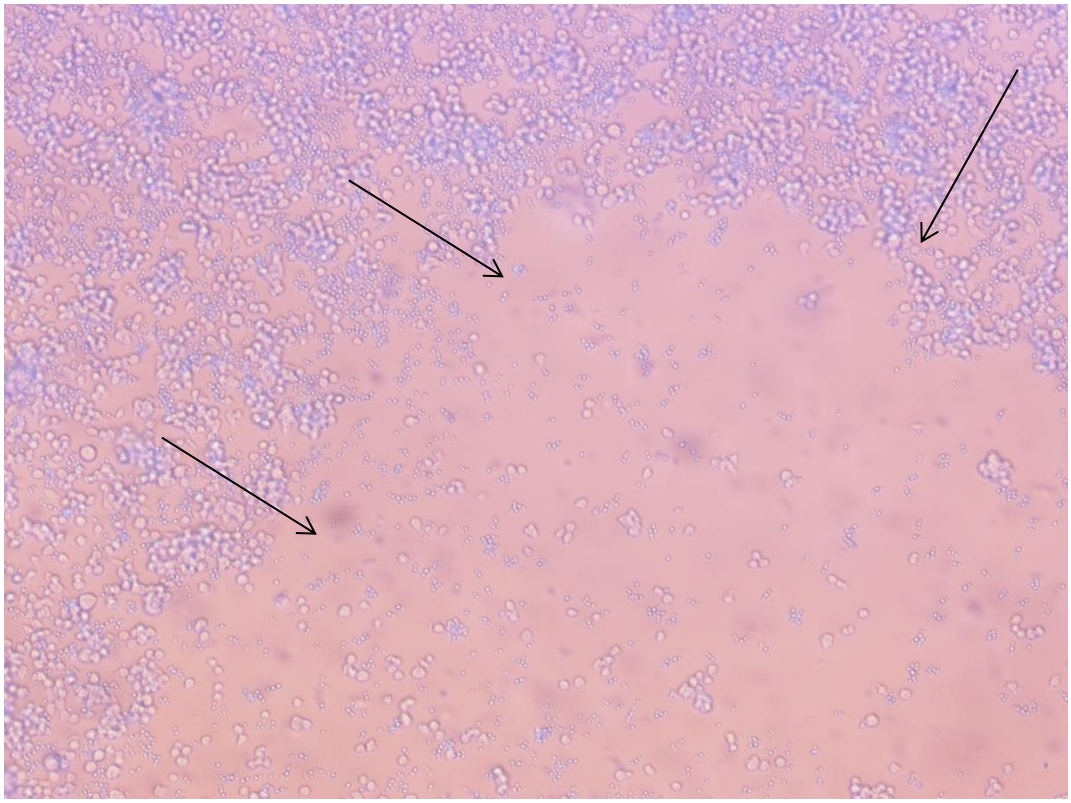

Figure 20: Result of mechanical damage from the shell touching the CHO K1 INS/GFP cells from a direct contact assay. As seen above where the arrows are pointing indicates where the edge of the shell was. It can clearly be seen in the image that there is a loss of cells where the lobster shell piece was on top of the cells.

3.3.2 Neutral red assay

In order to avoid mechanical damage to the cells observed during the direct contact assay, it was then decided that an adaptation to the MEM elution assay (ISO 109935:2009) would be used. The shell would be added in MEM media to a 24 well cell culture insert and the insert and shell placed in a well with cell monolayers. This experimental set up allowed us to determine the effect of the shell on the cells' viability while avoiding any mechanical damage. Figure 21 illustrates that the shell did not have any toxic effects on the cells up to 96 hours exposure to the shell ($2.5x10^3$ cells per well with 1 mL media. This was measured using neutral red).

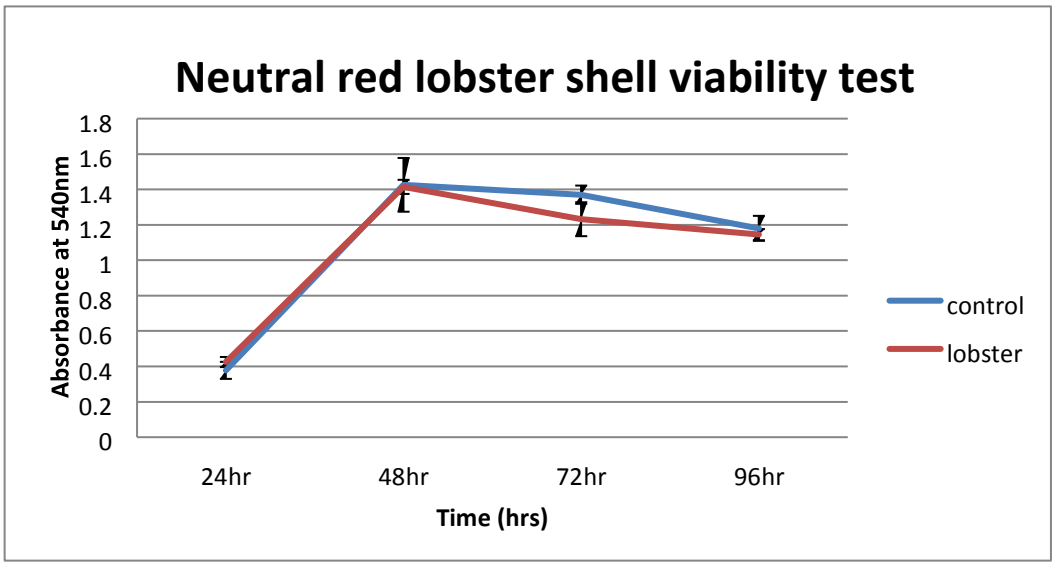

Figure 21: Viability testing of lobster shell: to test for effects of shell on CHO K1 INS/GFP cell viability over a 96 hour period. As seen above there is no difference in viability at 96 hours. (n=3X3).

3.4 Pilot absorption and release

To the best of our knowledge, lobster shell has not yet been used for such adsorption and release; little is known regarding the shell's ability for adsorption or release of sodium butyrate. Accordingly, a pilot study was launched to determine the dose and exposure time required for sodium butyrate adsorption onto shell and subsequent release.

Due to the quantity of samples to be analysed one sample from each experimental condition was initially run on the GC-MS (120 samples X two dilutions) to identify the range of concentrations and times which would be relevant to subsequent cell experiments.

3.4.1 Sodium butyrate adsorption

The shell was placed into a 24 well cell culture plate with sodium butyrate containing cell media and left to adsorb the Sodium Butyrate for 24, 48 and 72 hrs. Following adsorption, the media was analysed on GC-MS to determine how much butyrate remained *i.e.* not adsorbed.

3.4.2 Calculating sodium butyrate adsorption into the shell substrate

In order to determine the amount of butyrate that the shell had adsorbed we worked backwards from the amount of butyrate which remained in the media following the adsorption period. For example, in yellow highlighted row from Table 6 (100mM sample at 24 hour adsorption), 17.2201mM sodium butyrate has been adsorbed by the shell. The final concentration from the GC-MS analysis was 4.1389 mM. As the sample was diluted to 5 mM (for the purpose of GC-MS standard curve analysis) it must be multiplied back up (a 1 in 20 dilution was performed) therefore 4.1389 x 20 = 82.7798 mM. This value is the amount of sodium butyrate which was not adsorbed by the lobster. As the original concentration added for this sample was 100 mM we must subtract the 82.7798 mM from 100 mM which gives 17.2201 mM.

$$4.1389 * 20 = 82.7798\, mM$$

$$100 - 82.7798 = 17.2201\, mM$$

It can be seen from Table 6, the best adsorption was for the 100, 250, 500 and 1000 mM across all three time points.

Table 6: Amount of butyrate adsorbed by the shell. This table shows the adsorption values for each butyrate concentration at each adsorption time point n=1.

Adsorption values (mM)			
	24hr adsorption	48hr adsorption	72hr adsorption
0mM	-0.0708	-0.28418	-0.00124
10 mM	7.215911	1.583244	10
25 mM	-15.6451	-0.70222	14.02295
50 mM	-51.3064	15.00492	20.93355
100 mM	17.2201	57.48517	33.00736
250 mM	138.4141	136.4457	165.5841
500 mM	440.1358	374.043	424.9933
1000 mM	853.8422	852.9987	869.2201

3.4.3 Release of sodium butyrate from the shell substrate

After the adsorption period, the shell was placed into fresh media and left to release the sodium butyrate for 4, 8, 24, 48 and 72 hrs. At each release time point, the media which the butyrate released into was removed and stored. This was then replaced with fresh media. This was repeated at each time point (*i.e.* after 4 hrs of release, this media is removed and stored for later analysis; once the media is removed it is then replaced with fresh media for the 8 hr release).

To calculate the amount released in Table 7 in this instance, we multiply the final concentration from the GC-MS analysis by the dilution factor (Sections showing UM (Unable to Measure) are samples which the GC-MS was unable to measure, possibly due to the concentration of Sodium Butyrate being too low).

Table 7: Release values obtained after 24 hrs of adsorption. The shell here was left to adsorb sodium butyrate for 24 hrs at 37°C. Release was measured over a period of 72 hrs (n=1). (Sections showing UM (Unable to Measure)are samples which the GC-MS was unable to measure, possibly due to the concentration of Sodium Butyrate being too low).

24hr adsorption plate							
Release values							
	4hr	8hr	24hr	48hr	72hr	Total amount released (mM)	% release
0 mM	0.0093	0.0023	0.0010	0.0017	0.0070	0.0213	N/A
10 mM	UM	0.4926	0.0138	0.0713	0.0138	0.5915	8.1972
25 mM	0.6383	0.6740	0.0379	0.0068	0.0123	1.3693	-8.7521
50 mM	7.8769	0.7536	0.1168	0.0035	0.0225	8.7733	-17.0999
100 mM	13.8531	2.7490	0.4718	0.0354	0.0164	17.1259	99.4528
250 mM	28.5424	3.0879	0.4828	0.0701	0.0341	32.2173	23.2760
500 mM	53.7625	UM	0.6397	0.0803	0.0102	54.4928	12.3809
1000 mM	88.3718	5.5403	1.1909	UM	0.0379	95.1410	11.1427

Table 8: Release values obtained after 48 hrs of adsorption. The shell here was left to adsorb sodium butyrate for 48 hrs at 37°**C**. Release was measured over a period of 72 hrs (n=1). (Sections showing UM (Unable to Measure) are samples which the GC-MS was unable to measure, possibly due to the concentration of Sodium Butyrate being too low).

48hr adsorption plate,							
release values							
	4hr	8hr	24hr	48hr	72hr	total release	% release
0 mM	0.0525	0.0068	0.0119	0.0100	0.0018	0.0830	N/A
10 mM	0.4480	0.1970	0.0344	0.0169	0.0019	0.6982	44.0969
25 mM	2.6753	0.4225	0.0274	0.0209	0.0003	3.1463	-448.0574
50 mM	5.2483	0.6220	0.0615	0.0208	UM	5.9526	39.6709
100 mM	8.3148	1.2777	0.1272	0.0094	UM	9.7292	16.9247
250 mM	33.7763	1.4391	0.1984	0.0310	UM	35.4449	25.9773
500 mM	38.5609	1.7807	0.8188	0.0278	UM	41.1882	11.0116
1000 mM	88.2914	13.5571	2.9816	0.1533	UM	104.9834	12.3076

Table 9: Release values obtained after 72 hrs of adsorption. The shell here was left to adsorb sodium butyrate for 72 hrs at 37°C. Release was measured over a period of 72 hrs (n=1). (Sections showing UM (Unable to Measure)are samples which the GC-MS was unable to measure, possibly due to the concentration of Sodium Butyrate being too low).

72hr adsorption plate,							
release values							
	4hr	8hr	24hr	48hr	72hr	total release	% release
0 mM	0.0064	0.0011	0.0004	0.0003	0.0008	0.0089	N/A
10 mM	0.1349	0.0281	0.0008	0.0029	0.0002	0.1669	1.6687
25 mM	1.2306	0.0541	0.0050	UM	UM	1.2897	9.1974
50 mM	1.3455	0.1106	0.0034	UM	0.0006	1.4600	6.9744
100 mM	7.8016	0.6491	0.0823	0.0022	UM	8.5353	25.8586
250 mM	19.1403	3.9922	0.4823	0.0496	UM	23.6644	14.2915
500 mM	30.0337	8.3413	0.1224	0.0401	0.0172	38.5546	9.0718
1000 mM	68.4392	7.1183	0.3925	UM	UM	75.9500	8.7377

3.4.4 Pilot study summary

The samples from the initial pilot study were analysed and the optimal concentration and time point was selected. Between the 1 mM and 5 mM dilutions, it was found that the 5 mM dilutions gave more robust data as these dilutions fell within the range of the GC-MS standard curve. 1mM dilutions are not shown as the samples were too dilute to fit within the range of the standard curve.

It was found that for 24 hour, 48 hour and 72 hour adsorption for 0-50 mM samples, minimal to no butyrate was adsorbed (Table 6). Anything that did adsorb was released at 0-4 hours (Tables 7, 8, 9); therefore, concentrations of 0, 10 and 25 mM at all time points were not examined further.

For the higher concentrations of 500 and 1000 mM, a greater percent of sodium butyrate was absorbed at each time point (*e.g.* approx. 85% absorption for all three time points). However, the release was very low across all three adsorption time points (between 8-12% - Tables 7, 8, 9) and it seemed for the 500 mM samples the majority of the sodium butyrate was being retained and not released. Therefore, it was decided not to further examine 500 and 1000 mM at 0-4hrs so these concentrations and time points were not pursued further.

Overall, findings from the pilot study are that the concentrations of 100 mM and 250 mM showed an adsorption of between 17 – 57% with better adsorption shown at 48 hours and 72 hours for the 100 mM samples and 72 hours for the 250 mM samples than 24 hours for both (Table 6). The release values in terms of butyrate concentration in mM for these conditions are in line with the bolus dose concentrations studied and shown to have an enhanced effect on protein production. Therefore, it was decided to focus on the 100 and 250 mM concentrations. The 48 hour and 72 hour adsorption times seemed to give more favourable adsorption than 24 hours and there was no difference between 48 and 72 hours. Therefore, 48 hours was selected as the adsorption time going forward, as it was sensitive enough to move forward with.

3.5 Analysis of full Replicate Data from Pilot Study

Given the large number of samples in the pilot adsorption and release study, initially only one of a three replicates were analysed. This initial analysis allowed us to narrow the field of investigation to 50, 100 and 250 mM (as illustrated previously). To complete the pilot study, the remaining replicates of samples from 50, 100 and 250 mM were analysed from the adsorption and release studies and are presented here. From the pilot test it was decided to move forward with and analyse the triplicate samples of 48 hour adsorption and release times and sodium butyrate concentrations of 50, 100 and 250mM

The remaining two samples of the triplicates of the 100 and 250 mM samples (48 hour adsorption) were analysed on GC-MS in order to complete analysis of the dataset. Table 10 shows the concentration of sodium butyrate added, the amount adsorbed, amount released along with total release and percent release. From the addition of 50 mM sodium butyrate the shell adsorbed 10.18 mM, for 100 mM sodium butyrate the shell adsorbed 28.025 mM and for 250 mM adsorbed 72.47 mM (Table 10).

Percent release (Table 11) was calculated by getting the sum of the release values from each time point, this gives total release. Then the total release is divided by the amount adsorbed, multiplying the result by 100 giving percent release (n=3). Approximately 50% of the amount adsorbed was released within the first 4 hours.

Table 10: Release values after 4-72 hrs of sodium butyrate release from the lobster shell into cell culture media N=3.

Amount added	Amount adsorbed	4hr release (mM)	8hr release (mM)	24hr release (mM)	48hr release (mM)	72hr release (mM)	total release (mM)	% release
0mM	-0.1180 (+/- 0.14)	0.0222 (+/- 0.0263)	0.0049 (+/- 0.0017)	0.0057 (+/- 0.0053)	0.0052 (+/- 0.0042)	0.0019 (+/- 0.0002)	0.0398	-33.7406
50mM	10.1813 (+/- 5.23)	4.6768 (+/- 0.7602)	0.5353 (+/- 0.2553)	0.0838 (+/- 0.0517)	0.0323 (+/- 0.0107)	0.0255 (+/- 0.0078)	5.3537	52.5836
100mM	28.0257 (+/- 25.53)	9.1736 (+/- 0.9910)	1.0439 (+/- 0.2166)	0.1204 (+/- 0.0092)	0.0371 (+/- 0.0242)	0.0730 (+/- 0.0636)	10.4481	37.2803
250mM	72.4702 (+/- 55.45)	29.7288 (+/- 6.8241)	3.3580 (+/- 2.0082)	0.3428 (+/- 0.1433)	0.1037 (+/- 0.0647)	0.0950 (+/- 0.0141)	33.6283	46.4029

Table 11: Percent release at each timepoint (n=3).

Percent release at each timepoint	50mM	100mM	250mM
4hr	54.3204 (+/- 24.94)	53.5411 (+/- 35.51)	54.5124 (+/- 31.50)
8hr	5.4171 (+/- 1.30)	5.4495 (+/- 3.02)	7.5795 (+/- 6.57)
24hr	0.9122 (+/- 0.46)	0.6613 (+/- 0.38)	0.7277 (+/- 0.52)
48hr	0.4194 (+/- 0.30)	0.2616 (+/- 0.21)	0.2401 (+/- 0.20)
72hr	0.2388 (+/- 0.22)	0.3503 (+/- 0.42)	0.1560 (+/- 0.14)

3.6 Controlled release of sodium butyrate in cell culture.

From analysis of triplicate samples on GC-MS adsorption and release, and bolus dose experiments, section 3.7, it was determined that 100 mM and 250 mM Sodium Butyrate were the optimal adsorption concentrations to move forward with. These concentrations were considered optimal as they released concentrations of Sodium Butyrate which should be tolerated by the cells with little effect on viability while still increasing protein production. The 100 mM sample released an average 10 mM and the 250 mM released an average 33 mM (Table 13). As seen from the bolus dose data, 10 mM and 25 mM resulted in an increase in protein production (Figure 25). From the bolus dose viability results (Figure 22), it can be seen that the percent viability of the cells treated with 10 mM and 25 mM butyrate have a viability of greater than 90%. It was also found that a 48 hr period of adsorption and release was optimal.

To investigate controlled release of butyrate from lobster shell on protein production (section 3.9), the lobster was exposed to 100 mM and 250 mM sodium butyrate (n=3 for each timepoint) and left to absorb for 48 hours. After this time, the shell was rinsed and added to CHO-K1 INS/GFP cells in culture in an insert. The adsorption values were obtained by collecting the media in which the shell was in for 48 hours to adsorb, and analysing by GC-MS. The amount adsorbed was calculated by taking the amount of sodium butyrate left behind by the shell away from the initial concentration added. In this experiment, the media was removed at each timepoint and measured for both sodium butyrate adsorption (Table 12) and release (Table 13) (by GC-MS). At the same time, cells were stained and cell viability was quantified (Figure 23).

Table 12: Adsorption values from controlled release in cell culture experiment showing adsorption values for each concentration at each time point tested. The shell was left to adsorb the Sodium Butyrate for 48 hrs. Following this release, values were measured (n=3X3).

	Adsorption	
Time (hrs)	100mM	250mM
4hr	15.17 (+/-4.46)	45.59 (+/- 6.47)
8hr	17.32 (+/- 5.35)	32.19 (+/-9.67)
24hr	17.10 (+/-4.78)	37.72 (+/- 10.68)
48hr	17.89 (+/-6.30)	36.68 (+/- 14.69)

Table 13: Release values (mM) from controlled release cell culture experiment showing the release values for each concentration of sodium butyrate added at each time point tested. Concentrations added were 100 and 250 mM sodium butyrate. The shell was left to release the Sodium Butyrate over a 48 hour period. Following this period, milimolar values of sodium butyrate release were measured by GC-MS analysis. (n=3X3).

Release	100mM	250mM	100mM % release	250mM % release
4hr	7.88 (+/- 2.96)	21.23 (+/- 7.44)	55.03 (+/- 22.45)	48.00 (+/- 20.83)
8hr	7.36 (+/-1.66)	19.16 (+/- 5.32)	47.00 (+/- 22.39)	66.40 (+/- 35.15)
24hr	7.69 (+/-3.42)	19.57 (+/- 4.83)	49.00 (+/- 27.72)	55.95 (+/- 23.19)
48hr	7.47 (+/- 2.85)	21.86 (+/- 9.66)	46.90 (+/- 23.87)	68.96 (+/- 39.64)

3.7 Cell viability

3.7.1 Bolus dose percent viability

A bolus dose of a drug is one in which the drug is released immediately after administration with no deliberate effort made to modify the rate of release.

Increasing concentrations of sodium butyrate was added to the CHO K1 INS/GFP cells and left to incubate for a period of 48 hours, with images taken at each time point (4, 8, 24 and 48 hrs).

In order to determine viability of the CHO K1 INS/GFP cells, the fluorescent images of Hoechst and propidium iodide stained cells were taken during the bolus dose experiment were analysed using ImageJ analysis. From this analysis, the viability of the cells was determined. It can be seen in Figure 22 that the viability of the cells is negatively impacted over time and as the concentration of sodium butyrate increased the viability of the cells decreased. A significant decrease in cell viability can be seen at 8 hours for 250 mM and from 24 hours to 48 hours with concentrations 100 mM, 175 mM and 250 mM (Figure 22). This shows that while sodium butyrate addition does increase INS/GFP production, (as demonstrated in Figure 25) it negatively impacts cell viability.

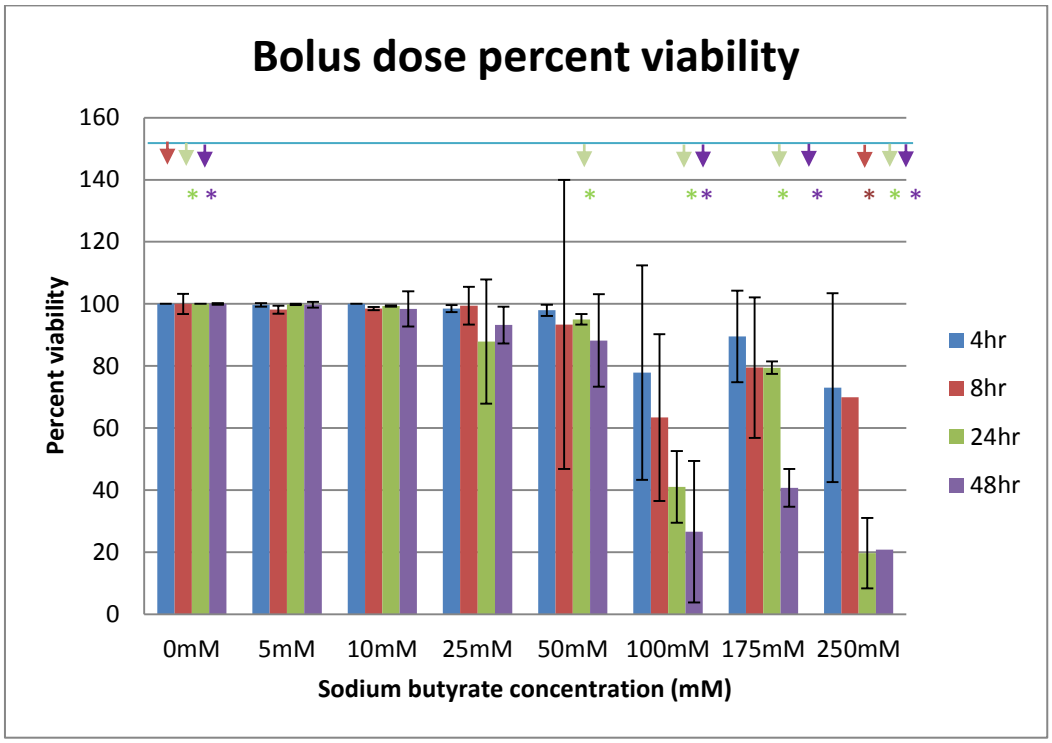

Figure 22: Percent viability of CHO K1 INS/GFP cells following exposure to bolus dose of 0 – 250 mM sodium butyrate over a 48 hour time period(n=3X3). * represents statistical significance by two tailed t-test ($p<0.05$).

3.7.2 Controlled release Viability

To evaluate the effect of controlled release of sodium butyrate on the viability of CHO K1 INS/GFP cells, 100 and 250 mM sodium butyrate was adsorbed onto the pieces of lobster shell for 48 hours (as described in Section 3.6). Following adsorption, lobster shell pieces were placed into a 24 well plate insert and then exposed to the cells for 48 hours. As seen from Figure 23 there is no significant decrease in percent viability of the cells at and time point with any concentration of sodium butyrate released. It should be noted that 100mM released approximately 7 mM sodium butyrate onto the cells and 250 mM released approximately 20 mM onto the cells as can be seen in Table 13.

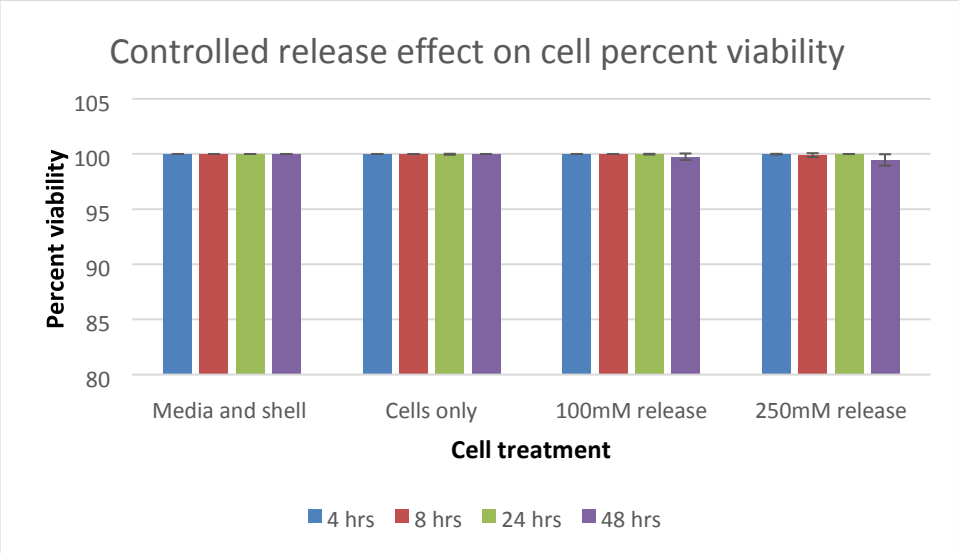

Figure 23: Percent viability of CHO K1 INS/GFP cells following controlled release of 100 and 250 mM sodium butyrate over a 48 hour time period (n=3X3).

Figure 24 shows a comparison of percent viability for bolus dose and controlled release of sodium butyrate. As it was not possible to determine percent viability on a per milimolar basis, it was decided to compare 5 mM, 10 mM and 25 mM from the bolus dose experiment to 100 mM and 250 mM from the controlled release experiment (controls from both experiments are also present). It should be noted that 100mM released approximately 7 mM sodium butyrate onto the cells and 250 mM released approximately 20 mM onto the cells (Table 13).

For this reason, 5 mM, 10 mM and 25 mM from the bolus dose experiment are used for comparison against the controlled release values as they represented the closest milimolar values. As seen from Figure 24 there is a statistical difference in percent viability between 100 mM Controlled Vs 10 mM bolus at 24 hr, and 250 mM controlled Vs 10 mM bolus at 24 hr. In both cases it is the controlled release values show a significantly higher viability than that of the bolus dose values. 250 mM released approximately 20 mM onto the cells resulting in a higher percent viability compared to 10 mM bolus dose.

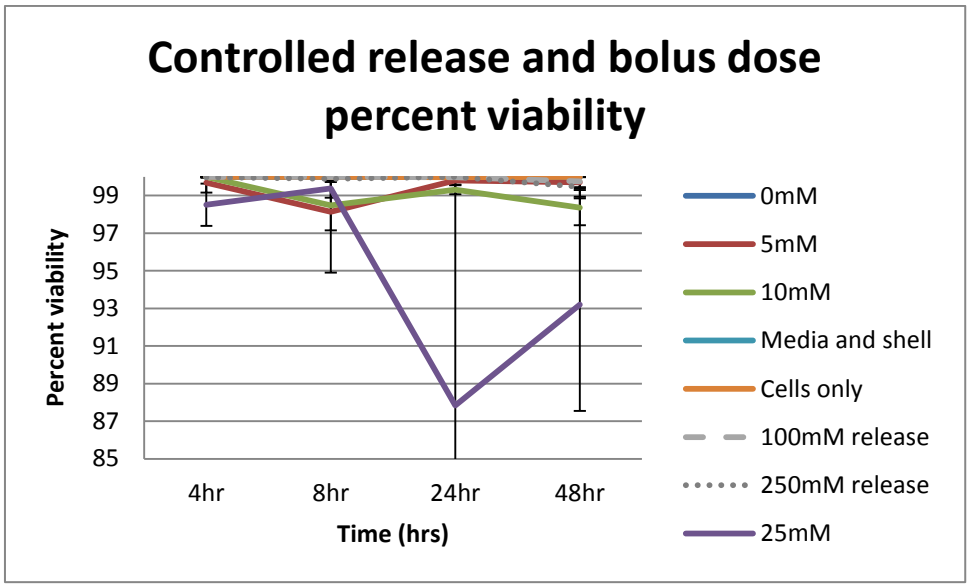

Figure 24: Controlled vs bolus viability test graph, scale 85-100%. Controlled release data is shown by dotted lines. There is a statistical difference between 100 mM Controlled Vs 10 mM bolus at 24 hr, and 250 mM controlled Vs 10 mM bolus at 24 hr ($P<0.05$, two tailed t-test).

3.8 Increasing Recombinant INS/GFP protein by bolus dose sodium butyrate

To examine the effect of sodium butyrate on recombinant INS/GFP fusion protein (INS/GFP) production, CHO K1 INS/GFP cells were exposed to a range of sodium butyrate concentrations (0, 5, 10, 25, 50, 100, 175 and 250 mM) over time (4, 8, 24 and 48 hours). INS/GFP protein production was measured by quantifying GFP fluorescence using Image J. Bolus doses of Sodium Butyrate were added to the cells; at concentrations indicated in Figure 25. INS/GFP protein production was measured at each time point (using ImageJ analysis and fluorescent dyes) up to and including 48 hours as indicated. Adding bolus doses of sodium butyrate to the cells (up to 10 mM) results in an increase in protein production over time. At doses of 25 mM and greater, there is no difference in protein production compared to 0 mM at any time point. The finding in Figure 25 indicates that the addition of sodium butyrate at concentrations of 100 mM, 175 mM and 250 mM resulted in a statistically significant decrease in the amount of INS/GFP protein produced compared to 0mM, 48 hours. There is also a significant decrease in production between 0 mM and 100 mM at 4 hours (p value = 0.003918, t-Test: Paired Two Sample for Means).

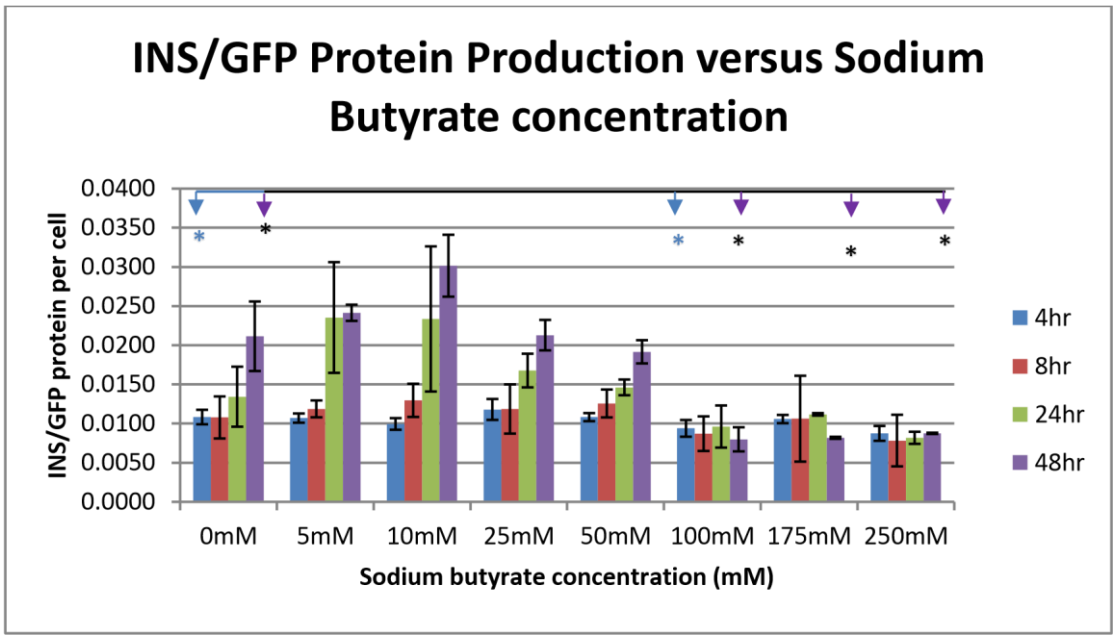

Figure 25: The effect of varying bolus concentrations of sodium butyrate on recombinant INS/GFP protein production in CHO K1 INS GFP cells over time. Bars represent the average of three independent runs (n=3 for each run) ± standard deviation. * represents statistical significance by two tailed t-test ($p<0.05$). (n=3X3).

3.9 Protein production from controlled release in cell culture

Cells were seeded at $2.5x10^3$ cells per mL. Cells were left to adhere for 48 hours. During this 48 hours, the lobster shell samples ($0.25cm^2$) were in sodium butyrate containing media to adsorb. The controls in this experiment were samples of shell and cells, and cells only. At each time point the media was removed and stored for analysis on GC-MS (section 3.6 Controlled release of sodium butyrate in cell culture, for analysis). Following the removal of the media the cells were stained using Hoechst dye and propidium iodide. This was done to measure total live cells and dead cells under fluorescent microscope imaging, during this imaging protein production was also measured by capturing the fluorescence of the GFP produced by the cells (from this analysis it was possible to determine the amount of protein produced per cell).

Figure 26 illustrates the effect of controlled release on protein production. Controlled release of Sodium butyrate resulted in a statistically significant increase in protein production between 250 mM release and media and shell only control at 24 hours, and between 100 mM release and media and shell only at 48 hours (paired one tailed t-test ($p<0.05$).

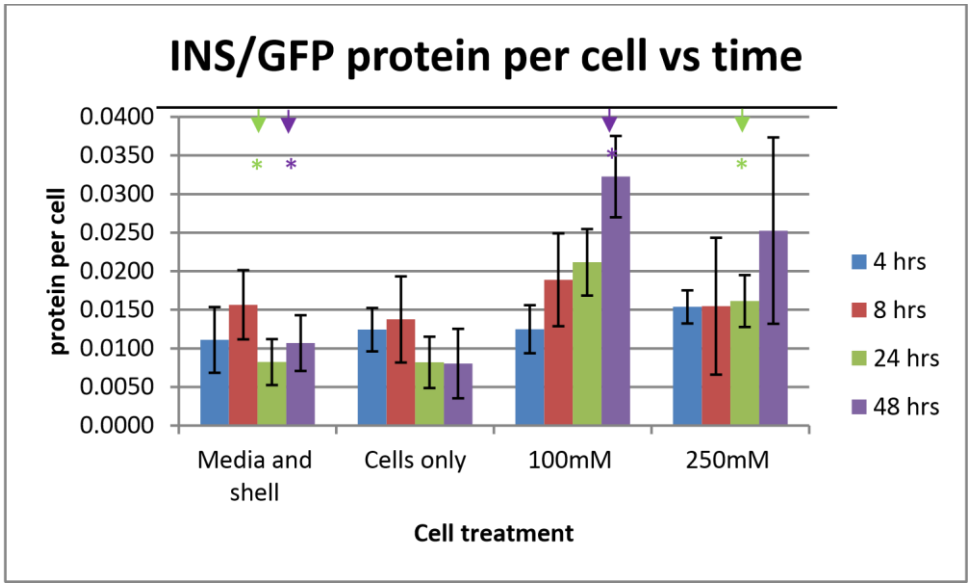

Figure 26: To determine the effects of controlled release of sodium butyrate on INS/GFP protein production in CHO K1 INS GFP cells (n=3X3). A piece of lobster shell which had adsorbed Sodium Butyrate (100 and 250 mM), was added to the cells. The protein production was measured at each time point (using Nikon basic research software analysis and fluorescent dyes). * indicates statistical significance.

3.10 Fold change in INS/GFP protein production for bolus dose experiment

Fold change in INS/GFP was calculated by dividing each INS/GFP Protein per cell result for the experimental group by the control group. Table 14 indicates a trend of increasing protein production with the addition of up to 50 mM sodium butyrate (fold change >1). The highest fold change in INS/GFP protein production per cell can be seen at 24 hours with 10 mM sodium butyrate added to the cells. A decline in INS/GFP protein production can be seen from 100 mM to 250 mM sodium butyrate addition (fold change <1). No statistically significant differences in fold change was found.

Table 14: Table of fold change in recombinant INS/GFP protein per cell (plus or minus standard deviation) for CHO K1 INS/GFP cells, following exposure to 5, 10, 25, 50, 100, 175 and 250 mM sodium butyrate over a 48 hour time period (+/- standard deviation).

Fold change of INS/GFP protein per cell n=3 X 3 (mM)							
	5mM	**10mM**	**25mM**	**50mM**	**100mM**	**175mM**	**250mM**
4 hours	1.0006 (+/- 0.05)	0.9389 (+/- 0.16)	1.1030 (+/- 0.12)	1.0170 (+/- 0.09)	0.8763 (+/- 0.02)	0.9993 (+/- 0.15)	0.8189 (+/-0.16)
8 hours	1.1995 (+/- 0.33)	1.3531 (+/- 0.37)	1.1743 (+/- 0.28)	1.2831 (+/- 0.30)	0.8430 (+/- 0.20)	0.9672 (+/0.26)	0.7350 (+/- 0.14)
24 hours	1.9539 (+/0.79)	2.2612 (+/- 1.68)	1.4068 (+/- 0.35)	1.2781 (+/- 0.46)	0.8272 (+/- 0.34)	0.9601 (+/- 0.31)	0.7079 (+/- 0.24)
48 hours	1.3642 (+/- 0.33)	1.8533 (+/- 0.95)	1.2143 (+/- 0.30)	1.1482 (+/- 0.32)	0.4545 (+/- 0.12)	0.4798 (+/- 0.18)	0.4978 (+/- 0.19)

3.10.1 Fold change analysis from controlled release

When compared to the control (0 mM sodium butyrate added) it can be seen in Table 15 that there is a significant increase in protein production when a controlled release of Sodium Butyrate is added to the cells. In table 15, at 48 hours there is a 5.3 fold increase in the 100 mM sodium butyrate treatment when compared to the control of 0 mM (the 100 mM Sodium Butyrate released 17.8 mM with the controlled release system which resulted in a 5.3 fold increase in protein production).

At 24hrs, 100 mM butyrate resulted in 2.8 fold increase in protein production and 250 mM resulted in a 2.1 fold increase when compared to the control of cells only. At 48 hrs 100 mM butyrate resulted in a 3.6 fold increase compared to the control of cells only. There was also no significant difference in protein production between the two controls used, of cells only and cells with shell.

Table 15: Fold increase in protein production (per cell) from controlled release of Sodium Butyrate.

	100mM	250mM
4hrs	1.0348 (+/- 0.06)	1.3156 (+/- 0.22)
8hrs	1.4344 (+/- 0.32)	1.1135 (+/- 0.18)
24hrs	2.8367 (+/- 0.95)	2.1242 (+/- 0.43)
48hrs	5.3962 (+/- 3.36)	3.5579 (+/- 0.93)

Percent change in INS/GFP protein per mM bolus dose sodium butyrate

The percent change of INS/GFP protein production between 0 mM butyrate added and each concentration was calculated. Results were then calculated per mM, this was to normalise the data for comparative analysis, against control release, in later experiments. Briefly, results for protein production were divided by the amount of sodium butyrate added (*e.g.* 10 mM, 25 mM etc). The greatest percent change can be seen for the 5 mM and 10 mM concentrations (Figure 27). At 24 hours, the percent change for both 5 mM and 10 mM is significantly greater than percent change for 50 mM and all concentrations greater than 50 mM (t-Test: Paired Two Sample for Means).

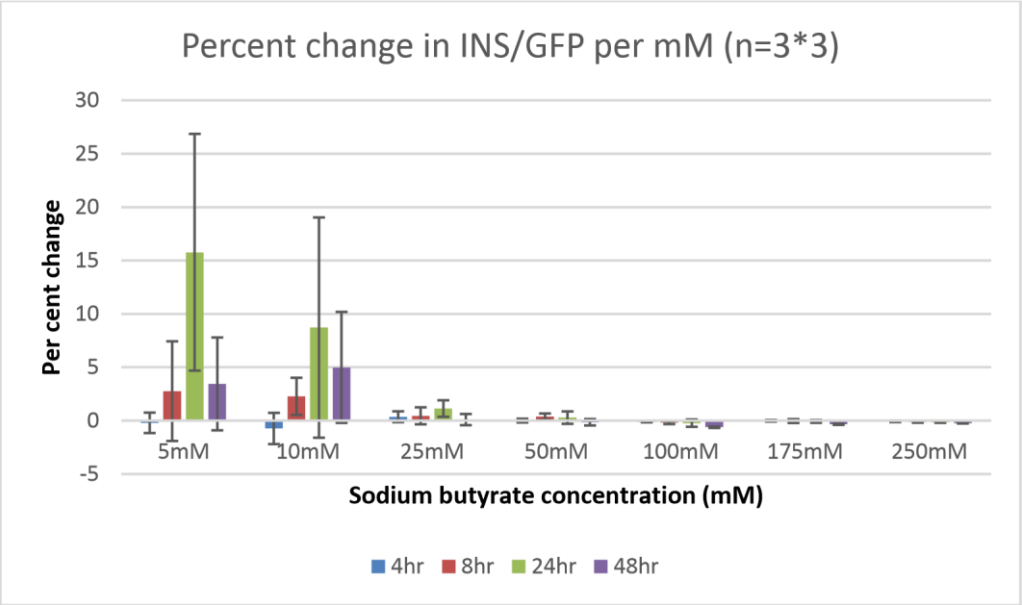

Figure 27: Percent change of INS/GFP protein per milimolar sodium butyrate. Three independent experiments were carried out in triplicate giving a final sample size of n=3X3. CHO K1 INS/GFP cells were exposed to a bolus dose of sodium butyrate (0, 5, 10, 25, 50, 100, 175 and 250 mM) for a period of 48 hours.

Percent change INS/GFP protein per milimolar controlled release

The percent change of INS/GFP protein production between 0 mM butyrate added and each concentration was calculated. Results were then calculated per mM. The greatest percent change can be seen for the 100 mM at 24 hours and 48 hours (Figure 28).

Figure 29 compares the bolus dose and controlled release percent change in INS/GFP protein per milimolar. For this comparison concentration 5 mM, 10 mM and 25mM were selected from the bolus dose experiment and compared to 100 mM and 250mM from the controlled release experiment. From figure 29 you can see that there is a significant increase in the percent change at 24 hours from 25 mM compared to 100 mM. There is also a significant increase present at 48 hours from 25 mM compared to both 100 mM and 250 mM.

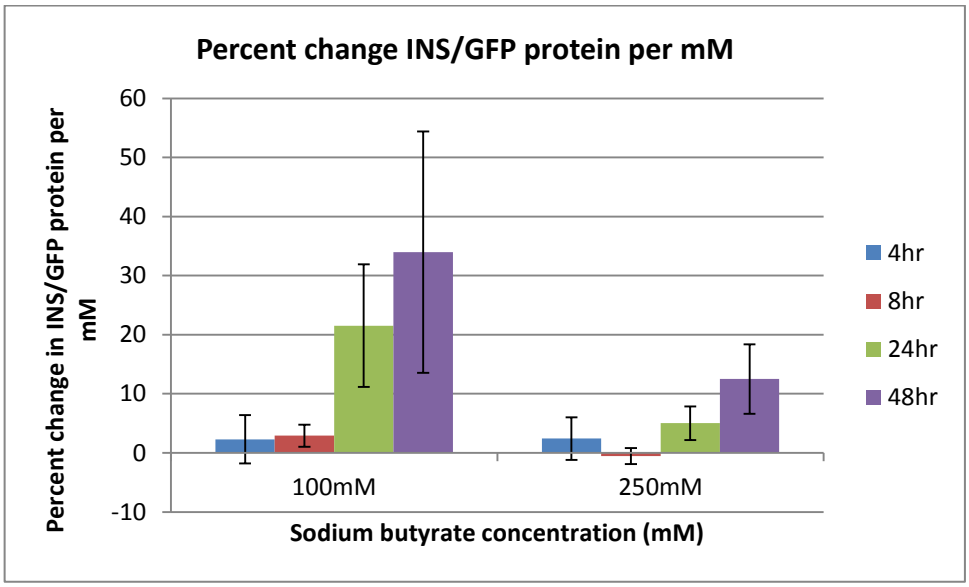

Figure 28: Percent change in INS/GFP protein per mM for controlled release of sodium butyrate.

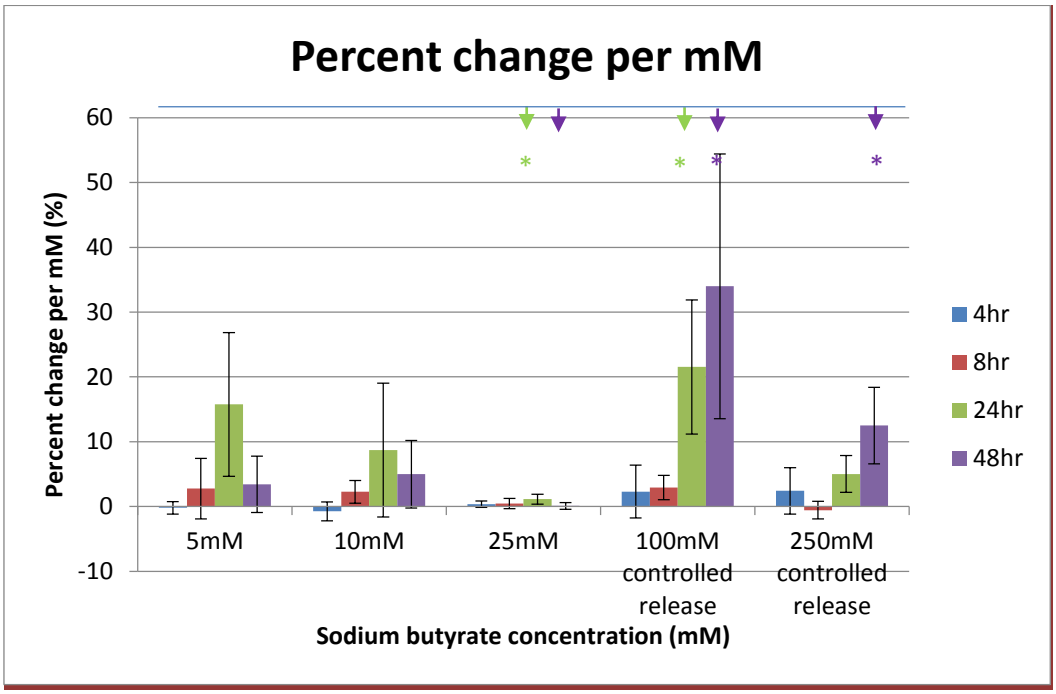

Figure 29: Percent change per mM comparing 5 mM, 10 mM and 25 mM from the bolus dose with 100 mM and 250 mM controlled release. * indicates statistical significance.

4.0 Discussion

4.1 Measurement of Protein Production

The hypothesis of this research was that controlled release of sodium butyrate would result in enhanced protein production from CHO-K1 cells while minimizing the impact on cell viability. One of the first research questions to be addressed was how to measure protein production efficiently.

Various methods can be employed to measure protein production, including ELISA, immunostaining. In this thesis, it was decided to measure the amount of fluorescence emitted by the GFP fusion protein as a measure of recombinant INS/GFP protein production by the CHO K1 INS/GFP cells using image analysis.

First, it was necessary to validate Image J analysis as a method for measuring protein production. Image J is a software program designed for processing scientific images; one use of this software is for measuring fluorescence in images. As such, an ELISA was carried out to measure the protein produced from increasing numbers of cells. This is in agreement with other methods described in literature.

In our study, fluorescent images of the cells were also captured and analysed using Image J and Nikon basic research package to measure the fluorescence emitted by the cells (Figure 15). Correlation analysis showed that a strong correlation was present between protein production and fluorescence (Pearson's Correlation r=0.715) (Figure 17). Therefore, our own analysis corroborated with the literature and showed that measuring fluorescence emitted using Image J can be used as a method for the analysis of protein production rather than ELISA.

Fluorescence detection is widely used in biotechnology due to its sensitivity, specificity and convenience; fluorescence can be up to 1000 times more sensitive than other spectrophotometric techniques (Karoui, 2017). Several examples exist in the literature whereby fluorescence has been compared to ELISA measurements and utilized to quantitate protein expression. Dolled-Filhart *et al*., (2006) examined the relationship between β-catenin expression and breast cancer prognosis. Quantification of β-catenin was assessed by using automated quantitative analysis (AQUA), which was linked to a fluorescence microscopy system. This enabled rapid analysis of immunofluorescence on tissue microarrays. β-catenin protein levels were detected by ELISA and this was compared to AQUA analysis results, which gave a correlation of 0.853. Therefore, through the use of ELISAs and AQUA analysis the concentration of βcatenin could be quantitatively measured.

The use of immunofluorescent microscopy and Image J analysis has also been used by Kaneyoshi *et al*., (2019) in order to determine the location of IgG within CHO cells, with the intention of improving IgG production. Similarly Van der Weken, Cox, & Devriendt, (2019) used Image J analysis to determine the mean fluorescence intensity of CHO cells in order to identify high expressing clones after transfection. This image analysis was then correlated to an anti-porcine IgA sandwich ELISA (which measured the level of antibody in the supernatant). Using Pearson correlation, a strong correlation (r=0.55) was found between antibody production and GFP expression. Based on this correlation and justification, the authors used image analysis instead of ELISA to rapidly select GFP expressing clones.

4.2 Lobster as a Biomaterial

In our study, we used lobster as a delivery vehicle as it is a waste product, accounting for approximately 6,000 tonnes of crab waste a year (Archer, 2008), which is costly to dispose of. Marine organisms are well studied for their biomedical applications (Clarke, Walsh, Maggs *et al*, 2011). Marine organisms have evolved elaborate hierarchical structures giving superior mechanical properties (Studart, 2012). Extensive research has been performed aiming to utilise this hierarchical template in organisms such as coral, cuttlefish, sponges and algae for applications as scaffolds in tissue engineering (Clarke, Walsh, Maggs *et al*, 2011). Efforts to recreate these structures using a biomimetic approach have also been extensively studied. However, the mechanical strength of the bio inspired, synthetic materials differs greatly from that of the natural marine organisms at a nano/microstructural level (Walsh, Fee, Clarke *et al*, 2018). While these studies have used exoskeleton of crab and shrimp for a source of chitin by crushing it, to the best of our knowledge lobster shell has not been utilized in its whole state before (not crushed). Other marine organisms such as coral derived scaffolds have been used to deliver growth factors such as rhVEGF165 to promote angiogenesis in bone healing (Du, Gao, Deng *et al*, 2015) and delivery rhBMP-2 to a critical-sized cranial defect rabbit model (Hou, Chen, Yang *et al*). In line with these studies, it would seem that utilising the hierarchical structure of the lobster shell would harness its natural ability to transport molecules. The lobster shell is mainly composed of chitin; in order for us to obtain a high purity chitin for biomedical applications such as a vehicle for controlled release of the sodium butyrate onto the CHO K1 cells it was important that we first prepared the lobster shell for use in cell culture. To do this it is necessary to remove all proteins, minerals and pigments from the shell which may pose as contaminants to the cell culture (AbdelRahman *et al.*, 2015; Soon *et al.*, 2018).

Demineralisation and deproteination were carried out on the shell using acids and bases, as reported previously by Romano, Fabritius, & Raabe, 2007. In order to confirm that demineralisation was complete, Armin's method was used. This method has been described in a histopathology textbook (reference: Luna LG. Histopathologic methods and color atlas of special stains and tissue artifacts. Gaithersburg (MD): American Histolabs; 1992) and also used by Romano, Fabritius, & Raabe, 2007. Other methods to test for demineralisation include immunohistochemistry, evaluating weight loss of sample and µCT (Fang *et al.*, 2013; Savi *et al.*, 2017).

Previous research in our laboratory of EDX analysis of pretreated and post treated lobster samples showed complete removal of Calcium after treatment with HCL solution (Patton, 2014). This validated Armin's method as a reliable method of determining demineralisation.In Figure 19 it can be seen that all pigments, minerals and proteins have been removed from the shell, resulting in a much more pliable shell, which is free from impurities and can now be used for further analysis. As the shell is much more pliable after removing all the proteins, pigments and minerals this allowed it to be cut into desired sizes easily.

We did not analyse if the removal of proteins was complete. However, it has been reported in the literature that 1M NaOH is widely used for removal of proteins (Younes and Rinaudo, 2015). The absence of pigmentation is a strong indicator that all proteins had been removed. Nuclear magnetic resonance spectroscopy of proteins (NMR), is a method of analysing organic compounds including proteins, the intensity of the peaks produced is directly proportional to the amount of protein present (King *et al.*, 2017). Is it possible that this method could have been used to analyse our lobster samples. Bautista *et al.*, 2001 used NMR to show that demineralisation and deproteinisation were effective for their crayfish samples. They found that before demineralisation the spectrum contained peaks which indicated that large amounts of protein were present however in the demineralised chitin the peaks were not observed in the, showing that proteins were removed by the demineralisation. Sayari *et al.*, 2016 also found no peaks in their NMR spectra, indicating that deacetylation of their lobster samples was complete.

4.3 Analysis of Lobster Biocompatibility

In order to evaluate the effects of the lobster shell on cell viability, testing was carried out which included a direct contact assay and a MEM elution assay. As is evident from Figure 20, the direct contact method of measuring cell viability was not suitable to be used in this instance as the direct contact of the shell onto the cells caused physical damage to the cells which reduced cell viability. However, this is not likely as a result of any toxic effects of the shell to the cells, it is from the physical contact of the shell to the cells. The disadvantage of the direct contact assay is reported in the literature as the risk of physical damage to the cells caused by the sample moving or the weight of the sample crushing the cells, this damage is evident from the patches of missing cells within the healthy cells (Ratner *et al.*, 2004).

Similary Lehmann & Richardson, (2010) carried out experiments to test the impact of assay selection on the outcome of cytotoxicity for the testing of contact lens multi-purpose solutions (MPS) and contact lenses. They found that with the direct contact assay there was significant issues relating to movement and mechanical damage.

The contact lens moved along the cell monolayers resulted in mechanical damage to the cells, causing the lens to fail the cytotoxicity test. They performed a MEM elution assay where extracts prepared from contact lenses were soaked in MPS. All extract strengths passed the criteria of this assay at all time-points, therefore the materials were not found to be cytotoxic.

Kempf, Kimble, & Cuttle, (2011) tested the cytotoxicity of wound dressings using a modified MEM assay; the wound dressings were placed onto cell culture inserts and incubated with a monolayer of cells. This assay allows for testing of the wound dressings without direct contact to the cells, without the inserts as a barrier the dressings would be in direct contact with the cells causing physical damage to the cells which would result in inaccurate results.

After our initial investigation by direct contact assay, a modified MEM elution assay was used to measure the effect of the shell on cell viability. In an attempt to minimise any physical damage to the cells through the direct contact of the shell on the cells, we placed the shell into a cell culture insert. The addition of the shell within the insert into the well with cell monolayers prevented the shell from touching the cells, thereby avoiding any mechanical damage. Figure 21 shows the effect of the shell on the viability of the cells, as measured using neutral red. It can be seen from this that there is no difference in cell viability up to 96 hours of exposure to the shell. Although at 72 hours there is a significant difference between the control and the shell, this is not a concern as it is possible that this difference could be due to variability between shell pieces or cells. Also it should be noted that for all further experiments involving both shell and cells that 48 hours was the maximum time of exposure. From Figure 21 there is no significant difference in the viability of the shell sample compared to the control.

4.4 Pilot Analysis of Sodium Butyrate Adsorption and Release from Lobster Shell

As the lobster shell has not previously been used for the controlled release of sodium butyrate, little was known about its abilities for adsorption and release. For this reason, a pilot study was conducted to determine the dose, exposure time for adsorption onto the shell and release. Initially a wide range of sodium butyrate concentrations were tested along with multiple adsorption and release times. In order for all sample concentrations to fit within the standard curve for GC-MS analysis it was necessary to dilute all samples down to final concentrations of 1 mM and 5 mM. Due to the large number of samples which needed to be analysed from each concentration, dilution, adsorption and release time points, one sample from each experimental condition was analysed on GC-MS before narrowing down the range of experimental conditions to focus on in further investigations.

It was quickly found that samples which had been diluted to 1 mM would not be investigated further as a number of samples were too low to be measured by the GCMS and fell outside the range of the standard curve.

For this reason, samples which had been diluted to 5 mM will be discussed in more detail moving forward. From Table 6 it can be seen that the adsorption values for concentrations 0-25 mM resulted in minimum and inconsistent adsorption of butyrate across all time points tested. In addition, the release values for these concentrations were very low (under 3 mM Tables 7, 8, 9), due to lack of adsorption. It is unlikely that such low milimolar concentrations of sodium butyrate would have much of an effect on increasing protein production as seen in Figure 25. While 5 mM did increase protein production, it is unlikely that anything lower than this would have much of an effect on protein production. For these reasons concentrations of 0, 10, 25 mM were not examined further.

The results from the higher concentrations of sodium butyrate used for adsorption and release (500 and 1000 mM) indicate that the adsorption is more efficient, as approximately 85% of the sodium butyrate was adsorbed by the shell (Table 6). However the release for 500 mM and 1000 mM was low across all time points with a percentage release of less than 15%.

It would seem that the butyrate while adsorbed was not being released efficiently at these concentrations. For this reason both 500 mM and 1000 mM were not investigated further.

For the concentrations 100 mM and 250 mM it was found that the adsorption here was better as both concentrations adsorbed approximately 17-57%, with the better adsorption shown at 48 and 72 hours compared to 24 hours (Table 6). The release values for these concentrations are similar to concentrations tested for the bolus dose study which showed an increase in protein production. With 100 mM releasing 8-17 mM and 250 mM releasing 23-35 mM (Tables 7, 8, 9). It was decided to move forward with a 48 hour adsorption and release time as at 24 hours 100 mM sample only adsorbed 17.22 mM compared to 48 hours where 57.49 mM was adsorbed from the 100 mM sample (Table 6).

4.5 Analysis of Adsorption and Release Data

From the pilot test it was decided to move forward with and analyse the triplicate samples of concentrations of 50, 100 and 250 mM sodium butyrate and 48 hour adsorption time and up to 72 hours release times.

As seen in Table 10, the average release values for 100 mM and 250 mM were 10.45 mM and 33.63 mM respectively. These values were close to that of the bolus dose study concentrations of 10 mM and 25 mM, which showed an increase in protein expression (Figure 25).

4.6 Controlled Release of Sodium Butyrate

For the main controlled release study, the sodium butyrate concentrations used were 100 mM and 250 mM. These concentrations were chosen based on the pilot study and due to the fact that the concentrations released would be tolerable to the cells based on the bolus dose study. The average percent adsorption for 100 mM is 16.87% and for 250 mM is 15.22%.

Concerning adsorption / drug loading, it is common that the percent adsorption is relatively low, Peng *et al*., (2019) found that the percent drug loading of BSA into chitin nano whisker hydrogels was only 10-30%. Gayathri *et al*. (2017) conducted a study comparing the binding efficiencies of different antibacterial drugs using chitin nanocarriers. The adsorption of hydrophilic methacycline (MET) was found to be 25% and the adsorption of hydrophobic ethionamide (ETA) was 45%. It is evident that the hydrophilic drug had a lower binding ability. They found that hydrophobic drugs have a better binding energy towards polymeric nanosystems such as chitin compared to lipophilic drugs. It is possible therefore that the low percent adsorption of sodium butyrate to the lobster shell in our study is due to its hydrophilic nature (Gandhinagar, 2018).

The cumulative percent release for 100 mM and 250 mM is approximately 50% and 60% respectively (Table 11). From our initial testing we also know that the majority of the sodium butyrate is released within the first four hours (Table 11). It is possible that as the majority of the sodium butyrate was released within in the first few hours that this could be a burst release. This mechanism of a burst release seems somewhat common with a number of researchers in controlled release systems. Burst release is the fast release of a large amount of the drug at the start of controlled release (Hezaveh and Muhamad, 2013). Thedrattanawong, Manaspon, & Nasongkla, (2018) noted that for water soluble drugs there is an initial burst release of drugs from the surface, which is then followed by a decreased release rate as the drug diffuses from inside the matrix through to the surface.

The amount of drug released (M_t) with an initial burst, from these systems is estimated by:

$$M_t = \frac{DC_0}{l}\left(t + \frac{l^2}{6D}\right)$$

Where D is the drug diffusion coefficient, C_0 is the drug concentration on the inside of the membrane, and l is the membrane thickness, t is the time (Huang and Brazel, 2001). D, the drug coefficient for sodium butyrate has been reported as 0.041 (Tatevossian, 1979).

When our data is fitted to this model, it predicts a release of 33 mM from the 100 mM sample at 4 hours, and 82 mM from the 250 mM sample at 4 hours. Actual experimental data showed an average release of 28 mM from the 100 mM sample and 72 mM from the 250 mM.

Cai *et al*., (2018) investigated the influence of composition ratios and pH values on the microstructure of chitosan sponges. As the sponge was prepared by freeze drying, this resulted in a porous structure which provides potential space and channels for the containment and delivery of bio factors. The presence of the pores in this sponge are similar to that of the naturally occurring pores of the lobster shell used in this research.

By recycling lobster shell waste, it is possible that the environmental impact of producing chitosan, through the use of strong acids and bases at different stages of demineralization, deproteination and deacetylation could possibly be reduced. The release of three drugs were studied, ibuprofen (IBU) and roxithromicin (ROX) which are hydrophobic drugs; and gentamicin (GEN) a hydrophilic drug. A burst release, which is a rapid release of drug in the initial stages of controlled release was found within the first hour for each sample, this release then stabilized after two hours. They found that after 12 hours the maximum cumulative release of GEN was 32.36% which is much higher than the release of the IBU and ROX which was 5.69% and 0.5% respectively. The sponge swelling was found to be the main driving force for the release of the two hydrophobic drugs.

In a study by Peng *et al*. (2019), investigating controlled release from a hydrogel matrix, a 30% release within the first 20hrs and 50% release within the first 60hrs was described. They hypothesised that the rapid release rates could be due to the concentration difference inside and outside the hydrogel which would accelerate the diffusion of the drug from the hydrogel. This could also be possible in our study with the sodium butyrate on the lobster shell. Dinesh Raja, Mohambed, Joji, *et al*, 2012) found that after 1 hour most of the drug was released from the chitosan nanoparticles; they put this mechanism of release down to non-fickian diffusion. The main difference between Fickian and Non Fickian Diffusion is the presence of boundaries; there are no boundaries in Fickian diffusion.

Non Fickian diffusion has a sharp boundary separating the highly swollen region from a dry, glassy region (Madhusha, 2018).

The equation governing Fickian diffusion is:

$$\frac{M_t}{M_0} = 4\left(\frac{Dt}{\pi h^2}\right)^2$$

Where M_t is the amount of drug released at time t, M_0 is the total mass of drug loaded into the device, D is the diffusion coefficient of the drug and h is the thickness of the scaffold (Fu and Kao, 2010).

This approximation holds for the release of the first 60% of cumulative release, which is applicable to our results. When we fit our data to this model, there is no correlation between the mathematical data and experimental with % differences as large as 90% at timepoints. Therefore, we can reject Fick's diffusion as a release mechanism.

Other models of diffusion proposed in the literature include degradation based and multicomponent systems, which do not apply here. As the burst release equation described above most closely fits our experimental data, we can theorize that the release is largely due to burst.

However it is possible that some of the sodium butyrate adsorbed into the pores present on the shell, and the mechanism of diffusion was due to a number of different diffusion mechanisms. Also Gayathri *et al.*, 2017 described the burst release of 20% in the first hour for both the hydrophilic and hydrophobic drugs. This initial burst levelled off with the hydrophilic MET releasing 54% within the first 24 hours compared to the hydrophobic ETA which released 36% within the same time period. This burst release could be caused by the drug being poorly entrapped inside the matrix or that the drug adsorbed onto the surface of the nanoparticle. Due to the fact that sodium butyrate is hydrophilic it follows the trend of the MET with releasing quickly from the lobster shell, it is also possible that the sodium butyrate simply adsorbed onto the surface of the shell and therefore was quickly released.

Nedjadi, Moran, Al-Rammahi, & Shirazi-Beechey, (2014) identified the mechanism of butyrate transport in equine intestine; they found that the transport of butyrate into the luminal membrane vesicles is energized by a pH gradient. The transport of butyrate is also time and concentration dependant. They found a six-fold increase in butyrate uptake at pH 5.5 compared to pH 8. It is possible that in this research, the pH (7.4) of the cell media could have an effect on the transport of the sodium butyrate. However, it would not be possible in our system to alter the pH of the cell culture media for potential improved sodium butyrate transport as a change in the pH would not be optimal for the cells.

Dozie-Nwachukwu *et al*. (2017) examined the extraction and encapsulation of prodigiosin in chitosan freeze dried microspheres for targeted drug delivery. Prodigiosin is a secondary metabolite extracted from bacteria; it is hydrophilic and exhibits anti-cancer properties. They had encapsulation efficiencies of 60-90%. With regards to drug release it was found that the initial drug released is due to diffusion and burst release, during early stages of release the drug can travel through the pores which formed during the hardening phase.

This is later followed by degradation controlled release for a smaller fraction of the drug. Something similar to this could be the cause for the sodium butyrate in the lobster shell. Any sodium butyrate remaining after the burst release at four hours could be released using chitinases to degrade the shell, releasing the sodium butyrate remaining.

4.7 Cell Viability in response to Bolus Sodium Butyrate Addition

The addition of sodium butyrate to CHO cell cultures for increasing recombinant protein production is known to induce apoptosis in a dose-dependent manner (Seong Lee and and Lee, 2012). It is known that sodium butyrate treatment increases histone acetylation by inhibiting deacetylases, leading to core histone hyperacetylation (Biermann *et al.*, 2011). However the mechanisms by which sodium butyrate induces apoptosis is not fully understood (Mu *et al.*, 2013; Huang *et al.*, 2019).

In order for us to evaluate the effects of varying concentrations of the bolus doses of sodium butyrate on the percent viability of cells fluorescent images were taken during the bolus dose experiment which were analysed using Image J. From the analysis of the fluorescent images, the effect of sodium butyrate on the percent viability on the CHO K1 cells could be determined.

Although apoptosis is the most well understood type of programmed cell death, there are other types of cell death, including pyroptosis, necrosis and autophagy (Kiraz *et al.*, 2016). Autophagy is mainly a pro-survival pathway that cells use when under stress or nutrient depletion; however if autophagy is activated for a long period than this leads to cell death (Zhang *et al.*, 2016).

Kasner *et al.*, (2013) state that autophagy is generally activated at early time points and at low doses of stress and apoptosis is generally activated at late time points and high doses of stress.

It is possible that in our research, the bolus additions of sodium butyrate resulted in immediate increased stress levels within the cells, which were too much for autophagy to control and resulted in the induction of apoptosis or cell cycle inactivation. As observed the addition of higher concentrations of sodium butyrate (100 mM, 175 mM and 250 mM), resulted in a statistically significant decrease in the amount of protein produced (Figure 25). This was probably due to cell death as the viability of the higher concentrations was reduced compared to the lower concentrations and the control (Figure 22). At concentrations greater than 50 mM, a decrease in the cell viability can be seen. Furthermore, a significant decrease in cell viability can be seen as early as 8 hours for 250 mM compared to the control. At 24 hours compared to the control, there is a significant decrease in viability of the cells treated with 50 mM, 100 mM, 175 mM and 250 mM. Finally, at 48 hours there is a significant decrease in viability of the cells treated with concentrations 100 mM, 175 mM and 250 mM. This demonstrates that while a bolus dose of sodium butyrate can increase protein production, it also has a negative impact on cell viability, this is in agreement with Wang *et al*., (2016) who showed a decrease in proliferation, which was linked to increased Bcl-2 expression, a marker of apoptosis at 48 hours.

It is possible that ER stress is induced in our bolus dose experiments but delayed in the controlled release experiments, resulting in reduced cell death. Similarly, Bialik, Dasari and Kimchi, (2018) state that the presence of autophagy does not mean that autophagy is the cause of cell death, rather it reflects that the cell is making efforts to prevent cell death in response to cell stress by removing damaged organelles and proteins. This link of sodium butyrate to endoplasmic reticulum stress is important to note as the endoplasmic reticulum is involved in protein folding, storage and is sensitive to minor changes in its environment such as glucose deprivation, oxidative stress, and infection.

ER stress causes the cell to activate the unfolded protein response which is a self-protection mechanism, however similarly to autophagy, if the unfolded protein response is overwhelmed than apoptosis could be activated. (Hussain, Maldonado-Agurto and Dickson, 2014; Liu *et al.*, 2017).

Conversely, in the controlled release experiments, it is possible that the slower addition of the sodium butyrate resulted in less stress to the cells. It is possible that this level of stress was not high enough to trigger apoptosis or endoplasmic reticulum stress. Seong Lee and & Lee, (2012) found that autophagy appears to work towards cell survival under sodium butyrate treatment, possibly by the elimination of damaged mitochondria.

Similarly Tang, Chen, Jiang, & Nie, (2011) found that under sodium butyrate treatment (1-3 mM) the elimination of damaged mitochondria could slow down the induction of apoptosis. Mitophagy is a selective type of autophagy, which removes damaged or excessive mitochondria (Ding and Yin, 2012).

Therefore, in the controlled release of sodium butyrate-induced autophagy acted as a pro-survival tool for the cells, as the viability of the controlled release concentrations remained above 95% (Figure 23). Although we did not measure such events, we could in the future measure apoptosis (Bcl-2 and PARP-1 cleavage) and autophagy (LC3-II and parkin) using a western blot. It is possible that the cells are undergoing autophagy in the controlled release experiment which could delay cell death.

This evidence of the time of activation of apoptosis and autophagy could be an indicator of why in our research that the controlled release of sodium butyrate resulted in higher cell viability. As suggested previously, autophagy could serve a protective role to cells under sodium butyrate treatment, which could account for the higher cell survival under controlled release exposure. Also, as the majority of sodium butyrate was released over 4 hours, with a further trickle of sodium butyrate release up to 24 hours, it is possible that this somewhat slower addition did not shock the cells and allowed time for autophagy to possibly occur and remove damaged mitochondria allowing for longer/ increased cell viability.

Zhang *et al.*, (2016) showed that under sodium butyrate treatment, autophagy in colorectal cancer cells was mediated by endoplasmic reticulum (ER) stress; they also found that blocking the endoplasmic reticulum stress prevented autophagy and enhanced sodium butyrate induced apoptosis. They suggest that ER stress may be a trigger for autophagy in these cells. The induction of autophagy was confirmed using western blot measuring LC3-II which is a common autophagy marker.

They found that after 24 hours exposure low doses of sodium butyrate (2 mM) induced autophagy, while higher doses (5 mM) showed lower levels of autophagy and high levels of apoptosis. Autophagy induction is consistent with the results published by Tang *et al.*, (2011) indicating autophagy occurred when HCT-116 cells were treated with 1–3mM butyrate.

Similar to our results in Figure 22, Sung, Song, Lim, Chung, & Lee, (2004) found that at day three of culture, up to 10 mM of sodium butyrate had a minimal effect on viability with all cultures remaining over 90%. As seen in Figure 22, the percent viability of the bolus dose cells is negatively impacted in a time and dose dependant manner. Sun *et al.*, (2011) measured apoptosis using Hoechst dye to evaluate the effects of sodium butyrate on nuclear condensation, which is a characteristic of apoptosis. They found that after 24 hours of treatment with 10 mM sodium butyrate that nuclear condensation and fragmentation were induced, which indicates induction of apoptosis.
Wang *et al.*, (2016) investigated sodium butyrate induced apoptosis in MCF-7 breast cancer cells. The concentrations of sodium butyrate added to the cells were 1, 2.5, 5, 10, or 20 mM, cells were cultured with sodium butyrate for 24 and 48 hours. Viability was measured using CCK-8 assays and the absorbance decreased as sodium butyrate concentration increased. In agreement with other studies they found that sodium butyrate reduces cell viability in a time and dose dependant manner. Seong Lee and & Lee, (2012) used a western blot to measure LC3-II protein, which is a marker for autophagy, they found that the percent of GFP positive cells increased with time and concentration of sodium butyrate addition, showing autophagy was induced by sodium butyrate.

Finally to examine the pro survival potential of autophagy, a western blot was carried out to measure the parkin protein (a mitophagy protein). The levels of parkin protein increased in proportion to sodium butyrate concentration indicating sodium butyrate induces mitophagy, which is a mitochondria specific type of autophagy. This indicates that through autophagy and the removal of damaged mitochondria, autophagy could be a pro survival tool as removal of damaged mitochondria prevents the activation of pro apoptotic proteins.

Zhang *et al.*, (2016) note that the mechanisms which determine the autophagic or apoptotic response to sodium butyrate at low and high doses remain to be determined. They also blocked autophagy in order to examine the connection between sodium butyrate induced autophagy and apoptosis. They found that through blocking autophagy, the toxic effects of sodium butyrate were increased, as shown by significantly increased levels of cleaved PARP, suggesting that autophagy protects the cells from apoptosis, as when autophagy was blocked there was an increase in apoptosis.

Similarly, Huang *et al*. (2019) examined the effects of sodium butyrate on both autophagy and apoptosis in NPC nasopharyngeal carcinoma cells. To determine to effect of sodium butyrate on autophagy, fluorescence microscopy was used to measure LC3 puncta, which is an indicator of autophagy flux. They found that with sodium butyrate addition (5 mM for 12 hours) the LC3 puncta significantly increased suggesting that sodium butyrate may induce autophagy. They also found by flow cytometry that autophagy was activated as early as 6 hours (LC3-II was up regulated) and that apoptosis was activated at 12 hours (cleaved-PARP), which suggests that autophagy is activated earlier than apoptosis.

4.8 Cell Viability in Response to Controlled Sodium Butyrate Release

During the controlled release of sodium butyrate experiment, along with measuring protein production and analysing sodium butyrate on GC-MS, fluorescent images were taken to be analysed in order to determine the effects of a controlled release of sodium butyrate on the cell viability.

Concentrations of 100 mM and 250 mM were adsorbed onto the shell and subsequently released into the cell culture. As seen in Table 13, the amount of sodium butyrate released from the 100 mM sample was approximately 7 mM and the amount released from the 250 mM sample was approximately 20 mM. It can be seen in Figure 23 that the percent viability of the 100 mM sample remained above 99.7% over the 48 hour period. Similarly, the 250 mM sample remained above 99% across the 48 hour period, with no significant difference in viability found for either sodium butyrate concentration compared to the control. Keeping in mind that the amounts released from these samples were approximately 7mM and 20 mM, this 99% and higher viability shows higher viability than the bolus dose addition of similar concentrations.

As you can see in Figure 24 comparing the viabilities of the cells for the controlled release experiment alongside the bolus dose experiment, it can be seen that the lowest viability is that of 20 mM sodium butyrate at 24 hours after bolus addition of sodium butyrate. There is a statistical difference between 100mM controlled release compared to 10 mM bolus dose at 24 hours. There is also a statistical difference between 250mM controlled release and 10 mM bolus dose at 24 hours.

This is important to note, keeping in mind that 250 mM actually released approximately 20 mM sodium butyrate onto the cells. While it is not possible to use this data and compare a per milimolar basis, it is fair to conclude that 20 mM of sodium butyrate added to the cells by controlled release using the lobster shell resulted in higher cell viability than 10 mM of a bolus dose of sodium butyrate over the same time period. While the majority of the sodium butyrate was released from the shell in the first 4 hours (Table 11), it is possible that this slower addition of sodium butyrate to the cells resulted in less toxic effects to the cells even though subjected to twice the concentration of sodium butyrate.

This observation could be explained by a dose-dependent effect of butyrate exposure on the cell cycle and a slower induction of pro-apoptotic process in the cell as outlined earlier.

We can compare the beneficial effect seen here with butyrate with other systems, such as glucose addition to cells. Glucose is necessary in mammalian cell culture to allow for consistent growth and protein production. Generally, glucose is added in a bolus dose and this bolus addition can result in a quick change to the cellular environment which results in metabolic deregulation of glucose uptake rate and also increases contamination risk. Goldrick *et al*., (2018) propose a system of glucose addition which correlates the consumption rate of glucose to the oxygen transfer rate, allowing for online glucose measurement. This strategy allows maintenance of glucose levels while avoiding adding bolus doses of glucose and shocking the cells, which could kill them. This glucose controlled system showed similar growth characteristics and product quality to the bolus glucose addition, while also reducing the contamination risk and avoids the risk of a bolus dose of glucose causing a rapid change to the cells environment which could have negative effects. This shows that while glucose is necessary for the cells to grow, a system of on-line glucose control where glucose is automatically added if the levels drop below a set point is preferred to a bolus dose system.

4.9 Increasing Recombinant INS/GFP Protein production by Sodium Butyrate Addition

A major limiting factor in the production of recombinant proteins is the processing events that proteins undergo in the endoplasmic reticulum (Hussain, Maldonado Agurto and Dickson, 2014). With increased protein production, ER stress can be induced by accumulation of misfolded protein, nutrient deprivation, infection, chemical insult all of which can affect recombinant protein production. One mechanism within the cell to try and minimise ER stress is the unfolded protein response (UPR), which tries to overcome ER stress by inhibiting protein synthesis or improving protein processing and translocation; however, if the amount of ER stress is excessive the UPR can induce autophagy, followed by apoptosis.

With regards to recombinant protein production, cell death in cultures limits the viable cell density and could cause changes to product quality due to the release of cellular substances into the media (Hussain, Maldonado-Agurto and Dickson, 2014). All of this results in a decrease in protein production which could result in a monetary loss for the companies producing the recombinant protein.

To date many attempts have been made to improve protein production *in vitro* including supplementation with short-chain fatty acids (Coronel *et al.*, 2016), optimisation of culture conditions (Krause *et al.*, 2010) and development of growth media (Huang *et al.*, 2010; Fan *et al.*, 2015).

Sodium butyrate is known to increase production of recombinant proteins (Chung *et al.*, 2001; Han *et al.*, 2005; Liu *et al.*, 2014). Therefore, it is not surprising that we found an increase in recombinant insulin/GFP production in both the bolus dose and controlled release studies. As found in our research, adding a bolus dose of sodium butyrate (up to 10 mM) to CHO K1 cells results in an increase in protein production over time, although there was no statistical significant increase in protein production, a trend of increasing protein production is evident (Figure 25). However, controlled release of sodium butyrate resulted in a statistically significant increase in protein production for concentrations 250 mM at 24 hours and 100 mM at 48 hours (Figure 26). Although there is no statistically significance at other time points, a trend of increasing protein production is evident from Figure 26.

As sodium butyrate is a histone deacetylase inhibitor, it causes histone acetylation as a result of inhibiting histone deacetylase, which loosens the chromatin packing, leaving the chromatin accessible to transcription factors, which increases transcription (Jeon and Lee, 2007). Jiang and Sharfstein, (2008) examined if sodium butyrate stimulates monoclonal antibody over-expression in CHO cells; of the eight clones tested, three of the clones showed a greater than 2 fold change in mAb production compared to the control, following 48 hours sodium butyrate treatment. Similarly Sung *et al.*, (2004) found that with the addition of 3 mM sodium butyrate resulted in a 6.4-fold increase in qTPO and a 3.3-fold increase in the final Human thrombopoietin (hTPO) concentration on day 4 after butyrate addition compared to the control.

Chung *et al.*, 2012 looked at the effects of sodium butyrate on the production of recombinant hepatitis A virus (HAV) capsid protein VP1 in the culture of stably transfected *Drosophila melanogaster* S2 cells. They found that on day four of culture that 10 mM of sodium butyrate resulted in VP1 production of 104% higher as compared to the control.

When we look at our protein data in terms of fold change for the bolus dose it can be seen that the highest fold change in INS/GFP protein production per cell can be seen at 24 hours with the addition of 10 mM sodium butyrate (Table 14).

This data shows an increase in protein production up to the addition of 50 mM sodium butyrate (fold change = >1). From 100 mM to 250 mM sodium butyrate addition a decrease in protein production can be seen (fold change = <1).

In terms of fold change for the controlled release, it can be seen that the highest fold change in INS/GFP protein production per cell can be seen at 48 hours, with a 5.4 fold increase in protein production for the 100 mM sample compared to the 0 mM control. At 24 hours, 100mM resulted in a 2.8 fold increase and 250 mM resulted in a 2.1 fold increase in protein production (Table 15).

In order to look at the protein production results on a per milimolar basis, percent change per milimolar was calculated (Figure 27). Using per millimolar values allows for a comparison between experiments of the bolus dose and controlled release experiments. In the bolus dose experiment, it can be seen that the greatest percent change can be seen with the addition of 5 mM and 10 mM sodium butyrate.

For the controlled release results, the greatest percent change can be seen for the 100 mM sample at 24 hours (21.5%) and 48 hours (33.99%) (Figure 28). For the 250 mM sample, the greatest percent release was at 48 hours (12.49%). When these results are compared to the bolus dose experiment of 25 mM there is a statistically significant increase in protein production (Figure 29). There was also no significant difference in protein production between both controls of cells only and cells with shell.

4.10 Future Work

While events such as apoptosis or autophagy were not measured in this study, future progression of this work would investigate mechanism of cell death. Western blot could be used to measure for markers of apoptosis and autophagy such as LC3-II or PARP-1 cleavage (Hseu *et al.*, 2019).

Characterisation of lobster shell samples could be conducted using NMR to test for purity (Fukamizo *et al.*, 1986). In order for chitin to be used in medical applications it is important that it is of a high purity and free from any proteins, particularly any proteins which may induce an allergic reaction (King *et al.*, 2017). Thermogravimetric analysis (TGA) could be conducted to give information on absorbance and desorption rates (Zhang *et al.*, 2019), it also gives information on the thermal stability of a material which could be useful for processing the chitin for use in biomedical applications(Romano, Fabritius and Raabe, 2007). It is possible that the controlled release of sodium butyrate could be improved for a more gradual release; possibly through modification of the structural properties of the lobster shell to control pore size or by adding surface modifications to the lobster shell to enhance adsorption and release. Finally, it could be possible to explore using other naturally occurring porous and biocompatible materials.

5.0 Conclusion

The use of recombinant protein drugs in medicine are vital treatment options, especially for rare and genetic disorders and treatment of inflammatory disease. However, these drugs are also some of the most expensive in the marketplace. This is due to the cost of production of recombinant proteins as the production process is highly complex; therefore, the biotechnology industry is constantly striving for improved efficiency and enhanced protein yields. Media supplementation with short chain fatty acids, such as sodium butyrate, is one method which aims to increase recombinant protein production. However, this can often result in reduction in cell viability and therefore a reduction in protein yield due to toxic effects of the sodium butyrate.

The aim of the study was to examine the effects of controlled release of sodium butyrate on recombinant INS/GFP protein production in CHO K1 INS/GFP cells. The study hypothesised that a controlled release mechanism would deliver sodium butyrate in smaller but sustained doses and result in an increase in protein production while avoiding cell toxicity.

Lobster exoskeleton was chosen for the controlled release matrix in this study. As the exoskeleton of the lobster is composed of chitin, it is biocompatible and is available as reused waste from the seafood industry. The lobster shell also contains natural pores which are needed for the transport of nutrients and ions as the lobster moults and regrows its new exoskeleton. It was envisioned that the natural pore system would act as a conduit for the controlled release of sodium butyrate. Also chitin has been used for controlled release of drugs in the form of hydrogels. To examine the ability of the lobster shell for adsorption and release, a large pilot study was conducted examining sodium butyrate release to cell culture media. A range of adsorption and release times were analysed along with a number of sodium butyrate concentrations. Following this pilot study, we then further examined a narrower range of time points and sodium butyrate concentrations for determination of experimental parameters in the cell culture phase of the work. The adsorption and release of sodium butyrate was measured using GC-MS.

To prepare the lobster shell for use in our experiments, all the proteins and minerals had to be removed. Armin's method was used to confirm demineralisation. It was found that the lobster shell regulated the controlled release of sodium butyrate with most of sodium butyrate being released within the first four hours, and with small amounts released after that up to 48 hours. It is thought that the mechanism for this was a burst release.

To examine protein production in cells exposed to sodium butyrate, we correlated the use of ImageJ to measure GFP fluorescence to an indirect sandwich ELISA which used an antibody against GFP. This was done by plating increasing concentrations of CHO-K1 INS/GFP cells and taking fluorescent images. It was found through Pearson's correlation that there was a statistical correlation (Pearson's correlation value 0.715, $r^2 = 0.974$, $p<0.05$) between the GFP measured from fluorescent images and the protein measured by ELISA. This allowed us to move forward using fluorescent images to measure protein production.

Using optimised adsorption time and sodium butyrate concentration determined from the pilot study, exoskeleton samples were loaded with sodium butyrate and added to cells in culture. The cell culture media was saved for GC-MS analysis and cells examined for fluorescence for both GFP expression and cell viability. Through controlled release there was a significant increase observed in protein production at 24 hours for 250 mM and 48 hours for 100 mM. In order to normalise data for comparative analysis of bolus dose and controlled release, percent change per milimolar sodium buyrate was calculated. It was found that there is a significant increase in the percent change of protein production at 24 hours between 25 mM bolus and 100 mM controlled release; there is also a significant increase at 48 hours between 25 mM bolus and both 100 mM and 250 mM controlled release.

Comparing protein production per cell, it can be seen in the bolus dose that there is a trend of increasing protein production, however it is not significant. If we compare this to the controlled release, 100 mM and 250 mM sodium butyrate resulted in significant increases in protein production compared to the control. While this analysis is not per milimolar, the concentrations of sodium butyrate released from 100 mM and 250 mM during controlled release can roughly be compared to 5 mM, 10 mM and 25 mM of the bolus dose. There was no significant increase at these concentrations with bolus dose.

For measurement of cell viability following sodium butyrate exposure, cells were stained with Hoechst and propidium iodide. Following staining, images of the cells were taken using a fluorescent microscope and images were then analysed using ImageJ or the Nikon basic research package. It was found that for the bolus dose, there was a trend of decreasing viability, with a significant decrease at 24 and 48 hours for all concentrations after and including 100 mM. For the controlled release experiment, there was no significant decrease in viability with all samples remaining above 95%. Comparing the bolus dose and controlled release, there is a statistical difference in percent viability between 100 mM Controlled Vs 10 mM bolus at 24 hr, and 250 mM controlled Vs 10 mM bolus at 24 hr. In both cases it is the controlled release values show a significantly higher viability than that of the bolus dose values.

We hypothesise that through controlled release of sodium butyrate to the cells, the toxic effects of sodium butyrate were avoided, particularly early induction of apoptosis and ER stress, resulting in greater protein yields. It is possible that for the controlled release study, autophagy was activated and acted as a pro survival tool for the cells, which resulted in high percentage viability. Compared to the bolus addition of sodium butyrate which resulted in lower cell viability, this possibly overwhelmed the autophagic response and resulted in apoptosis which can be seen from the decline in cell viability in the bolus dose. This research could be used in the production of recombinant proteins including insulin and could result in improved yields and cost savings for companies manufacturing biopharmaceutical drugs, which will ultimately benefit patients through cost reductions.

The use of naturally abundant and biocompatible waste material can potentially enhance the production of recombinant proteins and evade the necessity for synthetic material development while also reducing our carbon footprint. This lobster substrate has never been used for the release of any molecule, this work presents a very novel use of a waste product.

6.0 Bibliography

Abdel-Mohsen, A. M. *et al.* (2016) 'Novel chitin/chitosan-glucan wound dressing: Isolation, characterization, antibacterial activity and wound healing properties', *International Journal of Pharmaceutics*. Elsevier, 510(1), pp. 86–99. doi: 10.1016/J.IJPHARM.2016.06.003.

Abdel-Rahman, R. M. *et al.* (2015) 'Chitin and chitosan from Brazilian Atlantic Coast: Isolation, characterization and antibacterial activity', *International Journal of Biological Macromolecules*. Elsevier, 80, pp. 107–120. doi: 10.1016/J.IJBIOMAC.2015.06.027.

Agarwal, S. K. and Weinstein, L. S. (2017) *Chapter 2 - Epigenetics*. Second Edi, *Genetics of Bone Biology and Skeletal Disease*. Second Edi. Elsevier Inc. doi: 10.1016/B978-012-804182-6/00002-2.

Ahmad, I. *et al.* (2018) 'Overcoming challenges for amplified expression of recombinant proteins using Escherichia coli', *Protein Expression and Purification*. Academic Press, 144, pp. 12–18. doi: 10.1016/J.PEP.2017.11.005.

Ahmed, E. M. (2015) 'Hydrogel: Preparation, characterization, and applications: A review', *Journal of Advanced Research*. Elsevier, 6(2), pp. 105–121. doi: 10.1016/J.JARE.2013.07.006.

Ahuja, G. and Pathak, k (2009) 'Porous carriers for controlled/modulated drug delivery', *Indian Journal of Pharmaceutical Sciences*.

Almo, S. C. and Love, J. D. (2014) 'Better and faster: improvements and optimization for mammalian recombinant protein production.', *Current opinion in structural biology*, 26, pp. 39–43. doi: 10.1016/j.sbi.2014.03.006.

Archana, D., Dutta Kumar, P. and Dutta, J. (2015) 'Chitosan: A Potential Therapeutic Dressing Material for Wound Healing', in *Chitin and Chitosan for Regenerative Medicine*, pp. 193–227.

Archer, M. (2008) 'Management of crustacea processing waste'.

Asiedu, S. *et al.* (2017) 'Microbial Degradation of Lobster Shells to Extract Chitin

Derivatives for Plant Disease Management', *Frontiers in Microbiology*, 8(May), pp. 1–

14. doi: 10.3389/fmicb.2017.00781.

Azad, G. K. *et al.* (2018) 'Modifying Chromatin by Histone Tail Clipping', *Journal of Molecular Biology*. Academic Press, 430(18), pp. 3051–3067. doi: 10.1016/J.JMB.2018.07.013.

Baek, S. W. *et al.* (2018) 'Shellac Films as a Natural Dielectric Layer for Enhanced Electron Transport in Polymer Field-Effect Transistors', *ACS Applied Materials and Interfaces*, 10(22), pp. 18948–18955. doi: 10.1021/acsami.8b03288.

Bandaranayake, A. D. and Almo, S. C. (2014) 'Recent advances in mammalian protein production', *FEBS Letters*. No longer published by Elsevier, 588(2), pp. 253–260. doi:

10.1016/J.FEBSLET.2013.11.035.

Bautista, J. *et al.* (2001) 'Preparation of crayfish chitin by in situ lactic acid production', *Process Biochemistry*, 37(3), pp. 229–234. doi: 10.1016/S0032-9592(01)00202-3.

Berg, J., Tymoczko, J. and Stryer, L. (2001) *Biochemistry 2001*.

Bernkop-Schnürch, A. and Dünnhaupt, S. (2012) 'Chitosan-based drug delivery systems', *European Journal of Pharmaceutics and Biopharmaceutics*. Elsevier, 81(3), pp. 463–469. doi: 10.1016/J.EJPB.2012.04.007.

Bertrand, P. (2010) 'Inside HDAC with HDAC inhibitors', *European Journal of Medicinal Chemistry*, 45(6), pp. 2095–2116. doi: 10.1016/j.ejmech.2010.02.030.

Bialik, S., Dasari, S. K. and Kimchi, A. (2018) 'Autophagy-dependent cell death – where, how and why a cell eats itself to death', *Journal of Cell Science*, 131(18), p. jcs215152. doi: 10.1242/jcs.215152.

Biermann, J. *et al.* (2011) 'Histone deacetylase inhibitors sodium butyrate and valproic acid delay spontaneous cell death in purified rat retinal ganglion cells.',

Molecular vision, 17(October 2010), pp. 395–403. Available at: http://www.pubmedcentral.nih.gov/articlerender.fcgi?artid=3036563&tool=pmcentrez&rendertype=abstract.

Bose, P., Dai, Y. and Grant, S. (2014) 'Histone deacetylase inhibitor (HDACI) mechanisms of action: Emerging insights', *Pharmacology and Therapeutics*, 143(3), pp. 323–336. doi: 10.1016/j.pharmthera.2014.04.004.

Boßelmann, F. *et al.* (2007) 'The composition of the exoskeleton of two crustacea: The American lobster Homarus americanus and the edible crab Cancer pagurus', *Thermochimica Acta*, 463(1–2), pp. 65–68. doi: 10.1016/j.tca.2007.07.018.

Cai, B. *et al.* (2018) 'Preparation, characterization and in vitro release study of drugloaded sodium carboxy-methylcellulose/chitosan composite sponge', *Plos One*, 13(10), p. e0206275. doi: 10.1371/journal.pone.0206275.

Carinhas, N. *et al.* (2013) 'Metabolic signatures of GS-CHO cell clones associated with butyrate treatment and culture phase transition', *Biotechnology and Bioengineering*, 110(12), pp. 3244–3257. doi: 10.1002/bit.24983.

Catalano, M. G. *et al.* (2005) 'Valproic acid induces apoptosis and cell cycle arrest in poorly differentiated thyroid cancer cells', *Journal of Clinical Endocrinology and Metabolism*, 90(3), pp. 1383–1389. doi: 10.1210/jc.2004-1355.

Chakravarty, J. *et al.* (2018) 'Fabrication of porous chitin membrane using ionic liquid and subsequent characterization and modelling studies', *Carbohydrate Polymers*. Elsevier, 198, pp. 443–451. doi: 10.1016/J.CARBPOL.2018.06.101.

Chen, F. *et al.* (2011) 'The combined effect of sodium butyrate and low culture temperature on the production, sialylation, and biological activity of an antibody produced in CHO cells', *Biotechnology and Bioprocess Engineering*, 16(6), pp. 1157–1165. doi: 10.1007/s12257-011-0069-8.

Chen, J. S., Faller, D. V and Spanjaard, R. A. (2003) 'Short-chain Fatty Acid inhibitors of histone deacetylases: promising anticancer therapeutics?', *Curr Cancer Drug Targets*, 3(3), p. 219–36. doi: 10.2174/1568009033481994.

Chen, P.-Y. *et al.* (2008) 'Structure and mechanical properties of crab exoskeletons', *Acta Biomaterialia*. Elsevier, 4(3), pp. 587–596. doi: 10.1016/J.ACTBIO.2007.12.010.

Chrun, E. S., Modolo, F. and Daniel, F. I. (2017) 'Histone modifications: A review about the presence of this epigenetic phenomenon in carcinogenesis', *Pathology - Research and Practice*. Urban & Fischer, 213(11), pp. 1329–1339. doi: 10.1016/J.PRP.2017.06.013.

Chung, B. S. *et al.* (2001) 'Effect of sodium butyrate on glycosylation of recombinant erythropoietin', *Journal of Microbiology and Biotechnology*, 11(6), pp. 1087–1092.

Chung, I. S. *et al.* (2012) ' Enhancement of Protein Productivity of Recombinant Hepatitis A Virus VP1 in Stably Transfected Drosophila melanogaster S2 Cells ', *Journal of Bacteriology and Virology*, 42(1), p. 69. doi: 10.4167/jbv.2012.42.1.69.

Coffey, W. D. *et al.* (2017) 'Ocean acidification leads to altered micromechanical properties of the mineralized cuticle in juvenile red and blue king crabs', *Journal of Experimental Marine Biology and Ecology*. Elsevier, 495, pp. 1–12. doi: 10.1016/J.JEMBE.2017.05.011.

Connolly, R. M., Rudek, M. A. and Piekarz, R. (2017) 'Entinostat: A promising treatment option for patients with advanced breast cancer', *Future Oncology*, 13(13), pp. 1137–1148. doi: 10.2217/fon-2016-0526.

Coronel, J. *et al.* (2016) 'Valeric acid supplementation combined to mild hypothermia increases productivity in CHO cell cultivations', *Biochemical Engineering Journal*. Elsevier, 114, pp. 101–109. doi: 10.1016/J.BEJ.2016.06.031.

Dash, S. (2010) 'kinetic modeling on drug release from controlled drug delivery systems', 67(3), pp. 217–223. doi: 10.2307/3237001.

Datta, J. *et al.* (2016) 'Suberoylanilide hydroxamic acid inhibits growth of head and neck cancer cell lines by reactivation of tumor suppressor microRNAs', *Oral Oncology*. Elsevier Ltd, 56, pp. 32–39. doi: https://doi.org/10.1016/j.oraloncology.2016.02.015.

Davies, C. E. *et al.* (2014) 'A comparison of the structure of American (Homarus americanus) and European (Homarus gammarus) lobster cuticle with particular reference to shell disease susceptibility', *Journal of Invertebrate Pathology*. Academic Press, 117, pp. 33–41. doi: 10.1016/J.JIP.2014.01.001.

Deacetylase, H. and Davie, J. R. (2003) 'Inhibition of Histone Deacetylase Activity by Butyrate', *Breast Cancer Research*, 133(7 Suppl), pp. 2485–2493. doi: 10.1359/JBMR.040123.

Demain, A. L. and Vaishnav, P. (2009) 'Production of recombinant proteins by microbes and higher organisms', *Biotechnology Advances*. Elsevier, 27(3), pp. 297–306. doi: 10.1016/J.BIOTECHADV.2009.01.008.

Dhaliwal, S. *et al.* (2008) 'Mucoadhesive Microspheres for Gastroretentive Delivery of Acyclovir: In Vitro and In Vivo Evaluation', *The AAPS Journal*.

Dinesh Raja, A. *et al.* (2012) 'Design and evaluation of chitosan nanoparticles as novel drug carriers for the delivery of donepezil', *Iranian Journal of Pharmaceutical Sciences*, 8(3), pp. 155–164.

Ding, W. X. and Yin, X. M. (2012) 'Mitophagy: Mechanisms, pathophysiological roles, and analysis', *Biological Chemistry*, 393(7), pp. 547–564. doi: 10.1515/hsz-20120119.

Dolled-Filhart, M. *et al.* (2006) 'Quantitative in situ analysis of β-catenin expression in breast cancer shows decreased expression is associated with poor outcome', *Cancer Research*, 66(10), pp. 5487–5494. doi: 10.1158/0008-5472.CAN-06-0100.

Dozie-Nwachukwu, S. O. *et al.* (2017) 'Extraction and encapsulation of prodigiosin in chitosan microspheres for targeted drug delivery', *Materials Science and Engineering: C*. Elsevier, 71, pp. 268–278. doi: 10.1016/J.MSEC.2016.09.078. *drugs.com* (2019).

Duan, B. *et al.* (2018) 'Recent advances in chitin based materials constructed via physical methods', *Progress in Polymer Science*. Pergamon, 82, pp. 1–33. doi: 10.1016/J.PROGPOLYMSCI.2018.04.001.

Eckschlager, T. *et al.* (2017) 'Histone deacetylase inhibitors as anticancer drugs', *International Journal of Molecular Sciences*, 18(7), pp. 1–25. doi: 10.3390/ijms18071414.

Edelstein, L. C. *et al.* (2009) 'Short Communication: Activation of Latent HIV Type 1 Gene Expression by Suberoylanilide Hydroxamic Acid (SAHA), an HDAC Inhibitor Approved for Use to Treat Cutaneous T Cell Lymphoma', *AIDS Research and Human Retroviruses*, 25(9), pp. 883–887. doi: 10.1089/aid.2008.0294.

Elgadir, M. A. *et al.* (2015) 'Impact of chitosan composites and chitosan nanoparticle composites on various drug delivery systems: A review', *Journal of Food and Drug Analysis*. Elsevier, 23(4), pp. 619–629. doi: 10.1016/J.JFDA.2014.10.008.

Elvir, L. *et al.* (2017) 'Epigenetic regulation of motivated behaviors by histone deacetylase inhibitors', *Neuroscience and Biobehavioral Reviews*. Elsevier, (January), pp. 0–1. doi: 10.1016/j.neubiorev.2017.09.030.

Fan, Y. *et al.* (2015) 'Amino acid and glucose metabolism in fed-batch CHO cell culture affects antibody production and glycosylation', *Biotechnology and Bioengineering*, 112(3), pp. 521–535. doi: 10.1002/bit.25450.

Fazary, A. E., Ju, Y. H. and Abd-Rabboh, H. S. M. (2017) 'How does chromatin package DNA within nucleus and regulate gene expression?', *International Journal of Biological Macromolecules*. Elsevier B.V., 101, pp. 862–881. doi: 10.1016/j.ijbiomac.2017.03.165.

Fang, J. K. H. *et al.* (2013) 'Methods to quantify components of the excavating sponge Cliona orientalis Thiele, 1900', *Marine Ecology*, 34(2), pp. 193–206. doi: 10.1111/maec.12005.

FDA (2018) *What Are 'Biologics' Questions and Answers*. Available at: https://www.fda.gov/AboutFDA/CentersOffices/OfficeofMedicalProductsandTobacco/CBER/ucm133077.htm.

Fisher, A. *et al.* (2010) 'Pharmacokinetic comparisons of three nasal fentanyl formulations; pectin, chitosan and chitosan-poloxamer 188', *Int. Journal of Clinical Pharmacology and Therapeutics*, 48, pp. 138–145.

Fu, Y. and Kao, W. J. (2010) 'Drug release kinetics and transport mechanisms of nondegradable and degradable polymeric delivery systems', *Expert Opinion on Drug Delivery*, 7(4), pp. 429–444. doi: 10.1517/17425241003602259.

Fukamizo, T. *et al.* (1986) 'Analysis of chitin structure by nuclear magnetic resonance spectroscopy and chitinolytic enzyme digestion', *Archives of Biochemistry and Biophysics*. Academic Press, 249(1), pp. 15–26. doi: 10.1016/0003-9861(86)90555-2.

Gandhinagar, G. (2018) *Bluecross Animal Healthcare Pvt Ltd*.

Gayathri, N. K. *et al.* (2017) 'Preparation, characterization, drug release and computational modelling studies of antibiotics loaded amorphous chitin nanoparticles', *Carbohydrate Polymers*. Elsevier, 177, pp. 67–76. doi: 10.1016/J.CARBPOL.2017.08.112.

Ginsburg, E. *et al.* (1973) 'Growth Inhibition and Morphological Changes Caused by Lipophilic Acids in Mammalian Cells', *Proceedings of the National Academy of Sciences*, 70(8), pp. 2457–2461. doi: 10.1073/pnas.70.8.2457.

Giri, T. K. *et al.* (2012) 'Modified chitosan hydrogels as drug delivery and tissue engineering systems: present status and applications', *Acta Pharmaceutica Sinica B*. Elsevier, 2(5), pp. 439–449. doi: 10.1016/J.APSB.2012.07.004.

Goldrick, S. *et al.* (2018) 'On-Line Control of Glucose Concentration in High-Yielding Mammalian Cell Cultures Enabled Through Oxygen Transfer Rate Measurements', 1700607. doi: 10.1002/biot.201700607.

Goodsell, D. S. (2003) 'The Molecular Perspective: Histone Deacetylase', *The Oncologist: Fundamentals of Cancer Medicine*, 8, pp. 389–391. Available at: http://www.scripps.edu/pub/goodsell.

Grant, S. and Dai, Y. (2012) 'Chapter Six – Histone Deacetylase Inhibitors and Rational Combination Therapies', *Advances in cancer research*, 116, p. 199.

Griffith, D. M. *et al.* (2011) 'Novel trans-platinum complexes of the histone deacetylase inhibitor valproic acid; synthesis, in vitro cytotoxicity and mutagenicity', *Journal of Inorganic Biochemistry*, 105(6), pp. 793–799. doi:

10.1016/j.jinorgbio.2011.03.001.

Haberland, M., Montgomery, R. L. and Olson, E. N. (2009) 'The many roles of histone deacetylases in development and physiology: implications for disease and therapy.', *Nature reviews. Genetics*, 10(1), pp. 32–42. doi: 10.1038/nrg2485.

Hamed, I., Özogul, F. and Regenstein, J. M. (2016) 'Industrial applications of crustacean by-products (chitin, chitosan, and chitooligosaccharides): A review', *Trends in Food Science & Technology*. Elsevier, 48, pp. 40–50. doi: 10.1016/J.TIFS.2015.11.007.

Han, K. O. *et al.* (2005) 'Effect of N-acetylcystein on butyrate-treated chinese hamster ovary cells to improve the production of recombinant human interferon-β-1a', *Biotechnology Progress*, 21(4), pp. 1154–1164. doi: 10.1021/bp050057v.

Handy, D., Castro, R. and Loscalzo, J. (2011) 'Epigenetic Modifications Basic Mechanisms and Role in Cardiovascular Disease', *Circulation*, 123(19), pp. 2145–2156. doi: 10.1161/CIRCULATIONAHA.110.956839.Epigenetic.

Harcum, S. W. and Lee, K. H. (2016) 'CHO Cells Can Make More Protein', *Cell Systems*. Cell Press, 3(5), pp. 412–413. doi: 10.1016/J.CELS.2016.11.007.

Hassainia, A., Satha, H. and Boufi, S. (2018) 'Chitin from Agaricus bisporus: Extraction and characterization', *International Journal of Biological Macromolecules*. Elsevier, 117, pp. 1334–1342. doi: 10.1016/J.IJBIOMAC.2017.11.172.

Hezaveh, H. and Muhamad, I. I. (2013) 'Controlled drug release via minimization of burst release in pH-response kappa-carrageenan/polyvinyl alcohol hydrogels', *Chemical Engineering Research and Design*. Institution of Chemical Engineers, 91(3), pp. 508–519. doi: 10.1016/j.cherd.2012.08.014.

Hoffman, A. S. (2008) 'The origins and evolution of "controlled" drug delivery systems', *Journal of Controlled Release*. Elsevier, 132(3), pp. 153–163. doi: 10.1016/J.JCONREL.2008.08.012.

Horton, R. *et al.* (2006) 'Principles of Biochemistry Fourth Edition', in *Principles of biochemistry Fourth edition*, pp. 599–604.

Huang, W. *et al.* (2019) 'Sodium butyrate induces autophagic apoptosis of nasopharyngeal carcinoma cells by inhibiting AKT/mTOR signaling', *Biochemical and Biophysical Research Communications*. Academic Press. doi: 10.1016/J.BBRC.2019.04.111.

Huang, X. and Brazel, C. S. (2001) 'On the importance and mechanisms of burst release in matrix-controlled drug delivery systems', *Journal of Controlled Release*. Elsevier, 73(2–3), pp. 121–136. doi: 10.1016/S0168-3659(01)00248-6.

Huang, Y. M. *et al.* (2010) 'Maximizing productivity of CHO cell-based fed-batch culture using chemically defined media conditions and typical manufacturing equipment.', *Biotechnology progress*, 26(5), pp. 1400–1410. doi: 10.1002/btpr.436.

Hseu, Y.-C. *et al.* (2019) 'Kalantuboside B induced apoptosis and cytoprotective autophagy in human melanoma A2058 cells: An in vitro and in vivo study', *Free Radical Biology and Medicine*. Pergamon, 143, pp. 397–411. doi: 10.1016/J.FREERADBIOMED.2019.08.015.

Hussain, H., Maldonado-Agurto, R. and Dickson, A. J. (2014) 'The endoplasmic reticulum and unfolded protein response in the control of mammalian recombinant protein production', *Biotechnology Letters*, 36(8), pp. 1581–1593. doi: 10.1007/s10529-014-1537-y.

Jefferis, R. (2016) 'Posttranslational modifications and the immunogenicity of biotherapeutics', *Journal of Immunology Research*, 2016. doi: 10.1155/2016/5358272.

Jenkins, N., Murphy, L. and Tyther, R. (2008) 'Post-translational modifications of recombinant proteins: Significance for biopharmaceuticals', *Molecular Biotechnology*, 39(2), pp. 113–118. doi: 10.1007/s12033-008-9049-4.

Jeon, M. K. and Lee, G. M. (2007) 'Correlation between enhancing effect of sodium butyrate on specific productivity and mRNA transcription level in recombinant Chinese hamster ovary cells producing antibody', *Journal of Microbiology and Biotechnology*, 17(6), pp. 1036–1040.

Jiang, Z. and Sharfstein, S. T. (2008) 'Sodium butyrate stimulates monoclonal antibody over-expression in CHO cells by improving gene accessibility', *Biotechnology and Bioengineering*, 100(1), pp. 189–194. doi: 10.1002/bit.21726.

Joon, C. Y. *et al.* (2008) 'Genomic and proteomic exploration of CHO and hybridoma cells under sodium butyrate treatment', *Biotechnology and Bioengineering*, 99(5), pp. 1186–1204. doi: 10.1002/bit.21665.

Kaneyoshi, K. *et al.* (2019) 'Analysis of intracellular IgG secretion in Chinese hamster ovary cells to improve IgG production', *Journal of Bioscience and Bioengineering*. Elsevier, 127(1), pp. 107–113. doi: 10.1016/J.JBIOSC.2018.06.018.

Kantardjieff, A. *et al.* (2010) 'Transcriptome and proteome analysis of Chinese hamster ovary cells under low temperature and butyrate treatment', *Journal of Biotechnology*, 145(2), pp. 143–159. doi: 10.1016/j.jbiotec.2009.09.008.

Karoui, R. (2017) 'Methodologies for the Characterization of the Quality of Dairy Products', *Advances in Food and Nutrition Research*. Academic Press, 82, pp. 237–275. doi: 10.1016/BS.AFNR.2016.12.007.

Kasner, E. *et al.* (2013) 'Self-consumption: the interplay of autophagy and apoptosis Guillermo', *Nat Rev Mol Cell Biol. 2014*, 70(4), pp. 646–656. doi: 10.1002/ana.22528.Toll-like.

Kawata, M. *et al.* (2016) 'Biomineralization of calcium phosphate crystals on chitin nanofiber hydrogel for bone regeneration material', *Carbohydrate Polymers*. Elsevier, 136, pp. 964–969. doi: 10.1016/J.CARBPOL.2015.10.009.

Kempf, M., Kimble, R. M. and Cuttle, L. (2011) 'Cytotoxicity testing of burn wound dressings, ointments and creams: A method using polycarbonate cell culture inserts on a cell culture system', *Burns*. Elsevier, 37(6), pp. 994–1000. doi: 10.1016/J.BURNS.2011.03.017.

Kim, Y. J. *et al.* (2001) 'Controlled release of insulin from injectable biodegradable triblock copolymer', *Pharmaceutical Research*, 18(4), pp. 548–550. doi: 10.1023/A:1011074915438.

Kim, Y. J. *et al.* (2013) 'Autophagy and its implication in Chinese hamster ovary cell culture', *Biotechnology Letters*, 35(11), pp. 1753–1763. doi: 10.1007/s10529-0131276-5.

King, C. *et al.* (2017) 'Measuring the Purity of Chitin with a Clean, Quantitative Solid-State NMR Method', *ACS Sustainable Chemistry and Engineering*, 5(9), pp. 8011–8016. doi: 10.1021/acssuschemeng.7b01589.

Kiraz, Y. *et al.* (2016) 'Major apoptotic mechanisms and genes involved in apoptosis', *Tumor Biology*, 37(7), pp. 8471–8486. doi: 10.1007/s13277-016-5035-9.

Kohrs, N. J. *et al.* (2019) 'Drug Delivery Systems and Controlled Release', *Encyclopedia of Biomedical Engineering*. Elsevier, pp. 316–329. doi: 10.1016/B978-0-12-801238-
3.11037-2.

Kouzarides, T. (2007) 'Chromatin Modifications and Their Function', *Cell*, 128(4), pp. 693–705. doi: 10.1016/j.cell.2007.02.005.

Krause, M. *et al.* (2010) 'Microbial Cell Factories A novel fed-batch based cultivation method provides high cell-density and improves yield of soluble', *Microbial Cell Factories*, pp. 1–11. doi: 10.1186/1475-2859-9-11.

Kumar, A., Vimal, A. and Kumar, A. (2016) 'Why Chitosan? From properties to perspective of mucosal drug delivery', *International Journal of Biological Macromolecules*. Elsevier, 91, pp. 615–622. doi: 10.1016/J.IJBIOMAC.2016.05.054.

Kumar, N., Gammell, P. and Clynes, M. (2007) 'Proliferation control strategies to improve productivity and survival during CHO based production culture: A summary of recent methods employed and the effects of proliferation control in product secreting CHO cell lines', *Cytotechnology*, 53(1–3), pp. 33–46. doi: 10.1007/s10616007-9047-6.

Kwon, K.-C. *et al.* (2019) 'An evaluation of microalgae as a recombinant protein oral delivery platform for fish using green fluorescent protein (GFP)', *Fish & Shellfish Immunology*. Academic Press, 87, pp. 414–420. doi: 10.1016/J.FSI.2019.01.038.

Lagassé, H. A. D. *et al.* (2017) 'Recent advances in (therapeutic protein) drug development', *F1000Research*, 6, p. 113. doi: 10.12688/f1000research.9970.1.

Lakshmaiah *et al.* (2014) 'Epigenetic therapy of cancer with histone deacetylase inhibitors', *J Cancer Res Ther*, 10(3), p. 469. doi: 10.4103/0973-1482.137937.

Lalonde, M.-E. and Durocher, Y. (2017) 'Therapeutic glycoprotein production in mammalian cells', *Journal of Biotechnology*. Elsevier, 251, pp. 128–140. doi: 10.1016/J.JBIOTEC.2017.04.028.

Lam, J. *et al.* (2015) 'Strategies for controlled delivery of biologics for cartilage repair',

Advanced Drug Delivery Reviews. Elsevier, 84, pp. 123–134. doi: 10.1016/J.ADDR.2014.06.006.

Lawrence, M., Daujat, S. and Schneider, R. (2016) 'Lateral Thinking: How Histone Modifications Regulate Gene Expression', *Trends in Genetics*. Elsevier Current Trends, 32(1), pp. 42–56. doi: 10.1016/J.TIG.2015.10.007.

Lehmann, D. M. and Richardson, M. E. (2010) 'Impact of assay selection and study design on the outcome of cytotoxicity testing of medical devices: The case of multipurpose vision care solutions', *Toxicology in Vitro*. Pergamon, 24(4), pp. 1306–1313. doi: 10.1016/J.TIV.2010.02.018.

Liaqat, F. and Eltem, R. (2018) 'Chitooligosaccharides and their biological activities: A comprehensive review', *Carbohydrate Polymers*. Elsevier, 184, pp. 243–259. doi: 10.1016/J.CARBPOL.2017.12.067.

Lim, S. H. and Hudson, S. M. (2003) 'Review of chitosan and its derivatives as antimicrobial agents and their uses as textile chemicals', *Journal of Macromolecular Science - Polymer Reviews*, 43(2), pp. 223–269. doi: 10.1081/MC-120020161.

Ling, S. *et al.* (2018) 'Biopolymer nanofibrils: Structure, modeling, preparation, and applications', *Progress in Polymer Science*. Pergamon, 85, pp. 1–56. doi: 10.1016/J.PROGPOLYMSCI.2018.06.004.

Liu, B. *et al.* (2017) 'Quantitative assessment of cell fate decision between autophagy and apoptosis', *Scientific Reports*, 7(1), pp. 1–14. doi: 10.1038/s41598-017-18001-w.

Liu, Y. *et al.* (2014) 'Sodium butyrate enhances the acidic isoform content of recombinant human erythropoietin produced by Chinese hamster ovary cells', *Biotechnology Letters*, 36(5), pp. 907–911. doi: 10.1007/s10529-013-1442-9.

Madhusha (2018) *Difference Between Fickian and Non Fickian Diffusion*.

Market Watch (2018) *Advanced Drug Delivery Systems - A Global Market Overview*, *Controlled Release Drug Delivery Market Analysis Report By Technology (Implants, Transdermal, Microencapsulation, Targeted Delivery), By Release Mechanism, By Application, And Segment Forecasts, 2018 – 2025.*

Matthews, T. E. *et al.* (2016) 'Closed loop control of lactate concentration in mammalian cell culture by Raman spectroscopy leads to improved cell density, viability, and biopharmaceutical protein production', *Biotechnology and Bioengineering*, 113(11), pp. 2416–2424. doi: 10.1002/bit.26018.

MBL INTERNATIONAL (2016) *MBL International Corporation*.

McCabe, C. (2015) *A study of the effects of sodium propionate on IgG expression of CHO-DP12 cells*.

McKenzie, E. A. and Abbott, W. M. (2018) 'Expression of recombinant proteins in insect and mammalian cells', *Methods*. Academic Press, 147, pp. 40–49. doi: 10.1016/J.YMETH.2018.05.013.

Miao, T. *et al.* (2018) 'Polysaccharide-Based Controlled Release Systems for Therapeutics Delivery and Tissue Engineering: From Bench to Bedside', *Advanced Science*, 5(4). doi: 10.1002/advs.201700513.

Micelli, C. and Rastelli, G. (2015) 'Histone deacetylases: structural determinants of inhibitor selectivity', *Drug Discovery Today*. Elsevier Current Trends, 20(6), pp. 718–735. doi: 10.1016/J.DRUDIS.2015.01.007.

Mimura, Y. *et al.* (2001) 'Butyrate increases production of human chimeric IgG in

CHO-K1 cells whilst maintaining function and glycoform profile', *Journal of Immunological Methods*, 247(1–2), pp. 205–216. doi: 10.1016/S00221759(00)00308-2.

Misztak, P., Pańczyszyn-Trzewik, P. and Sowa-Kućma, M. (2018) 'Histone deacetylases (HDACs) as therapeutic target for depressive disorders', *Pharmacological Reports*. Elsevier, 70(2), pp. 398–408. doi: 10.1016/J.PHAREP.2017.08.001.

Moncada, C. (2018) *Post-Translational Modification (PTM) Antibodies*. Available at: https://rockland-inc.com/post-translational-modification-antibodies.aspx (Accessed: 11 December 2018).

Moorkens, E. *et al.* (2017) 'The market of biopharmaceutical medicines: A snapshot of a diverse industrial landscape', *Frontiers in Pharmacology*, 8(JUN). doi: 10.3389/fphar.2017.00314.

Mottamal, M. *et al.* (2015) 'Histone Deacetylase Inhibitors in Clinical Studies as Templates for New Anticancer Agents', *Molecules*, 20(3), pp. 3898–3941. doi: 10.3390/molecules20033898.

Mu, D. *et al.* (2013) 'Sodium Butyrate Induces Growth Inhibition and Apoptosis in Human Prostate Cancer DU145 Cells by Up-Regulation of the Expression of Annexin A1', *PLoS ONE*, 8(9), pp. 2–9. doi: 10.1371/journal.pone.0074922.

Na, L. *et al.* (2010) 'Comparison of different absorption enhancers on the intranasal absorption of isosorbide dinitrate in rats', *International Journal of Pharmaceutics*. Elsevier, 397(1–2), pp. 59–66. doi: 10.1016/J.IJPHARM.2010.06.048.

Nayak, A. K. *et al.* (2018) 'Drug delivery: Present, past, and future of medicine', *Applications of Nanocomposite Materials in Drug Delivery*. Woodhead Publishing, pp. 255–282. doi: 10.1016/B978-0-12-813741-3.00012-1.

Nedjadi, T. *et al.* (2014) 'Characterization of butyrate transport across the luminal membranes of equine large intestine', *Experimental Physiology*, 99(10), pp. 1335–1347. doi: 10.1113/expphysiol.2014.077982.

Nguyen, A. H. *et al.* (2015) 'Gelatin methacrylate microspheres for controlled growth factor release', *Acta Biomaterialia*. Elsevier, 13, pp. 101–110. doi: 10.1016/J.ACTBIO.2014.11.028.

Noh, S. M., Sathyamurthy, M. and Lee, G. M. (2013) 'Development of recombinant Chinese hamster ovary cell lines for therapeutic protein production', *Current Opinion in Chemical Engineering*, 2(4), pp. 391–397. doi: 10.1016/j.coche.2013.08.002.

Osswald, C. R. and Kang-Mieler, J. J. (2016) 'Controlled and Extended In Vitro Release of Bioactive Anti-Vascular Endothelial Growth Factors from a Microsphere-Hydrogel Drug Delivery System', *Current Eye Research*, 41(9), pp. 1216–1222. doi: 10.3109/02713683.2015.1101140.

Overton, T. W. (2014) 'Recombinant protein production in bacterial hosts', *Drug Discovery Today*. Elsevier Current Trends, 19(5), pp. 590–601. doi: 10.1016/J.DRUDIS.2013.11.008.

Park, J. *et al.* (2017) *Deacetylase Inhibitors*. Second Edi, *Handbook of Epigenetics*. Second Edi. Elsevier Inc. doi: 10.1016/B978-0-12-805388-1/00040-7.

Pastor, E. *et al.* (2011) 'Protein delivery based on uncoated and chitosan-coated mesoporous silicon microparticles', *Colloids and Surfaces B: Biointerfaces*. Elsevier B.V., 88(2), pp. 601–609. doi: 10.1016/j.colsurfb.2011.07.049.

Pastor, E. L. *et al.* (2015) 'Pore size is a critical parameter for obtaining sustained protein release from electrochemically synthesized mesoporous silicon microparticles', *PeerJ*, 2015(10), pp. 1–12. doi: 10.7717/peerj.1277.

Patton, D. (2014) *A Preliminary Investigation into the Exoskeleton of European Lobster (Homarus gammarus) and Edible Crab (Cancer pagurus) as a source of Hierarchically Structured Chitin based Tissue Engineering Scaffolds for the Regeneration of Human Bone*.

Peng, C. *et al.* (2019) 'The preparation of α-chitin nanowhiskers-poly (vinyl alcohol) hydrogels for drug release', *International Journal of Biological Macromolecules*. Elsevier B.V, p. #pagerange#. doi: 10.1016/j.ijbiomac.2019.03.015.

Petrich, A. and Nabhan, C. (2016) 'Use of class I histone deacetylase inhibitor romidepsin in combination regimens', *Leukemia and Lymphoma*, 57(8), pp. 1755–1765. doi: 10.3109/10428194.2016.1160082.

Puvvada, Y. S., Vankayalapati, S. and Sukhavasi, S. (2012) 'Extraction of chitin from chitosan from exoskeleton of shrimp for application in the pharmaceutical industry', *International Current Pharmaceutical Journal*. doi: 10.3329/icpj.v1i9.11616.

Qiu, X. *et al.* (2017) 'Histone deacetylases inhibitors (HDACis) as novel therapeutic application in various clinical diseases', *Progress in Neuro-Psychopharmacology and Biological Psychiatry*. Elsevier, 72, pp. 60–72. doi: 10.1016/J.PNPBP.2016.09.002.

Raabe, D. *et al.* (2006) 'Microstructure and crystallographic texture of the chitinprotein network in the biological composite material of the exoskeleton of the lobster Homarus americanus', *Materials Science and Engineering A*. doi: 10.1016/j.msea.2005.09.115.

Raabe, D., Sachs, C. and Romano, P. (2005) 'The crustacean exoskeleton as an example of a structurally and mechanically graded biological nanocomposite material', *Acta Materialia*. doi: 10.1016/j.actamat.2005.05.027.

Ratner, B. D. *et al.* (2004) *Biomaterials Science: An Introduction to Materials in Medicine*. Available at: https://books.google.ie/books?id=9PMU1iYGe34C&lr=&source=gbs_navlinks_s.

Rbpaonline (2018) *rbpaonline.com*, *October 31st, 2018*.

Repetto, G., del Peso, A. and Zurita, J. L. (2008) 'Neutral red uptake assay for the estimation of cell viability/ cytotoxicity', *Nature Protocols*, 3(7), pp. 1125–1131. doi: 10.1038/nprot.2008.75.

Richelle, A. and Lewis, N. E. (2017) 'Improvements in protein production in mammalian cells from targeted metabolic engineering', *Current Opinion in Systems Biology*. Elsevier, 6, pp. 1–6. doi: 10.1016/J.COISB.2017.05.019.

Rikiishi, H. (2011) 'Autophagic and Apoptotic Effects of HDAC Inhibitors on Cancer Cells', *Journal of Biomedicine and Biotechnology*, 2011, pp. 1–9. doi: 10.1155/2011/830260.

Rinaudo, M. (2006) 'Chitin and chitosan: Properties and applications', *Progress in Polymer Science*. Pergamon, 31(7), pp. 603–632. doi: 10.1016/J.PROGPOLYMSCI.2006.06.001.

Roda, A. *et al.* (2007) 'A new oral formulation for the release of sodium butyrate in the ileo-cecal region and colon', *World J Gastroenterol*, 13(7), pp. 1079–1084. Available at: www.wjgnet.com.

Romano, P., Fabritius, H. and Raabe, D. (2007) 'The exoskeleton of the lobster Homarus americanus as an example of a smart anisotropic biological material', *Acta Biomaterialia*, Volume 3(Issue 3), p. Pages 301-309. doi:10.1016/j.actbio.2006.10.003.

de Ruijter, A. J. M. *et al.* (2003) 'Histone deacetylases (HDACs): characterization of the classical HDAC family.', *The Biochemical journal*, 370(Pt 3), pp. 737–749. doi: 10.1042/BJ20021321.

Sachs, C., Fabritius, H. and Raabe, D. (2007) 'Influence of microstructure on deformation anisotropy of mineralized cuticle from the lobster Homarus americanus'. doi: 10.1016/j.jsb.2007.09.022.

Sachs, C., Fabritius, H. and Raabe, D. (2008) 'Influence of microstructure on deformation anisotropy of mineralized cuticle from the lobster Homarus americanus', *Journal of Structural Biology*. Academic Press, 161(2), pp. 120–132. doi: 10.1016/J.JSB.2007.09.022.

Samrot, A. V. *et al.* (2018) 'Synthesis of curcumin loaded polymeric nanoparticles from crab shell derived chitosan for drug delivery', *Informatics in Medicine Unlocked*. Elsevier, 10, pp. 159–182. doi: 10.1016/J.IMU.2017.12.010.

Sasiak, A. B. and Sesardic, D. (1997) 'Controlled release vaccines', *Journal of Medical Microbiology*, 46(12), pp. 975–977. doi: 10.1007/978-3-642-29648-2. Savi, F. M. *et al.* (2017) 'Comparison of Different Decalcification Methods Using Rat Mandibles as

a Model', *Journal of Histochemistry and Cytochemistry*, 65(12), pp. 705–722. doi: 10.1369/0022155417733708.

Sayari, N. *et al.* (2016) 'Chitin and chitosan from the Norway lobster by-products: Antimicrobial and anti-proliferative activities', *International Journal of Biological Macromolecules*. Elsevier, 87, pp. 163–171. doi: 10.1016/J.IJBIOMAC.2016.02.057.

Sung, Y. H. *et al.* (2004) 'Effect of sodium butyrate on the production, heterogeneity and biological activity of human thrombopoietin by recombinant Chinese hamster ovary cells', *Journal of Biotechnology*. Elsevier, 112(3), pp. 323–335. doi: 10.1016/J.JBIOTEC.2004.05.003.

Seong Lee and, J. and Lee, G. M. (2012) 'Effect of sodium butyrate on autophagy and apoptosis in Chinese hamster ovary cells', *Biotechnology Progress*, 28(2), pp. 349– 357. doi: 10.1002/btpr.1512.

Shang, Y. *et al.* (2014) 'Chitin-based fast responsive pH sensitive microspheres for controlled drug release', *Carbohydrate Polymers*. Elsevier, 102, pp. 413–418. doi: 10.1016/J.CARBPOL.2013.11.039.

Sharifi-Sirchi, G. R. and Jalali-Javaran, M. (2016) 'Selecting appropriate hosts for recombinant proteins production : Review article Introduction ':, *Hormozgan Medical Journal*, 20(3), pp. 214–222.

Solá, R. J. and Griebenow, K. (2010) 'Glycosylation of Therapeutic Proteins: An Effective Strategy to Optimize Efficacy', *BioDrugs*, 24(1), pp. 9–21. doi: 10.2165/11530550-000000000-00000.

Soon, C. Y. *et al.* (2018) 'Extraction and physicochemical characterization of chitin and chitosan from Zophobas morio larvae in varying sodium hydroxide concentration', *International Journal of Biological Macromolecules*. Elsevier, 108, pp. 135–142. doi: 10.1016/J.IJBIOMAC.2017.11.138.

Sun, S. *et al.* (2011) 'Requirement for store-operated calcium entry in sodium butyrate-induced apoptosis in human colon cancer cells', *Bioscience Reports*, 32(1), pp. 83–90. doi: 10.1042/bsr20110062.

Sung, Y. H. *et al.* (2004) 'Effect of sodium butyrate on the production, heterogeneity and biological activity of human thrombopoietin by recombinant Chinese hamster ovary cells', *Journal of Biotechnology*. Elsevier, 112(3), pp. 323–335. doi: 10.1016/J.JBIOTEC.2004.05.003.

Sunley, K. and Butler, M. (2010) 'Strategies for the enhancement of recombinant protein production from mammalian cells by growth arrest', *Biotechnology Advances*, 28(3), pp. 385–394. doi: 10.1016/j.biotechadv.2010.02.003.

Tang, Y. *et al.* (2011) 'The role of short-chain fatty acids in orchestrating two types of programmed cell death in colon cancer', *Autophagy*, 7(2), pp. 235–237. doi: 10.4161/auto.7.2.14277.

Tatevossian, A. (1979) 'Diffusion of radiotracers in human dental plaque', *Caries Research*, 13(3), pp. 154–162. doi: 10.1159/000260396.

Teijeiro-Osorio, D., Remuñán-López, C. and Alonso, M. J. (2009) 'New generation of hybrid poly/oligosaccharide nanoparticles as carriers for the nasal delivery of macromolecules', *Biomacromolecules*, 10(2), pp. 243–249. doi: 10.1021/bm800975j.

Thedrattanawong, C., Manaspon, C. and Nasongkla, N. (2018) 'Controlling the burst release of doxorubicin from polymeric depots via adjusting hydrophobic/hydrophilic properties', *Journal of Drug Delivery Science and Technology*. Elsevier B.V., 46, pp. 446–451. doi: 10.1016/j.jddst.2018.06.001.

Thornton, P. (2016) *The use of submicron pore channels found in lobster shell to model drug and molecule delivery.* Institute Technology Sligo.

Uddin, M. J. *et al.* (2011) 'An in vitro controlled release study of valproic acid encapsulated in a titania ceramic matrix', *Applied Surface Science*, 257, pp. 7920–7927. doi: 10.1016/j.apsusc.2011.03.079.

Uretsky, N. J. *et al.* (1971) 'Morphologic Differentiation of mouse neuroblastoma cells induced in vitro by Dibutyryl adenosine 3':5'-cyclic monophosphate', *Nature New Biology*, 232(5), pp. 16–17. doi: 10.1038/229560a0.

Ververis, K. and Karagiannis, T. C. (2012) 'Overview of the Classical Histone

Deacetylase Enzymes and Histone Deacetylase Inhibitors', *ISRN Cell Biology*, 2012(Figure 1), pp. 1–12. doi: 10.5402/2012/130360.

Walsh, G. (2018) 'Biopharmaceutical benchmarks 2018', *Nature Biotechnology*. Nature Publishing Group, 36(12), pp. 1136–1145. doi: 10.1038/nbt.3040.

Walsh, G. and Jefferis, R. (2006) 'Post-translational modifications in the context of therapeutic proteins', *Nature Biotechnology*, 24(10), pp. 1241–1252. doi: 10.1038/nbt1252.

Wan, A. C. A. and Tai, B. C. U. (2013) 'CHITIN — A promising biomaterial for tissue engineering and stem cell technologies', *Biotechnology Advances*. Elsevier, 31(8), pp. 1776–1785. doi: 10.1016/J.BIOTECHADV.2013.09.007.

Wang, X. *et al.* (2012) 'Histone deacetylases and their inhibitors: molecular mechanisms and therapeutic implications in diabetes mellitus', *Acta Pharmaceutica Sinica B*, 2(4), pp. 387–395. doi: 10.1016/j.apsb.2012.06.005.

Wang, Y. *et al.* (2016) 'Sodium butyrate-induced apoptosis and ultrastructural changes in MCF-7 breast cancer cells', *Ultrastructural Pathology*, 40(4), pp. 200–204. doi: 10.3109/01913123.2016.1170083.

Wang, Y., Li, J. and Li, B. (2017) 'Chitin microspheres: A fascinating material with high loading capacity of anthocyanins for colon specific delivery', *Food Hydrocolloids*. Elsevier, 63, pp. 293–300. doi: 10.1016/J.FOODHYD.2016.09.003.

Weinhold, B. (2006) 'Epigenetics: the science of change.', *Environmental health perspectives.*, 114(3), pp. 160–167. doi: 10.1289/ehp.114-a160.

Weiser, J. R. and Saltzman, W. M. (2014) 'Controlled release for local delivery of drugs: barriers and models', *Journal of Controlled Release*. Elsevier, 190, pp. 664–673. doi: 10.1016/J.JCONREL.2014.04.048.

Van der Weken, H., Cox, E. and Devriendt, B. (2019) 'Rapid production of a chimeric antibody-antigen fusion protein based on 2A-peptide cleavage and green fluorescent protein expression in CHO cells', *mAbs*. Taylor & Francis, 0(0). doi: 10.1080/19420862.2019.1574531.

Witt, O. *et al.* (2009) 'HDAC family: What are the cancer relevant targets?', *Cancer Letters*, 277(1), pp. 8–21. doi: 10.1016/j.canlet.2008.08.016.

Wlaschin, K. F. *et al.* (2007) 'Recombinant protein therapeutics from CHO cells-20 years and counting', *Chemical Engineering Progress*, 103(10), p. 40. doi: 10.1017/CBO9781107415324.004.

Wright, J. A. (1973) 'Morphology and growth rate changes in Chinese hamster cells cultured in presence of sodium butyrate', *Experimental Cell Research*. Academic Press, 78(2), pp. 456–460. doi: 10.1016/0014-4827(73)90091-8.

Wurm, F. M. (2004) 'Production of recombinant protein therapeutics in cultivated mammalian cells', *Nature Biotechnology*, 22(11), pp. 1393–1398. doi: 10.1038/nbt1026.

Xiong, F., Mou, Y. Z. and Xiang, X. Y. (2015) 'Inhibition of mouse B16 melanoma by sodium butyrate correlated to tumor associated macrophages differentiation suppression', *International Journal of Clinical and Experimental Medicine*, 8(3), pp. 4170–4174.

Yang, X. and Gre, S. (2005) 'Class II Histone Deacetylases: from Sequence to Function, Regulation, and Clinical Implication', *MOLECULAR AND CELLULAR BIOLOGY*, 25(8), pp. 2873–2884. doi: 10.1128/MCB.25.8.2873.

Younes, I. and Rinaudo, M. (2015) 'Chitin and chitosan preparation from marine sources. Structure, properties and applications', *Marine Drugs*, 13(3), pp. 1133–1174. doi: 10.3390/md13031133.

Zhang, T. *et al.* (2019) 'The characteristics of free/bound biomarkers released from source rock shown by stepwise Py-GC-MS and thermogravimetric analysis (TGA/DTG)', *Journal of Petroleum Science and Engineering*. Elsevier, 179, pp. 526–538. doi: 10.1016/J.PETROL.2019.04.060.

Zhang, H. *et al.* (2017) 'The preparation and characterization of chitin and chitosan under large-scale submerged fermentation level using shrimp by-products as substrate', *International Journal of Biological Macromolecules*. Elsevier, 96, pp. 334– 339. doi: 10.1016/J.IJBIOMAC.2016.12.017.

Zhang, J. *et al.* (2016) 'Sodium Butyrate Induces Endoplasmic Reticulum Stress and Autophagy in Colorectal Cells: Implications for Apoptosis', *PLoS ONE*, 11(1), pp. 1–25. doi: 10.1371/journal.pone.0147218.

Zhu, J. (2012) 'Mammalian cell protein expression for biopharmaceutical production',

Biotechnology Advances. Elsevier, 30(5), pp. 1158–1170. doi: 10.1016/J.BIOTECHADV.2011.08.022.

7.0 Appendix

ELISA Reagent preparation

Samples and reagents were prepared on the day of the experiment, only the amount of reagent needed on the day was prepared.

Samples were defrosted and diluted to 1/1000 and 1/5000 using 1X cell extraction buffer PTR.

- 10ml 1X cell extraction buffer PTR ○ Combine 7.8 mL deionized water, 2 mL 5X cell extraction buffer PTR and 200 µL 50X cell extraction enhancer solution.
- 1X wash buffer PT ○ Combine 6 mL 10X wash buffer PT with 54 mL deionized water.
- 1X Antibody Diluent EB ○ Combine 1 mL 4X antibody diluent EB with 3 mL 1X wash buffer PT.
- Antibody cocktail ○ Combine 300 µL 10X capture antibody, 300 µL 10X detector antibody,

  2.4 mL 1X antibody diluent EB.

- Standard preparation ○ Reconstitute the GFP protein standard (4,000 pg/ml) by adding 250 µL deionized water. Mix gently using a pipette and hold at room temperature for 10 minutes. ○ Label eight tubes, standards 1-8.
  - Add 150 µL 1X cell extraction buffer PTR into tube number 1 and add 200 µL 1X cell extraction buffer PTR into tubes 2-8.
  - Use the stock standard (4,000 pg/mL) to prepare the dilutions.
  - Take 150 µL from the stock and add to tube 1. Mix gently before each step.
  - Take 100 µL from tube 1 and add to tube 2. Continue this for the remaining tubes. See diagram below.
  - Tube 8 contains no protein and is the blank control.

Standard curve of ELISA			
conc. (pg/ml)	O.D of standards at 450nm		Standard Deviation
	1	2	
0	0.136	0.124	0.008
2.7	0.177	0.167	0.007
8.2	0.201	0.206	0.004
24.7	0.273	0.263	0.007
74.1	0.526	0.516	0.007
222.2	1.398	1.349	0.035
666.7	3.305	3.289	0.011
2000	*****	*****	

y values (mean O.D) 1/5000 dilution		Protein concentration from equation of line (pg/mL)	Average fluorescence ImageJ
$1x10^3$	0.167	34.55	2.804
$2.5x10^3$	0.174	36.01	8.544667
$5x10^3$	0.204	42.33	9.7
$1x10^4$	0.320	66.56	19.71367
$2x10^4$	0.340	70.59	22.31633

GC-MS TIC Chromatograms

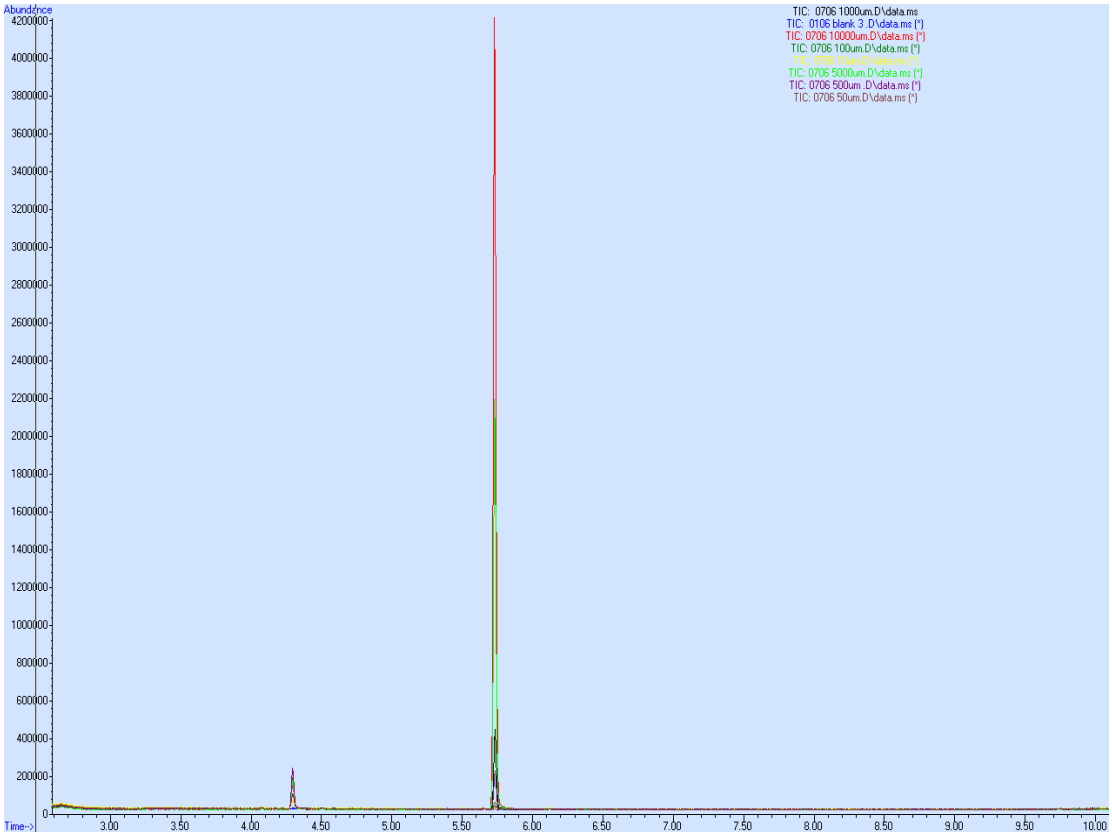

TIC chromatogram from GC-MS of standard curve for sodium butyrate

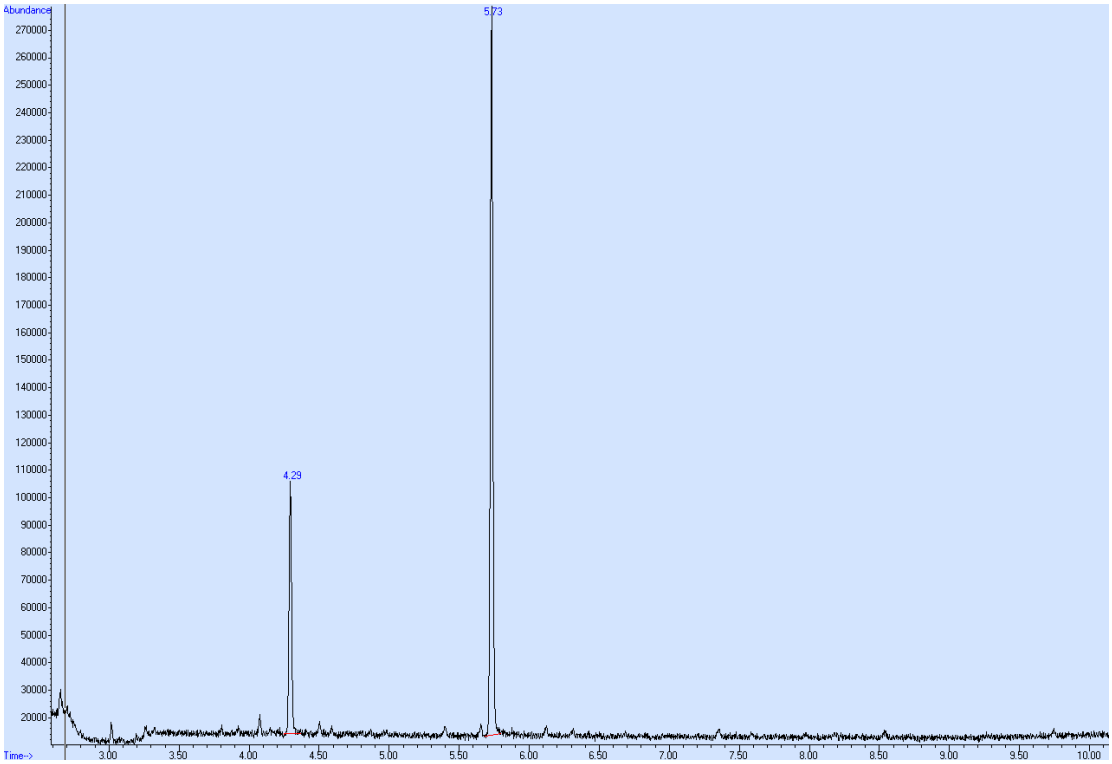

TIC chromatogram from GC-MS of 250mM sample sodium butyrate